

MSC THESIS

Enriching Conventional Sewer Condition Assessment Through Additional Data Interpretation and Visualization

WEI LIU

Student Nr: s2029774
Email: w.liu-2@student.utwente.nl

Course Code: 201800115

Examination Committee:

UT Supervisors: Dr. A. (Andreas) Hartmann
Dr. Ir. L.L. (Léon) olde Scholtenhuis
H. (Hengameh) Noshahri, MSc

External Supervisor: Dr. Hajo Molegraaf
Consultant / Software Engineer / Funder of Rolsch

Research Client: Rolsch Assetmanagement

Department of Construction Management & Engineering (CME)
Faculty of Engineering Technology
University of Twente
P.O. Box 217
7500 AE Enschede
The Netherlands

Version: Thesis _ Final
Date: August 24th, 2020

Preface

This research project is my master thesis about ***“Enriching Conventional Sewer Condition Through Additional Data Interpretation and Visualization”***. It was finished under the Master of Science Study Programme - Construction Management & Engineering at the University of Twente.

What drove me into the topic of sewers is twofold: my personal interest takes the first and major part; secondly, I want to help with improving the poor management work of the sewer industry in my home country - China, where many cities are facing frequent inner-city floodings, overflows, and other sewer problems. Such problems are essentially caused by insufficient sewer inspections and condition assessments, which consequently result in ineffective and late sewer maintenance activities. There is a Chinese saying says ***“the urban underground utilities, like the sewer system, represent the conscience of the city, and this conscience needs to be maintained by all of our people”***. It touched me so deeply because eventually, I will return to my homeland as an engineer, it will indeed be my responsibility to keep the cities’ conscience there and functioning well to serve our people.

As a master student who studies in the Netherlands - the nation that is well known for its outstanding water management achievements, the advancements of the Dutch sewer management industry impressed me. Thus, I started my master thesis on exploring the interpretation and visualization of sewer inspection data collected from new technologies and finished it by providing several innovative data visualization methods. Through this thesis, I contributed my thinking and creativity to both the scientific and industrial fields. But more importantly, the knowledge and experiences I gained from writing this thesis, are more than beneficial to my future career.

The past over six months was a rough but honorable journey, hereby I would like to deliver my sincere appreciation to all my supervisors, Mr. Hartmann, Mr. olde Scholtenhuis, and Miss. Noshahri from UT, and Mr. Molegraaf from the company Rolsch. They are very kind and friendly people and even better researchers. They kept supporting me with their expertise and insightful suggestions, which helped me through a lot of difficulties. Besides them, Rolsch and its great team (Peter, Ronald, Rimmert) also provided strong supports to this project and me personally. Thanks to all these amazing people, I went this far and accomplished this thesis even during the COVID-19 world pandemic.

Last but not the least, I want to express my deepest thanks to my beloved family (parents and sister), my girlfriend, and all my close friends. It has been more than four years since I left home, many things happened but their love and support to me never changed. It is them that encouraged and inspired me when I felt lost, they always have confidence in me and believe that one day I will come back to them with knowledge and skills that could make our life and the world around us better. They made me a better person, to all of them, thank you and I love you 3000!

I hope this thesis will not be the end of my academic thinking, I also hope the aforesaid hope is not just a hope.

希望这篇论文不会是我学术思考的终点，也希望前面这句话不只是希望。

I hope you get inspiration from this thesis and have fun reading!

Wei Liu

Enschede, August 2020

Summary

Municipalities and asset management companies use inspections methods to collect pipe condition data to assess the sewer conditions, and to make decisions about when and where they undertake what maintenance activities. Currently, CCTV (Closed-Circuit Television) is one of the most used methods to collect this condition data. However, the drawback of this method is that it can only inspect the interior of the pipeline visually, leaving other potentially existing defects unnoticed (e.g., voids behind or within the sewer wall).

Although additional methods like in-pipe GPR are able to detect such defects, they are not widely introduced and used by sewer asset managers. The in-pipe GPR uses high-frequency electromagnetic waves to “look through” the sewer pipe wall to collect data about anomalies in the structure of the pipe. To date, the interpretation of such data remains complicated since it requires additional filtering, processing and interpretation steps. One main challenge is also to visualize the collected data and present it to the sewer asset managers such that they can make maintenance decisions based on it. To stimulate the uptake of these additional inspection techniques, sewer management software developers such as Rolsch Assetmanagement B.V. (the client of this project), want to explore possible ways to visualize this new type of inspection data for uses of their future sewer management systems.

To date, the literature suggests to visualize conventional inspection data (from e.g., CCTV, laser and sonar inspections) for sewer pipes using full-range pipe fold-out images (Wirahadikusumah, et al., 1998; Kirkham, et al., 2000). The state-of-art in which data coming from other inspection methods such as impact echo and surface GPR is presented is, however, different. For example, literature uses 2D contour images, tomograms and defect maps for slab-like structures on pavements and bridge decks (Zhu, et al., 2007; Olson, et al., 2011; radarviewllc, 2020). These data visualization concepts are, however, not readily interpretable or presentable to sewer asset managers that conventionally work with the 2D CCTV pipe fold-out view. Nor are they implemented in sewer management software. Hence, the **objective of this project is to design a method that can visualize the additional sewer condition data collected by an in-pipe GPR sewer inspection.**

To achieve this goal, various steps were followed. The author conducted interviews, simulated dummy data from in-pipe GPR inspections, conducted a literature review, and finally developed (and verified) a graphical mock design to present this data. These steps and their outcomes are elaborated below.

Explorative interviews with two local sewer management organizations were first conducted to identify their additional sewer condition data needs and expectations of visualizing them. Questions such as “*Considering the limitations of CCTV inspections, what do you think are additional needs that make current sewer condition assessment more comprehensive?*” and “*How would you prefer the data collected (interpreted) from in-pipe GPR inspections to be presented?*” were asked. The interview results were analyzed qualitatively to formulate specific design requirements for the development of the data visualization method. This list was amended with requirements from the abstract tasks literature, which defines additional requirements for visualization systems (Ardito, et al., 2006; Shneiderman, 1996). Next, the formulated requirements were prioritized by the MoSCoW method (Mulder, 2017), and categorized based on eight descriptive aspects. These descriptive aspects are **area of application, visualized features, scale, depiction, compatible data types, viewing perspective, ease of creation**

and **future proof**. In total, sixteen requirements were formulated in line with these descriptive aspects (see Table 4-1), four important requirements were as follows:

1. The visualization must be applicable to sewer condition assessment practice. This specifically means that it should be able to visualize inspection data showing the interior space, wall and exterior environment of a pipe.
2. The visualization must contain the basic features of full-range pipe representation, defect representation, and a coordinate system that ranges the geometry of the pipe and locates the defects.
3. The visualization must be able to show an overview of all data collected from one inspection (of one pipe), which includes identified minor defects (and individual data points).
4. The visualization must include written characters to denote the characterizations and quantifications of defects (i.e., presence, location, type, size and severity).

After exploring the users' requirements, the second step was to run simulations with gprMax software to generate dummy data of possible sewer defects that in-pipe GPR sewer inspections can find. This was done since there was no access to empirical data from in-pipe GPR sewer inspection practices. Inspection data was needed to familiarize this study with the type of data (i.e., raw/post-processed data and characterizations and quantifications of defects) that could be collected and presented to sewer asset managers. The simulations were based on different soil and object types, voids at distinctive locations and with different sizes around the pipe. From the analysis of the simulation data, a routine for processing and interpreting in-pipe GPR sewer inspection data was provided.

Third, a literature review was conducted to identify inspection data visualization alternatives that might be able to present in-pipe GPR sewer inspection data to sewer asset managers. This took place by studying scientific databases such as *Google Scholar* and *Scopus*, using keywords searchers such as "inspection data visualization" and "sewer condition assessment". Over thirty papers from journals such as *Automation in Construction*, *Pipeline Engineering and Construction*, *Tunnelling and Underground Space Technology* as well as *Visualization in Engineering* were found.

The visualization alternatives identified from these papers covered inspection data visualization alternatives form different types of civil infrastructure and different types of inspection technology. The review resulted in eleven inspection data visualization alternatives (Table 4-2 provides a detailed overview). After excluding the alternatives that could not meet the first two requirements listed above, the following seven visualization alternatives remained:

1. The **2D representation of pipewall- soil interface** visualizes defects within and outside the sewer wall (e.g., wall thickness, grout loss and in/external voids) in a longitudinal front view of the pipewall-soil interface.
2. The **2D Pipe fold-out view** visualizes defects in the pipe and its inner surface (e.g., obstacles and cracks) in a longitudinal pipe fold-out view.
3. The **2D linear representation of pipe wall condition** visualizes pipe wall variations (e.g., thickness changes) and defects within the pipe wall (e.g., voids) in a longitudinal front view of the pipe thickness.
4. The **2D color-coded defects map** visualizes defects on and within the surface of slab-like structures (e.g., thickness losses and voids) in the top view of a map that outlines the shape of the inspected object.
5. The **3D pipe with inspection data projected on outer surface** visualizes sewer inner surface defects (e.g., corrosion) on a rotatable and zoomable 3D cylindrical surface.
6. The **3D pipe reconstruction** visualizes defects on and within the pipe wall surface (e.g., outer or inner surface damage, rebar configuration) in a rotatable and zoomable 3D pipe model (i.e., reconstructed from inspection data, with thickness) with certain forms (e.g., transparent, wireframe, X-ray).

7. The **3D Stereo AR sewer data visualization** visualizes the in-situ asset location and its registration information in a 3D AR model with certain forms (e.g. image-textured, transparent, wireframe, X-ray).

Fourth, an MCDA (Multi-Criteria Decision Analysis) was applied to systematically compare and rank these alternatives and find the most suited one for the purpose of this study. Six criteria from the list of descriptive aspects were included in the MCDA, these are: **area of application, scale, depiction, viewing perspective, ease of creation** and **future proof**. The MCDA was done by assessing whether these alternatives score low, mediocre or high (“bad”, “fair” or “good”) for the criteria. After placing weights to these criteria (0-100%), the total score of each alternative on all criteria was calculated. Table I shows the **2D representation of pipewall- soil interface** scored highest in the MCDA ranking with a score of 1.8.

Alternatives	Criteria	Area of application (30%)	Scaling (25%)	Depiction (15%)	Ease of creation (15%)	Future proof (10%)	Viewing perspective (5%)	Final Scores
3. 2D representation of pipewall- soil interface		2	2	1	2	2	1	1.8
2. 2D Pipe wall condition linear representation		0	2	1	2	1	1	1.1
1. 2D pipe fold-out view		0	2	2	2	1	1	1.25
6. 2D color-coded defects map		0	2	2	2	1	1	1.25
4. 3D pipe with inspection data projected on outer surface		1	1	1	1	1	2	1.05
8. 3D pipe reconstruction		1	1	2	1	2	2	1.3
11. 3D Stereo AR sewer data visualization		1	1	2	0	2	2	1.15

Table I: MCDA of selecting the optimal alternative for in-pipe GPR sewer inspection data visualization, “0” means this alternative is not specifically suitable for visualizing the in-pipe GPR inspection data collected from the exterior environment of the pipe.

Fifth, the features and elements from the highest-ranked alternative were integrated into one graphical mock design of the final in-pipe GPR sewer inspection data visualization method for asset managers. Figure I and Figure II present the outcome of this tailored design. The visualization shows the front view of a buried pipe and its upper and lower exterior condition. It depicts the type, location (e.g., longitudinal location, circumferential position and distance to the pipe), size and severity of defects (i.e., voids and unknown objects behind the pipe wall), and includes details of exterior defects around the pipe circumference with a “pop-up” window and “pipe-roller” view.

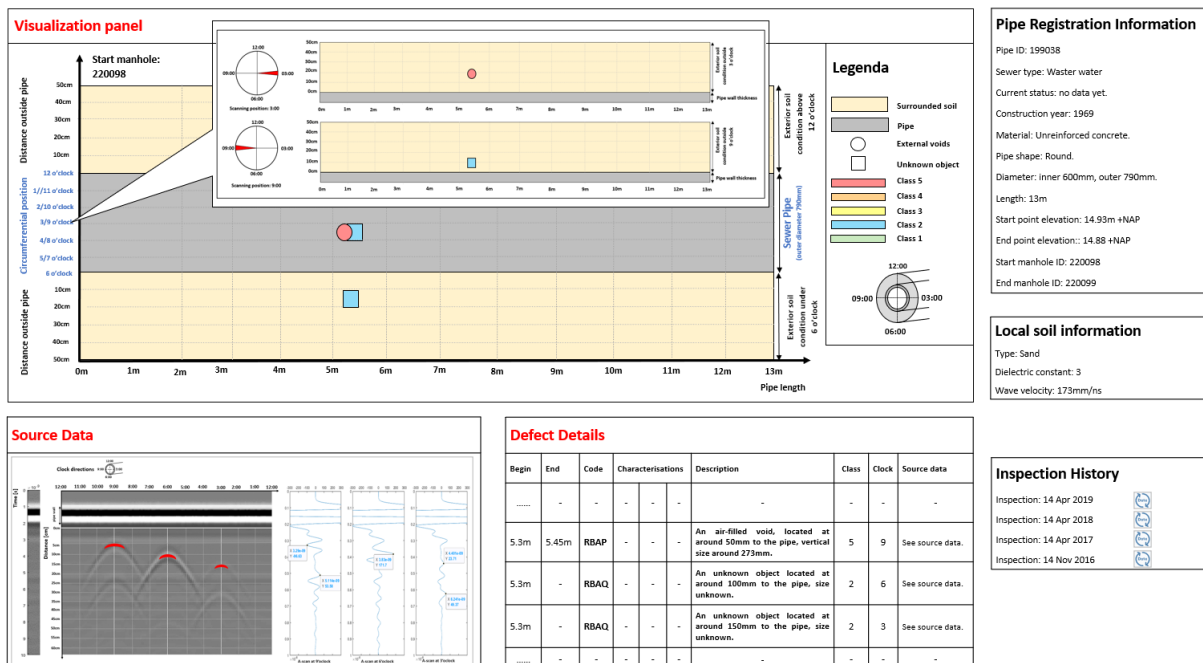


Figure II: The final developed in-pipe GPR sewer inspection data visualization method (pop-up version).

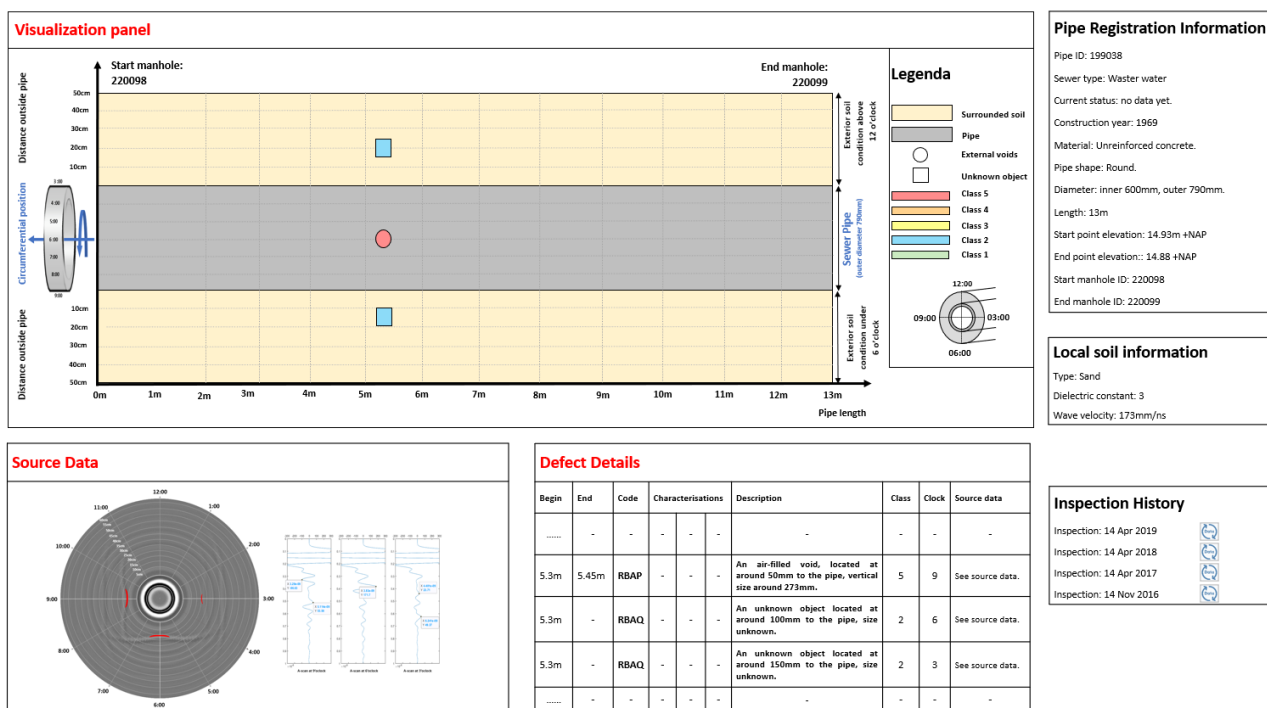


Figure III: The final developed in-pipe GPR sewer inspection data visualization method (pipe-roller version).

Finally, the developed visualization method was verified by assessing whether they are likely to fulfill the needs and expectations of the end-users, as was formulated in the requirements. The result turned out that the developed visualization method successfully realized eleven out of twelve highly prioritized requirements while one of such requirements was partly realized (i.e., the developed visualization is not fully in 3D). The requirements 1 and 2 were realized by providing a longitudinal front view of the pipe and its upper and lower exterior environment, and by including the “pop-up” window and “pipe-roller” view. Requirements 3 and 4 were realized by presenting defects in a similar fashion as in the conventional CCTV data visualization.

The main contributions of this thesis are the review of existing and potential data visualization alternatives for infrastructure inspections and the verified in-pipe GPR sewer inspection data visualization method. First, existing literature does not provide such a specific review. Further, only a few cases in grey literature (Ekes, et al., 2011; Ekes, et al., 2014; Ékes, et al., 2012) provide an approach to the visualization of in-pipe GPR data. The proposed visualization method adds to this by extending its visualization range and including the post-processed data and additional defect codes. These contributions, in turn, provide practitioners a way to process, interpret and visualize data from an alternative sewer inspection technology like in-pipe GPR, and may enable a more comprehensive sewer condition assessment in the future.

The limitations of this thesis project are that the in-pipe GPR data used for processing and interpreting was from simulations instead of real inspections or experiments. It may not be able to represent the variability of subsurface materials in reality. In addition, the developed visualization method is only a graphical mock design that could not be validated by real end-users (in terms of its workability and implementation feasibility). To overcome the limitations, the author recommends future studies to collect in-pipe GPR sewer inspection data in practice to assess whether the real data can be meaningfully interpreted and visualized, and to develop prototypes for the proposed visualization method (e.g., developing a workable visualization system) for users to verify and validate it from a more practical perspective.

Table of Contents

Preface.....	I
Summary.....	II
Table of Contents	VI
List of Abbreviation	VIII
1. Introduction.....	1
1.1. Problem Context.....	1
1.2. Problem Background	4
1.2.1. State of Art of In-pipe GPR Sewer Inspection.....	4
1.3. Problem Definition & Research Objective	7
1.4. Research Questions	8
1.5. Outline	8
2. Methodology	9
2.1. Data Collection Methods & Uses.....	9
2.2. Verification Setup	12
3. Simulating In-pipe GPR Data.....	13
3.1. Interpreting In-Pipe GPR Simulation Data	13
3.1.1. Simulation Mechanism & Setup	13
3.1.2. Considerations before the In-pipe GPR Inspection	15
3.1.3. Quantifications Analysis of Void.....	19
3.1.4. Standardized In-pipe GPR Data processing & Interpretation Routine	25
4. Visualization Method Development.....	30
4.1. Data Visualization in Sewer Condition Assessment.....	30
4.2. Available & Optimal Visualization Alternative(s) for in-pipe GPR Data.....	31
4.2.1. Descriptive Aspects & Requirements Development	31
4.2.2. Review of Available Inspection Data Visualization Alternatives	33
4.2.3. Selecting the Optimal Data Visualization Alternative	35
4.3. Designing the In-Pipe GPR Sewer Inspection Data Visualization Method.....	38

5.	Verifying the Developed Visualization Method.....	41
6.	Discussion	45
6.1.	Contribution	45
6.2.	Limitations & Recommendations	45
7.	Conclusion	46
	Appendixes	49
A.	Interview Setups and Questions.....	49
B.	Interview Results	50
C.	Translating Users' Additional Sewer Condition Data Needs into Specific Defects.....	51
D.	Technology Readiness Level Scale	53
E.	Time Zero Correction.....	53
F.	Coordinates Transformation	54
G.	Detailed Visualization Alternatives Found in Literature.....	57
H.	European Sewer Defects Coding System.....	61
I.	State of Art of Impact Echo Sewer inspection.....	62
J.	Solution to Unavailable Impact Echo Simulation	65
K.	Selecting Optimal Visualization Alternatives for Impact Echo & Sewer Condition Data Integration....	66
L.	Additional Sewer Defect Codes Development	67
M.	Impact Echo Sewer Inspection Data Visualization Method	69
N.	Integrated Sewer Condition Data Visualization Method.....	71
	References	73

List of Abbreviation

AR	Augmented reality
ARSI	Aerial Robot for Sewer Inspection
AutoCAD	Auto Computer-Aided- Design
CCTV	Closed-Circuit Television
COMSOL	A cross-platform finite element analysis, solver, and Multiphysics simulation software
FFT	Fast Fourier Transform
GPR	Ground Penetrating Radar
GIS	Geographic Information System
gprMax	An open-source software that simulates electromagnetic wave propagation.
HPC	High-Performance Computing cluster
IMU	Inertial Measurement Unit
Intelligent PIG	Intelligent pipeline inspection gauge
KLIC melding	Cables and Pipelines Information Report in Dutch, a report for excavation in the public space managed by the Dutch Land Registry (Kadaster).
LIDAR	Light Detection and Ranging, a method for measuring distances (ranging) by illuminating the target with laser light and measuring the reflection with a sensor.
MATLAB	Matrix Laboratory, a multi-paradigm numerical computing environment and proprietary programming language.
MCDA	Multiple-Criteria Decision Analysis, introduced on page 11.
MoSCow	A method for prioritizing requirements of a project or final product, introduced on page 11.
NDE	Non-Destructive-Evaluation
TISCALI	Technological Innovation for Sewer Condition Assessment - Long-Range Information System (the collaboration between three faculties of the University of Twente: Engineering Technology, Electrical Engineering Math and Informatics, and ITC (Faculty of Geo-Information Science and Earth Observation)).
TRL	Technology Readiness Level, see Appendix D for the detailed TRL table.
TWTT	Two-Way Travel Time, indicates the time duration from a GPR electromagnetic wave was transmitted into a medium to it gets reflected and received by the receiver.
TZC	Time Zero Correction
PPR	Pipe Penetrating Radar, particularly refers to the “SewerVUE surveyor” in-pipe GPR application.
SSET	Sewer Scanner and Evaluation Technology, a flexible non-destructive evaluation data acquisition tool.
VR	Virtual reality
WTDR	Width-to-depth ratio, $\frac{d}{T}$, d represents the size of the flaw and T represents the depth of the flaw.

1. Introduction

The topic of this thesis is part of the Technology Innovation for Sewer Condition Assessment - Long-distance-Information-system (TISCALI) project of the University of Twente, and was originally initiated by the local sewer management company - Rolsch Assetmanagement B.V. in Enschede, Netherlands. In this chapter, section 1.1 first introduces the conventional CCTV (Closed-Circuit Television) - led sewer condition assessment and its limitations, then the users' interests in additional sewer condition data arose from such limitations, which lead to the solution of applying additional inspection technologies to fulfill such needs. Subsequently, the current state and limitations of the in-pipe GPR method are elaborated in section 1.2. Based on that, the main research problem is defined and the research objective is formulated in section 1.3. Moreover, section 1.4 breaks down the research problem into specific questions while section 1.5 outlines the structure of this document.

1.1. Problem Context

An enormous amount of sewer pipes scatters around beneath cities globally, together they form up one of the most capital-intensive infrastructure systems for the society – the urban sewer system. The sewer pipes play an important role in keeping the city functional on discharging waste and storm water and providing the citizens with a hygienic living environment. However, many of these underground utilities are facing failure problems due to aging, misuse, and many other causes (Makar, 1999). This calls for a more proactive and cost-effective sewer inspection and maintenance strategy, which emphasizes on inspecting the sewer pipes regularly and replacing them once the severity of the deterioration outweighs the benefit of further maintenance (Fenner, 2000).

To plan the sewer rehabilitation work actively and effectively, valid condition assessments are the key, and they require good record keeping and a proficient information system (Fenner, 2000). As defined by the U.S. Environmental Protection Agency, sewer/pipeline condition assessment is: ***“the collection of data and information through direct and/or indirect methods, followed by analysis of the data and information, to make a determination of the current and/or future structural, water quality, and hydraulic status of the pipeline”*** ((EPA), 2007).

The data and information mentioned in the ((EPA), 2007) definition come from both the sewer registration information and the in-situ sewer inspection data, but only the inspection data is discussed in this thesis. The inspection data can greatly help to provide more enhanced and updated information relating to the current condition of the buried pipes (McDonald, et al., 2001), but the collection of it highly relies on the so-called NDE (non-destructive evaluation) technologies. Among such technologies, CCTV is currently the most dominating inspection technique available (Makar, 1999).

The idea of CCTV sewer inspection is mounting a camera on a small cart or float, cable-pulling or self-propelling it through the sewer line (Wirahadikusumah, et al., 1998). The operation is usually manual because the operator needs to stop and zoom in the camera (pan-and-tilt) when a defect is spotted. The acquired images and videos will be visually diagnosed by certified operators (see Figure 1-1 right), to determine the type, location, size and further information of the observed defects (Chae, et al., 2001; Duran, et al., 2002). The workflow of a CCTV inspection can be seen at the left of Figure 1-1.

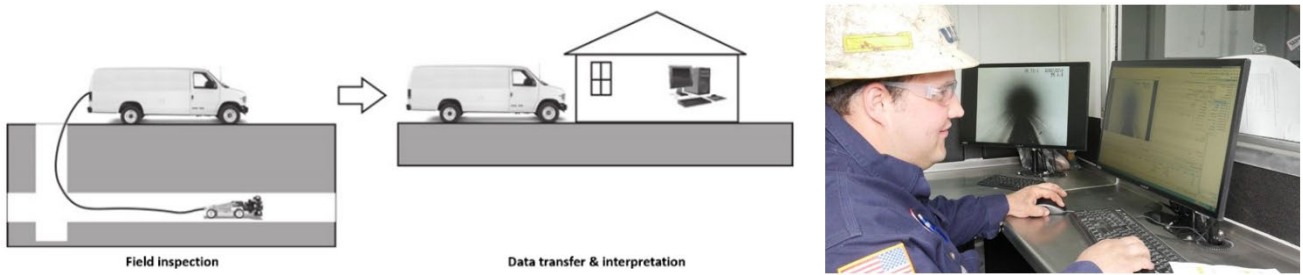


Figure 1-1: left: Workflow of CCTV inspections (Liu, et al., 2013); right: Defects recognition by a certified inspector, source from Google.

As seen in Figure 1-2, the CCTV data visualization first visualizes the geometry of the sewer pipe by “unfolding” it into a long rectangle along its length. The pipe circumference then becomes the rectangle width, denoted by the clock directions. After that, the defects are coded with the sewer defects coding system from (BS_EN_13508-2:2003+A1, 2011) and marked on the pipe-length long rectangle based on their longitudinal location and circumferential position. E.g., the selected red dot in Figure 1-2 represents a class 5 (heavily damaged) “BAP” (void visible through defect) defect, located at 26.5m and 12 o’clock of the pipe. Note this information is also listed in the table under the pipe-long rectangle. Besides that, the raw data (images/videos) is usually also provided and linked to the corresponding defects as evidence (see these small camera icons and the video in Figure 1-2).

Be noted, as currently the most standard and wide-used visualization method for sewer condition assessment, the visualization approach of the CCTV data visualization method is to visualize the pipe’s geometry and the interpreted defects (i.e., presence, type, location, size and severity), and classify the defects with the sewer defect coding system. Although images/videos are provided, they mainly act as evidence (source data) to the interpreted defects, which have little effect on the overall inspection data visualization. In other words, the conventional sewer condition assessment separates the data processing and interpretation from the visualization, what is visualized is mainly the results interpreted from the sewer inspection data.

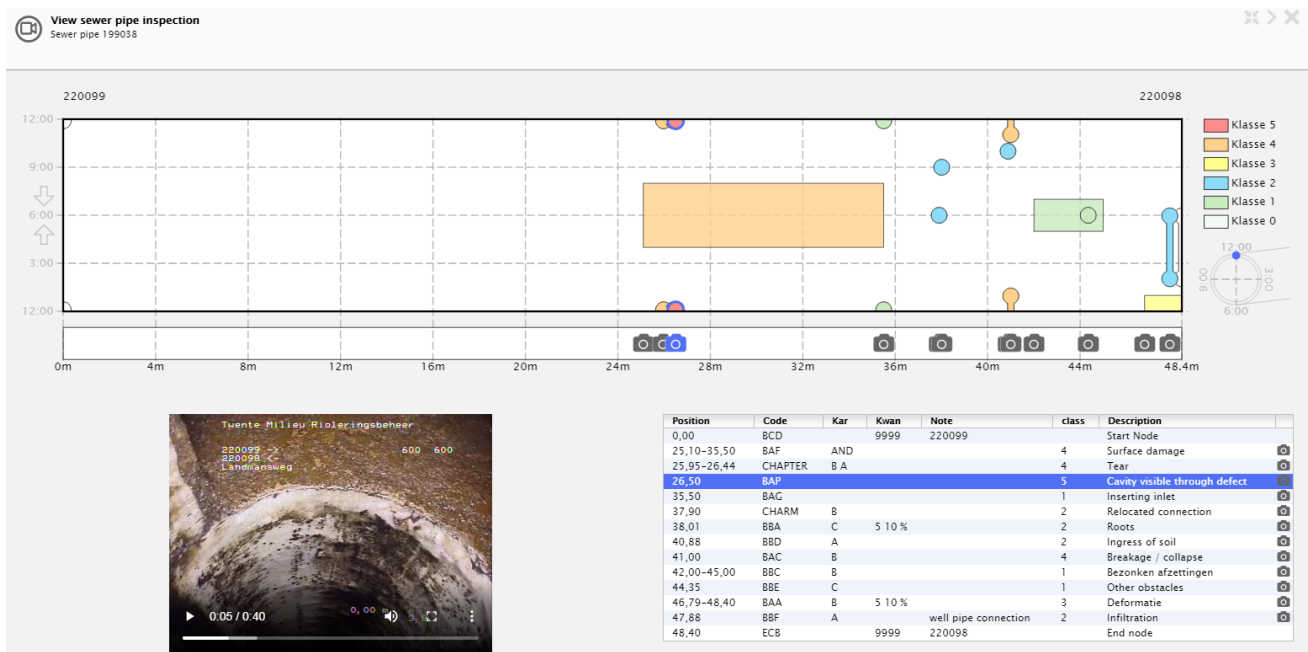


Figure 1-2: Visualization of CCTV inspection results, screenshot from Rolsch sewer management software - MapKit.

Even as the most dominating sewer inspection technique at the time, the CCTV inspection still has many limitations **1).** minor defects (e.g., invisible cracks/deformations that are severe enough to affect the structural integrity of the pipe) are tended to be missed or ignored in the CCTV inspection; **2).** anomalies within/of the sewer wall (e.g., delamination, voids, and (minor) wall thickness reduction) are out of the detecting range of CCTV; and the last but not the least **3).** CCTV inspections are not capable of finding pipe exterior deteriorations (e.g., voids) that might cause major structural integrity losses and capital-intensive failures (e.g., sinkholes) (Noshahri, et al., 2019).

These limitations essentially indicate that the visual-based data collection of the CCTV inspection is insufficient, which consequently causes the incomprehensiveness of the data visualization of the current CCTV-led condition assessment since it cannot visualize the sewer condition from where the CCTV camera cannot “see” or might ignore.

As the limitations of conventional sewer condition assessment techniques such as CCTV act as one main obstacle in the proactive sewer management strategy (Noshahri, et al., 2019), the users’ increasing data needs on a more comprehensive assessment becomes another important perspective of the context of this research. To acquire these needs in more details, interviews with sewer management professionals (mainly sewer managers and managers from the CCTV inspection companies in the Twente region) are arranged to identify users’ interests in additional sewer condition data (see Appendix A and B).

For example, the Hengelo sewer manager mentioned: *“the current CCTV inspection method cannot provide information about the pipe thickness and remaining strength”* and the Almelo CCTV inspector stated: *“more information about sewer problems like subsidence or cavities (not visible from inside the pipe) might be needed, it is advised to take an additional investigation to find out the cause or extent of such problems”*. These quotes reveal that the users would like to expand their knowledge of the sewer condition to problems that could occur within the pipe wall and in the pipe’s exterior environment. After communicating with the sewer management professionals and searching in the literature, the author made the following assumptions:

- The condition of the pipe exterior environment is partly defined by the presence, characterizations and quantifications of the void defect (particularly the air-filled voids).
- The condition of/within the sewer pipe wall (that represents the pipe’s remaining quality) is partly defined by the presence, characterizations and quantifications of defects such as pipe wall thickness losses, voids and delamination within the pipe wall, and (minor) crack on the pipe inner/outer surface.

These defects are further explained in terms of their causes and consequences in Appendix C. Be noted, besides the presence of defects, quantitative information about the characterizations and quantifications of a defect (i.e., location, type, size and severity) is especially important for users to execute an effective and accurate sewer condition assessment. Hence in Appendix C, characterizations and quantifications of these defects are particularly defined and suggested to collect.

In summary, the users’ data needs towards a more comprehensive sewer condition assessment arose from the insufficient visual-based data collection of conventional inspection methods such as CCTV. These needs can be translated into certain defects listed above, which calls for additional inspection technologies to investigate (Noshahri, et al., 2019). Hence, the in-pipe GPR method is applied as a complementary inspection method in this research.

1.2. Problem Background

Before introducing the in-pipe GPR method in more detail, the reasons for specifically choosing it as the complimentary inspection technology in this thesis are explained below.

As the condition of a sewer pipe involves its hydraulic, structural, environmental, and operational performance, pipe structural failures could occur in any one of these domains or their combinations (BS_EN-752:2017, 2018; Costello, et al., 2007). Hence, this thesis proposes a “pipe spaces” theory to simply divide these domains into three pipe spaces that they are related to, namely the **pipe inner space** (including the pipe inner surface, relates to the hydraulic, operational and structural domains), the **space within the pipe wall** (including the pipe outer surface, relates to the structural domain) and the **pipe exterior environment** (relates to the environmental domain).

As assumed in the last page, the users’ data needs can be translated to specific defects of/on/within the pipe wall and in the pipe exterior environment. In which, the latter is directly related to the detecting ability in-pipe GPR since it excels at detecting voids, rocks and other objects in the pipe bedding and surroundings (Makar, 1999; Noshahri, et al., 2019).

Overall, the technology selection is made based on matching the users’ data needs and the detecting ability of the inspection technique. Based on that, this thesis sets up to use in-pipe GPR for detecting anomalies in the pipe’s exterior environment, particularly the air-filled voids.

1.2.1. State of Art of In-pipe GPR Sewer Inspection

GPR is a conventional NDE electromagnetic geophysical technique for subsurface exploration, characterization, and monitoring. Due to its great ability of detecting subsurface objects and voids, there were many attempts made to use it for pipeline inspection in recent years, which is either through a surface GPR or in-pipe GPR (Makar, 1999; Feeney, et al., 2009). Different than the surface GPR, the in-pipe GPR is in a smaller size and examines the pipe from inside, thus also called PPR (Pipe Penetrating Radar). Because of the higher frequencies it uses and its relatively shallow detecting range, the in-pipe GPR could generate results in much higher resolutions. Also, because it performs the inspection from inside the pipe and the scanning is automated, it is easier to operate and consequently more effective in data collection. In short, the in-pipe GPR sewer inspection method appears to be more promising than using a surface GPR to detect the sewer from the ground above it (Makar, 1999).

There are also two ways to execute an in-pipe GPR inspection inside the sewer, one is by sending a robotic platform(see the left of Figure 1-3) into the pipe, which is the focus of this thesis. The other is inspecting the pipe via human entry and scanning the pipe wall with a handheld device, which is only feasible for pipe with a diameter larger than 1m (see the right of Figure 1-3).



Figure 1-3: Robotic in-pipe-GPR inspection (left) and man entry in-pipe GPR inspection (right), source from the SewerVUE website.

Figure 1-4 indicates the working principle of the “SewerVUE Surveyor” presented in Figure 1-3 left. Like other GPR applications, this in-pipe GPR device works by emitting a coherent beam of electromagnetic pulses that travel through the pipe material and soil as a function of their electrical properties. Some of the pulses will be reflected and refracted by any change in material properties, such as at the interface between pipe material and air or water. The greater the difference in the material properties, the greater is the amount of energy reflected back. The reflected waves are detected by a receiving antenna and recorded as single traces (A-scans). This process is repeated continuously as the antenna moves along the inspected pipe to build up a longitudinal profile (B-scans, see Figure 1-4B) (Donazzolo, et al., 2010).

Be noted, the “SewerVUE Surveyor” in-pipe

GPR device has two sets of adjustable transmitter and receiver to scan two circumferential positions of the pipe along its long axis, which has to go back and forth in the pipe several times if the pipe's full circumference needs to be completely scanned. But it is also possible to scan the pipe around its circumference and repeat such circular scanning as the antenna moves along the inspected pipe. This thesis focuses on the latter in-pipe GPR scanning method.

With an ideal resolution, data collected from in-pipe GPR inspections could provide information about **1).** the sewer structural condition, e.g., pipe wall thickness loss, cracks; **2).** the sewer-soil interface condition, e.g., leaks; and **3).** the exterior soil condition, e.g., voids and other adjacent utilities (Ekes, 2016; Wirahadikusumah, et al., 1998). However, this requires processing and interpreting the raw inspection data with a series of complicated procedures.

Same as the surface GPR, the raw in-pipe GPR data is often shown as wiggle traces of wave transit time vs. amplitude (A-scan, see Figure 1-5 left) or planar displays of wave transit time vs. distance (B-scans, see Figure 1-5 middle and right). The B-scan is made of multiple closely collected A-scans and is usually referred to as “radargram”. The A-scan and radargram are the most basic GPR data displays. Conventionally, the grey/color scaled radargrams are more often seen in GPR practices since the hyperbolas in them denote the presence and location of the detected object. The A-scans then provide further information such as the wave’s polarity change while reflecting on an object, which can be used to estimate the material of the detected object.

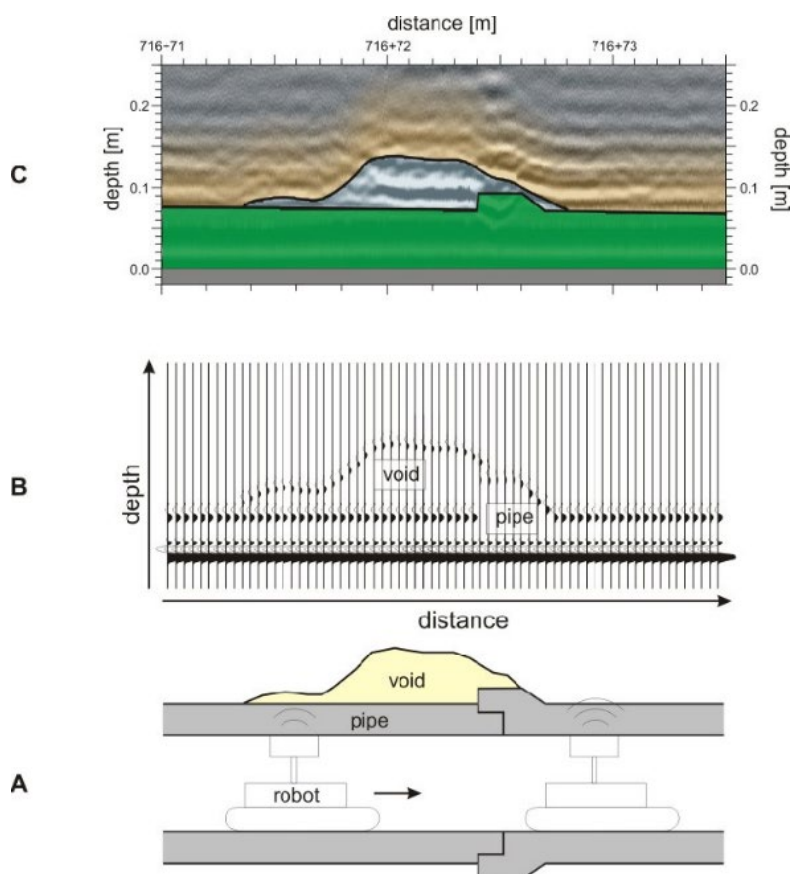


Figure 1-4: A: antenna emits and records GPR signals;
 B: A-scans making up the radar “wiggle” trace (B scan);
 C: interpreted radar plot; source from (Ekes, et al., 2011).

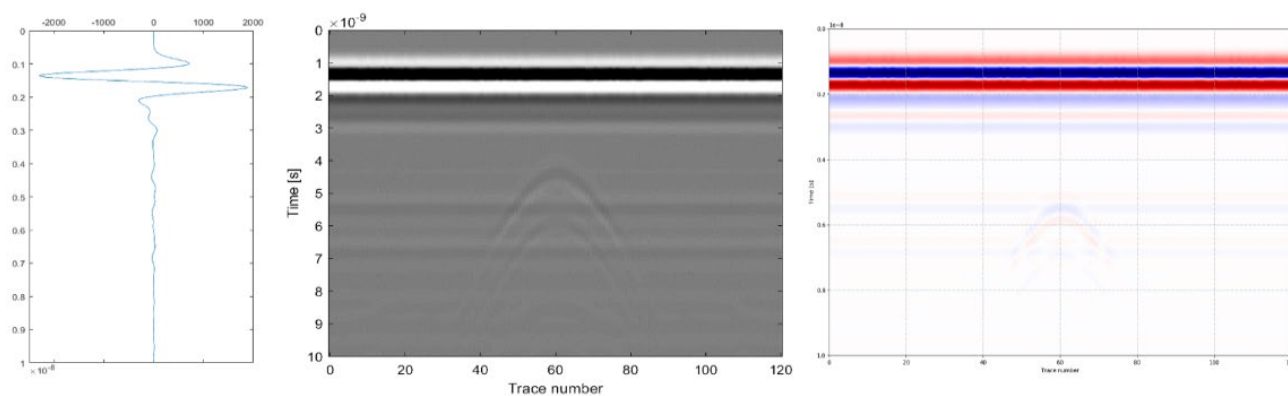


Figure 1-5: Raw GPR data in different forms, from left to right are: A-scan, gray-scaled, and color-scaled B-scan.

The interpretation of raw GPR data is essentially a process of applying different techniques to extract information (e.g., the presence, location, size and even the material) of the detected object from the collected wiggle traces and radargrams, which requires experts' level of data processing skills. After proper processing, the post-processed radargram and A-scan are usually displayed in axes of distance VS. depth (clock directions VS. distance in case of in-pipe GPR), which can be used to interpret the presence, location, size and even material of the detected object.

Worth to note, the post-processed radargram displays the raw data better but not yet a data visualization. Because one basic task of any information visualization system is to present a clear overview of the entire data collection^④ (Ardito, et al., 2006), but the radargram only represents a small group of data points in that. A metaphor here can be, the (raw) post-processed radargrams are just like the individual images collected in the CCTV inspection, they present the condition of certain defects but they do not visualize the sewer condition of a complete pipe segment.

Through searching in product reports of available sewer inspection technologies and various other scientific literature, the author found that the aforementioned "Sewer VUE surveyor" (Figure 1-3 left) is currently the only commercial-grade in-pipe GPR application that visualizes the in-pipe GPR sewer inspection data at a practical level. But it still owns some major imperfections, e.g., it is determined by its scanning method that it cannot visualize the sewer condition around the pipe's full circumference. There might be visualization methods or concepts from other inspection practices (e.g., other types of infrastructure and inspection technology) suitable to present the in-pipe GPR sewer inspection data, but current studies have not discussed them yet.

In summary, there are at least one commercial product and corresponding data visualization methods available for the in-pipe GPR sewer inspection purpose, and some practical cases from this product showing its ability to provide quantitative information about sewer pipe's external environment in high resolutions (Ekes, et al., 2011). Thus the in-pipe GPR sewer inspection can be concluded as developed to a TRL (technology readiness level, see full TRL table in Appendix D) of deployment 8: a few recorded implementations. However, despite these, the data interpretation of the in-pipe sewer inspection method remains complicated and its data visualization is not yet completely suitable and standardized for sewer condition assessment. These then need more development for its further implementation and popularization.

^④ For an in-pipe GPR sewer inspection, the entire data collection means the data collected for an complete pipe segment while the small group of data points means the data collected from a defective pipe cross-section or longitudinal profile (depends on the scanning method).

1.3. Problem Definition & Research Objective

Through searching in the literature, the author found most studies that explore the use of new sewer inspection technologies mainly focus on topics such as detecting ability, operation methods and implementation feasibility, whereas much less attention is given to interpreting and visualizing the inspection data. The introduction to in-pipe GPR in the previous section to some extent also revealed this issue. Although the in-pipe GPR method is one of the most promising quantitative sewer inspection technologies that emerged in recent years^②, its data interpretation and visualization still require further development for practical sewer inspections.

The main problem at the moment is, even if there were additional sewer condition data collected from this new technology, gaps are still lying among the raw inspection data, interpreted sewer condition information and the sewer condition visualization. The in-pipe GPR sewer inspection is in lack of a standardized data processing and interpretation routine and suitable visualization method in terms of sewer condition assessments^③.

The absence of such a data interpretation routine and visualization method then defines the main research problem of this thesis, see the line of argument from the problem context and background to the research problem below:

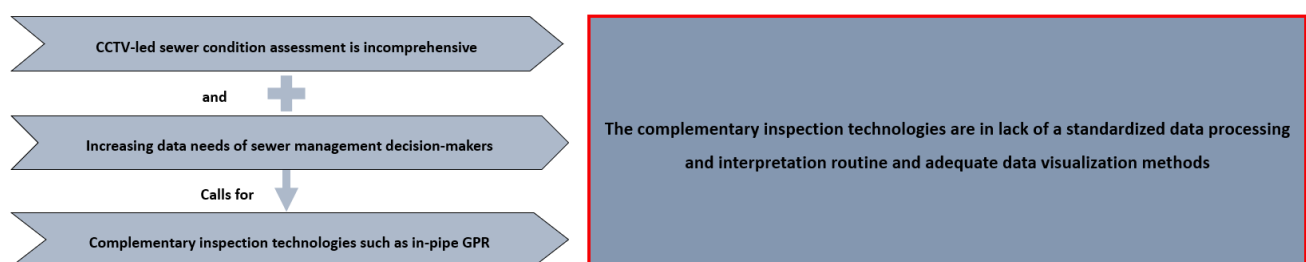


Figure 1-6: Line of the argument of the problem definition of this thesis.

As indicated in Figure 1-6, the main research problem of this thesis is defined as the absence of a standardized data interpretation routine and adequate data visualization method of the in-pipe GPR sewer inspection method. Meanwhile, the research objective for the final evaluation of this research is also formulated. The research can be called successful when the results of this master thesis accomplished:

To design a method that can visualize the additional sewer condition data collected by an in-pipe GPR sewer inspection.

To be more specific, the practical goal of this thesis is to conclude a standardized data processing and interpretation routine for the additional sewer inspection data collected by the in-pipe GPR method and develop a suitable visualization method to present the interpreted sewer condition information to decision-makers.

^② Despite the current state of the in-pipe GPR sewer inspections, (Noshahri, et al., 2019) compared it with many other inspection techniques on the types of defect that they can detect. The in-pipe GPR scored 10 (same as the conventional CCTV inspection method) in this competition, indicating that it has a great potential to be adapted for sewer condition assessment in the very near future.

^③ Be noted, the data processing and interpretation routine translates the raw inspection data into sewer condition information (e.g., presence, location, type, size, and severity of defects), whereas visualization methods visualize the interpreted sewer condition information in graphical forms and present it to decision-makers in an easy-to-understand way.

1.4. Research Questions

To tackle down the research problem step by step, the research objective is split into the following questions:

- 1) *What are users' data needs regarding the current CCTV-led sewer condition assessment?*
- 2) *As the complementary sewer inspection technology, what is the state of the in-pipe GPR method in terms of its data interpretation and visualization?*
- 3) *Which essential data processing procedures should be taken for interpreting raw in-pipe GPR inspection data into meaningful sewer condition information?*
- 4) *What are users' expectations of visualizing the sewer condition information interpreted from the in-pipe GPR inspection data?*
- 5) *Among all the available inspection data visualization methods and concepts, which is the most suitable one for visualizing the sewer condition information interpreted from the in-pipe GPR inspection data?*
- 6) *What is the feasibility of the final developed in-pipe GPR sewer inspection data visualization method?*

1.5. Outline

The remainder of this thesis is structured as follows:

Chapter 2 addresses the sources and uses of the involved information and data; introduces several specific research methods used in later chapters; and sets up the verification process for the main outcome of this thesis.

Chapter 3 first simulates in-pipe GPR sewer inspections to create dummy data to discuss and conclude its data processing and interpretation process, and saves a sample data as input for its final developed visualization method.

Chapter 4 first defines "data visualization" in sewer condition assessment and addresses the expected main outcome of this thesis. Secondly, it extracts criteria and design requirements from the users' expectations and system expectations for the development of the desired visualization method. Thirdly, it presents a literature review that explores the available inspection data visualization alternatives. Fourthly, it ranks the available alternatives through an MCDA and selects the optimal alternative for the final visualization method development. Finally, it modifies the selected alternative into the final visualization method and presents the graphical design of it.

Chapter 5 verifies the data visualization method developed from chapter 4 with the method set up in Chapter 2.

Chapter 6 summarizes the contribution of this thesis and makes recommendations for future research.

Chapter 7 answers the research questions and concludes the overall work of this thesis.

2. Methodology

In this chapter, section 2.1 addresses the sources and uses of the collected data and information in this thesis, and introduces the concepts and steps of several specific methods used in later chapters. After that, section 2.2 sets up the verification and validation for the main outcome of this thesis.

2.1. Data Collection Methods & Uses

There were both qualitative and quantitative data and information involved in this thesis research. The table below indicates the source, type and content of these data and information and particularly the purpose of use of them.

Table 2-1: The source and use of the data and information involved in this thesis.

Data sources	Data type	Data content	Purpose of use
Interviews	Qualitative	<ul style="list-style-type: none"> Users' interest in additional sewer condition data 	<ul style="list-style-type: none"> Define the research problem Additional sewer defect codes development
		<ul style="list-style-type: none"> Users' expectations of visualizing additional sewer condition data 	<ul style="list-style-type: none"> Identification of data visualization methods/concepts MCDAs criteria development Design requirement formulation
Simulated sewer inspections	Quantitative	<ul style="list-style-type: none"> In-pipe GPR simulation data 	<ul style="list-style-type: none"> Sewer inspection data processing and interpretation Interpreted as source data in the final developed data visualization method.
Literature review	Qualitative	<ul style="list-style-type: none"> Theories (e.g, definitions of various concepts) 	<ul style="list-style-type: none"> Supporting and smoothing the arguments and storyline of this thesis
		<ul style="list-style-type: none"> System expectations ("Abstract Tasks") on data visualization 	<ul style="list-style-type: none"> Identification of data visualization methods/concepts MCDAs criteria development Design requirement formulation
		<ul style="list-style-type: none"> Available inspection data visualization methods/concepts 	<ul style="list-style-type: none"> As alternatives in the MCDA

Besides the abovementioned data and information, there are several specific methods involved in the use of them, namely the Abstract Tasks, MCDA, and MoSCoW. These methods are all applied in section 4.2, the phase of finding the most suitable visualization alternative to visualize the additional sewer condition data collected by the in-pipe GPR method. Therefore, the following pages first introduce the overall methodology of section 4.2, then introduce each specific method in terms of the definition and steps and reasoning of applying them.

The workflow of section 4.2 consists of many research activities and methods (see Figure 2-1 below). Firstly, the users' expectations and system expectations on the desired visualization method were extracted from interviews and literature about the Abstract Tasks method (Ardito, et al., 2006; Shneiderman, 1996), then categorized by a series of descriptive aspects. By specifying these descriptive aspects and expectations, requirements for designing and assessing the desired visualization method were formulated and prioritized by the MoSCoW method (Mulder, 2017). Secondly, a literature review was conducted to explore the available inspection data visualization method

and concepts, whereas the descriptive aspects are used to describe and identify them. Thirdly, the descriptive aspects that can distinguish the alternatives the most are extracted and defined as criteria in the pre-selection and MCDA to select the most suitable alternative for the development of the desired visualization method.

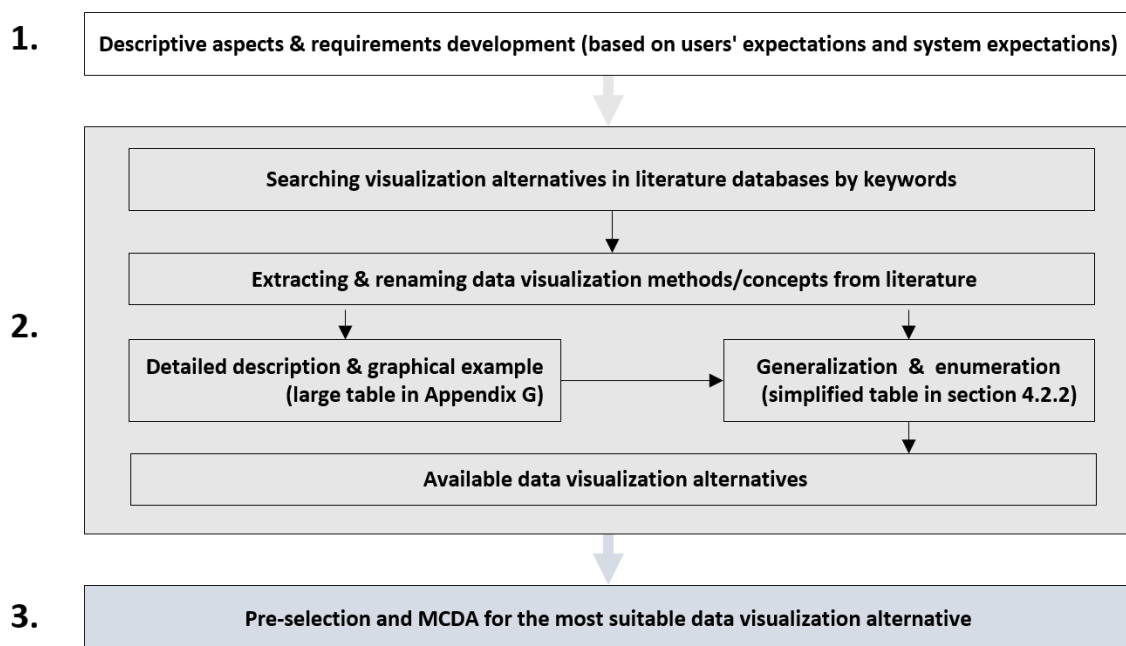


Figure 2-1: Workflow of finding the optimal data visualization alternative in section 4.2.

Abstract Tasks Method

The concept of “Abstract Tasks” is originally from the Abstract Tasks Inspection, which is a systematic usability evaluation method for information visualization systems (Ardito, et al., 2006). This method expresses specific actions that users wish to perform on the information visualization system as seven major abstract tasks **1). Overview** shows users an overview of the entire collection; **2). Zoom** allows users to zoom in/out on items of interest; **3). Filter** permits to filter out uninteresting items; **4). Details-on-demand** enables users to select an item or group to get details when needed; **5). Relate** shows relationships among items; **6). History** provides historical data records; **7). Extract** allows users to extract sub-collections and query parameters; see more of these abstract tasks in (Ardito, et al., 2006; Shneiderman, 1996).

Since the abstract tasks express the expected functions of the desired data visualization alternatives in a more systematic perspective, whereas the users’ expectations on the desired data visualization alternatives were elaborated rather fuzzy and incomprehensive. The abstract tasks were introduced as “system expectations” to enrich the users’ expectations. Together these expectations were used to develop the descriptive aspects for describing the found data visualization alternatives and systematically formulate specific requirements for designing and assessing the desired visualization method in section 4.2.1.

Worth to note, most of the abstract tasks are out of the scope of this thesis since they are about the actions that users wish to perform on an actual visualization system instead of the content that the visualization is ought to present for users to see. Out of this consideration, only the **overview**, **relate** and **history** abstract tasks were used in section 4.2.1.

MoSCoW

The MoSCoW method is a popular prioritization technique for managing requirements. The name of it has nothing in common with the capital of Russia, instead, it represents the importance of requirements that are categorized in groups of **Must-haves**, **Should-haves**, **Could-haves** and **Won't-haves** (Mulder, 2017).

This method was applied for prioritizing the design requirements formulated in Table 4-1 to ensure the final developed visualization methods to meet the requirements that are important for end-users. The priority of each requirement was partly determined by the users' and system expectations, which to some extent reflect the users' opinion on the importance of the requirements since they are formulated from these expectations. Moreover, the wide-used CCTV data visualization method was regarded as a standard for reference. By considering the visualization approach and elements used in this reference, the requirements that are directly related to the visualization process can be prioritized as **Must-haves** or **Should-haves**. On the other hand, the requirements that are less related to the visualization process but more about abstract considerations, such as financial and future proof concerns, were then prioritized as **Could-haves** and **Won't-haves**.

Multi-criteria Decision Analysis (MCDA)

The Multi-Criteria Decision Analysis (MCDA) is an analysis tool that evaluates multiple (conflicting) criteria as part of the decision-making process, most applicable to solving problems that are characterized as a choice among alternatives (Janse, 2018).

The MCDA was applied in section 4.2.3 to select the most suitable visualization alternative for in-pipe GPR sewer inspections among all the available visualization methods and concepts found in the literature. The reason for applying it is because trade-offs from multiple aspects were involved in this process (e.g., the users' and system expectations, characteristics of alternatives, design considerations, etc.). Hence a systematic method is needed to quantify the available options and make the selection transparently and quantitatively.

Six steps were followed to ensure the MCDA to be successfully executed, source from (Janse, 2018):

1) Define the objective

2) Define the criteria

In section 4.2.3 the criteria are selected from the descriptive aspects concluded from the users' and system expectations, but be noted that only the ones that distinguish available alternatives the most are selected.

3) Weight the criteria

In section 4.2.3, the criteria are weighted by comparing the criteria with each other, based on that, certain percentages are assigned to them as the weight coefficient (sum up to 100%).

4) List the options

5) Rate the options

Based on the classifications defined in section 4.2.3, scores (0-2) are given to each option on each criterion.

6) Calculate and select the most suitable option(s)

The scores for each criterion are multiplied with their weights, then summed up as the final score of each alternative on all criteria.

2.2. Verification Setup

This thesis plans to assess the final developed visualization methods through the verification and validation, which are two independent processes used for assessing if a product meets the predefined requirements (or specifications) and intended uses. In other words, the verification ensures “the product was built right” whereas the validation ensures “the built product is right” (Rajkumar, 2020).

More specifically, the verification process ensures the product was built according to the documented requirements (or design specifications), which means the final designed product should have met their specified requirements. On the other hand, the validation process ensures the product meets the users’ needs and the formulated requirements (or specifications) were correct in the first place (softwaretestingfundamentals, 2020).

In summary, the verification is about the realization of requirements (or specifications), which is more designer-oriented; whereas the validation is about the quality of the requirements and the actual performance of the final designed product, which is more user-oriented. Worth to note, because verification is guided by requirements, the requirements should be validated and approved first to prevent rework (Parker, 2011).

Hence, to validate the visualization method developed in this thesis, the quality of the formulated requirements shall first be evaluated by end-users of this visualization method (e.g., sewer asset managers) based on the criteria below, adapted from (Bahill, et al., 2005; Parker, 2011; Balci, 2004).

- **Requirements completeness:** all users’/system expectations shall be reflected in the developed requirements.
- **Requirements correctness/clearness:** the statement of requirements can only be interpreted one way, which means it needs to clarify the users’/system expectations accurately and be easily comprehended by all readers.
- **Requirements consistency:** the developed requirements should not conflict or overlap with each other.
- **Requirements priority:** the developed requirements should be ranked based on its importance of inclusion in the final product to ensure the features/elements that they reflected are necessary.

Further, to verify whether the final visualization method was designed accordingly and of high quality by ensuring the formulated requirements have been realized in the outcome, the criteria below is defined, adapted from (Yin, et al., 2020; Bahill, et al., 2005; Parker, 2011; Balci, 2004).

- **Requirements realization:** the formulated design requirements should be reasonably realized in the final developed visualization methods, e.g., the *must-haves* and *should-haves* requirements that reflected the major users’ and system expectations shall be particularly fulfilled.

Be noted, examples of visualizing the in-pipe GPR simulation data and the interpreted results with the developed visualization method shall be presented during the verification and validation. This can first provide a demonstration of the intended uses of the developed visualization method, moreover, show how it has addressed the predefined requirements in an easy-to-understand graphical form.

3. Simulating In-pipe GPR Data

To achieve the research objective of interpreting and visualizing the sewer inspection data collected by in-pipe GPR, the inspection data is first needed. Since this thesis research has no access to real in-pipe GPR inspections or experiments, the sewer inspection data from this new sewer inspection technology was acquired via computer simulations. Specifically, gprMax[®] is used to generate the raw sewer inspection data collected by in-pipe GPR.

3.1. Interpreting In-Pipe GPR Simulation Data

In this section, subsection 3.1.1 introduces the mechanism and general setups of the in-pipe GPR simulations, then subsection 3.1.2 explains two considerations that users might have before/during an in-pipe GPR inspection. Subsequently, subsection 3.1.3 analyzes the predefined quantifications of voids (see Appendix C), find out whether they can cause significant responses in the raw data display and how to extract sewer condition information out of it through certain data processing procedures. After that, subsection 3.1.4 summarizes the used data processing procedures into a standardized routine and produces post-processed radargrams with a sample simulation data.

3.1.1. Simulation Mechanism & Setup

The gprMax simulation mechanism in Figure 3-1 shows a pipe cross-section with a wall thickness of w . The in-pipe GPR transmitter (red dot), receiver (green dot) and coordinates of the cross-section are in a polar coordinate system (r, ϑ, z) , where r is the radius of the GPR from the pipe center (blue dot), ϑ denotes the rotation around the pipe center, and z is the long axis of the sewer pipe. The antenna separation a denotes the distance between the transmitter and receiver. A subsurface object is located at the common midpoint between the transmitter and receiver with a distance d to the outer sewer wall. As for one scan, the transmitter rotates 360° and the receiver follows based on the antenna separation (van Delft, 2019). When the antenna finishes one full circle (one single data point), the entire device moves along the z -axis to the next location in the sewer and repeats the scanning.

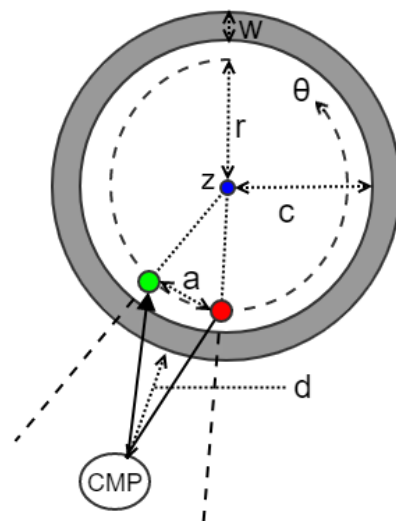


Figure 3-1: gprMax simulation mechanism.

For all in-pipe GPR simulations in this research, each of them executed a 120-trace scan to simulate the detection of the pipe external condition. The 120 traces were evenly distributed around the pipe's perimeter, each trace has a detecting range of 3° . The scans were simulated anticlockwisely and the starting point was 12 o'clock (regarding the pipe cross-section as a clock). The parameters below describe the basic setup of the simulations.

[®] Note the simulation software cannot model arbitrary subsurface environment in great detail, and the simulated result might be too optimistic in terms of noise and contrast since the assumed homogeneous materials can be contradictory to real materials (van Delft, 2019).

- The sewer simulated is an unreinforced concrete pipe (inner diameter 600mm, thickness 95mm).
- The antenna frequency used in the simulation is 10^9 Hz.
- The time window of the simulation is 10ns. This means only data of the first 10ns that the wave propagating the pipe wall and the soil is recorded, which will also be referred to as the “detecting range” in the later text.
- The clearance between the antenna and the sewer wall is 0mm (r equals to the pipe radius 300mm) to eliminate the attenuation caused by the gap between the antenna and the pipe wall.
- The antenna separation (between the transmitter and receiver) is 20mm.

On the other hand, electromagnetic properties (also called “constitutive parameters” in gprMax) of the used materials are needed in the simulation, namely the relative permittivity, conductivity, relative permeability, and magnetic loss. The latter two are always set to 1 and 0 for non-conductors like sand and concrete in gprMax. The properties of the used material can be found in the table below, note the velocity can be used to estimate the location and size of the objects. Be noted the electromagnetic property values listed below are from theories and could be different from the realistic situation.

Table 3-1: Material properties, adopted from (Reynolds, 2011).

Material	Relative permittivity, ϵ_r	Conductivity, σ (s/m)	Velocity (mm/ns)
Air	1	0	300
Concrete	4-30 (took 4.5)	0.001 – 0.1 (took 0.01)	55-250
Sand in NL	3-6 (took 3)	0.01 (the sand in NL has a conductivity of the coastal sand, so 0.01 is taken)	122-173
Clay (average)	2-40 (took 8)	0.002 – 1 (took 0.03)	134 - 212
Average (soil)	16	0.005	75
Peat (freshwater)	57-80 (took 60)	≤ 0.04 (took 0.01)	33-40
Water (fresh)	81	0.0005	33
Granite (average)	5-8 (took 6)	$10^{-8} - 10^{-6}$ (took 10^{-5})	106-120

Other than the abovementioned simulation setups and material properties, it is also important to know the GPR detecting resolution under such a simulation environment. The GPR detecting resolution includes the vertical and horizontal resolutions, which together determine the minimum object size that could be detected in the survey. The vertical resolution (VR) is equal to one-quarter of the wavelength λ while λ is equal to the wave velocity $V_{material}$ divided to the GPR operating frequency f . On the other hand, the horizontal resolution (HR) is usually considered equal to the width (or defined as the radius r) of the first Fresnel zone (Reynolds, 2011), hence, HR is equal to two times the radius of the first Fresnel zone. As defined by the equations below, source from (Reynolds, 2011).

$$VR = \frac{\lambda}{4} = \frac{v_{material}}{4f} = \frac{299.8/\sqrt{3}}{4*1} = 43.2\text{mm} \quad (3-1)$$

Where λ is the wavelength, in mm.

$v_{material}$ is the wave velocity determined by $\frac{c}{\sqrt{\epsilon_{material}}}$, in which c is the wave velocity in a vacuum (299.8 mm/ns), $\epsilon_{material}$ is the relative permittivity of the soil (since sand is used, 3 is taken for the calculation). f is the GPR operating frequency, set as 10^9 Hz in the simulations, converted to 1 GHz in this calculation.

$$HR = 2r = 2 * \left[\left(\frac{\lambda_c}{4} \right)^2 + \frac{\lambda_c * z}{2} \right]^{0.5} \approx 2 * \left(\frac{\lambda_c * z}{2} \right)^{0.5} = 2 * \left(\frac{1 * (0 + 95 + 300)}{2} \right)^{0.5} = 28.1 \text{mm} \quad (3-2)$$

Where r is the radius of the first Fresnel zone.

λ_c is the center-frequency wavelength, regarded as equal to λ mentioned in equation (3-1).

z is the largest distance from the transmitter to the point of reflection (including the gap between the transmitter and the pipe wall (0mm), the pipe wall thickness w (95mm), and the largest distance d (300mm) from the pipe outer wall to the target object).

As can see, the in-pipe GPR inspection resolution under the designed simulation environment is 43.2mm (take the larger one from VR and HR)⁵. Worth to note, the 120 traces defined for each scanning also influence the inspection resolution, calculated as $\pi * 600 / 120 = 15.7 \text{mm}$ (600 is the pipe diameter in mm), which is smaller than both the VR and HR . This means to ensure the target object is detectable to the in-pipe GPR, it needs to have a radius larger than 43.2mm (assuming it is a sphere). Hence, while designing the simulation scenarios, the resolution should be considered, more specifically, it is suggested to set the target object with a size a few times bigger than the resolution, which guarantees it forms reflections measurable by the in-pipe GPR.

3.1.2. Considerations before the In-pipe GPR Inspection

This subsection runs simulations to respond to two potential considerations from the user: **1)** How is the soil type influencing the detected result? **2)** How to determine if the detected object is a void or not?.

Soil Influences

To find out how different types of soil influence the in-pipe GPR inspection result on the radargram, simulations of detecting the same object in four typical soil types were run. Figure 3-2 below presents the simulation scenarios, a 600mm (inner diameter) unreinforced pipe with a thickness of 95mm, the target object is an air-filled void (radius of 100mm) located at 6 o'clock, and 150mm away from the pipe. Three of the soil types are commonly seen in the Netherlands, namely sand, clay and peat, the last one is the average soil (electromagnetic properties of them can be found in Table 3-1).

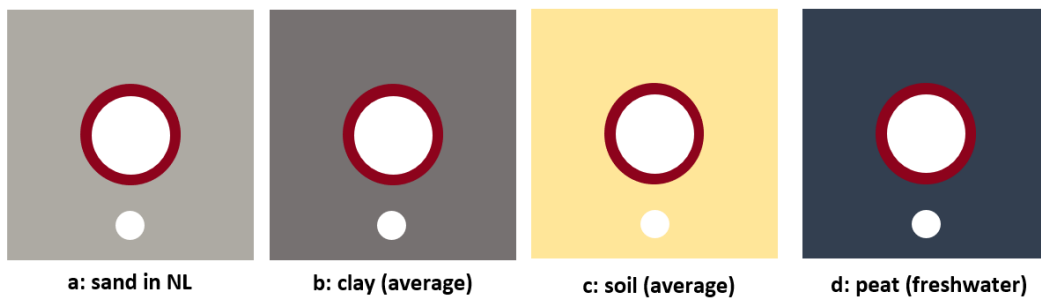


Figure 3-2: In-pipe GPR simulation scenarios for the four common soil types.

⁵ Note the VR and HR equations are originally used to calculate the resolution of planar GPR inspections. It is assumed the same principle also applies to the cylindrical in-pipe GPR inspection, hence the curvature of the pipe's cylindrical topology is neglected in the resolution calculation.

Figure 3-3 below presents the simulation results with minor contrast adjustment (to make the reflections more visible). The Y-axis in the radargram represents the TWTT (two-way travel time) of the reflected wave while X-axis represents the number of traces simulated around the pipe perimeter. On the other hand, the X-axis (vertical) in the A-scan represents the wave transit time while Y-axis (horizontal) represents the wave amplitude. Note the XY-axis representation of the radargram and A-scan remain the same for later simulation results.

As seen in Figure 3-3, the void reflections are shown as hyperbolas that are captured at different TWTTs[®]. From the sand radargram to the clay radargram and the average soil radargram, it can be seen clearly that the receiver took more time to receive the wave reflected by the void. Besides that, the hyperbolas from these radargrams show a minor change in shape (i.e., the hyperbola gets slightly narrower from the sand radargram to the clay radargram and the average soil radargram). These two major findings confirm that soil types indeed affect the in-pipe GPR measurements significantly even if all features of the object remain the same.

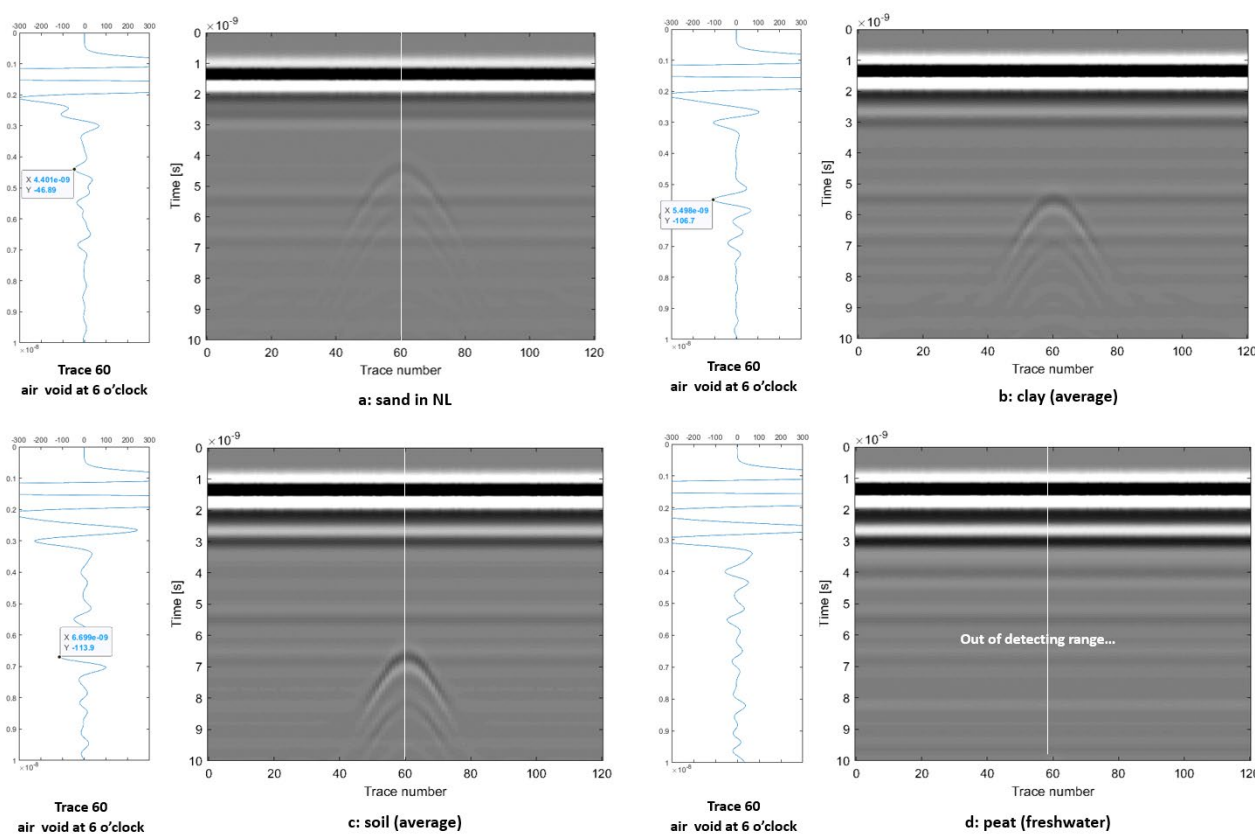


Figure 3-3: In-pipe GPR simulation results of detecting an air void in different soil types, with A-scans extracted from the center of the void.

The explanation is, the different relative permittivity and electrical conductivity of these soil types (see Table 3-1) influences the GPR operation and performance (Igel, 2008; Rhebergen, et al., 2004). More specifically, the different relative permittivity results in a different wave traveling velocities in the soil (see equation (3-1) and Table 3-1), which is why the reflections were captured at different TWTTs in Figure 3-3. The same applies to the hyperbolas' shape change. When the wave spreads faster, it reaches the target object earlier (for both peak and non-peak points), which results in a border hyperbola in the radargram and vice versa (Bigman, 2017).

[®] There is no reflection shown in the peat radargram because the wave velocity in peat is very slow, which took more than 10ns for the receiver to receive the reflection. This is out of the detecting range of this simulation.

On the other hand, the electrical conductivity of soil influences the wave attenuation. The GPR wave attenuation is proportional to the material's conductivity, which leads to high attenuation in materials with high electrical conductivity (Ingelise, 2006). This means the wave attenuates the quickest in clay (conductivity 0.03), then sand (conductivity 0.005) and average soil (conductivity 0.005), see Table 3-1. Unfortunately, this cannot be directly observed in the simulation result in this thesis. But the worst consequence of this early wave attenuation can be deduced. If the soil is highly conductive, the wave might attenuate to an extent that it is unable to reach the target object or get reflected and received by the receiver. In this case, there will be no reflection of the target object showing on the radargram at all, which misleads to an interpretation that there was nothing in the subsurface.

In summary, in-pipe GPR measurements can be affected by the soil types in several ways: **1).** it can cause different TWTTs of the expected reflection; **2).** it influences the shape of the hyperbola; and in worse cases, **3).** it might lead to false-negative interpretation (a defect is not observed although it is there). To eliminate such effects, it is strongly recommended to obtain sufficient knowledge of the local soil before starting the in-pipe GPR survey, based on that set up the configuration and parameters of the equipment properly.

Identifying the Detected Object

As known, GPR surveys are only able to reveal the interface between layers with different electromagnetic impedances, which makes it difficult to identify the detected object (Hong, et al., 2017). The same applies to inspect the sewer's exterior environment from inside, the detected objects may be adjacent utilities (e.g., other pipes or cables), rocks, or water/air-filled voids. However, in practice, the sewer manager needs to know what is actually found behind the sewer wall since voids impose more threats than other objects. To find answers to that, an in-pipe GPR simulation of detecting three different buried objects was run. The simulation scenario is presented at the right. The unreinforced 600mm concrete pipe is buried in sand, with a thickness of 95mm. The objects^⑦ outside the pipe are an air-filled void at 9 o'clock, a water-filled void at 6 o'clock, and a granite at 3 o'clock, which all have a radius of 100mm.

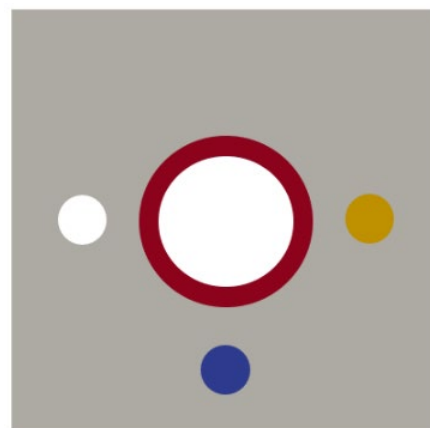


Figure 3-4: In-pipe GPR simulation scenario for different objects.

Figure 3-5 presents three pairs of hyperbolas, representing the air void, water void, and granite respectively. Besides the position difference, the other obvious difference is the distance between the upper hyperbola and lower hyperbola, representing the TWTT difference between the moment the wave was reflected by the top of the void and the bottom of the void^⑧. The reason for this distance difference is the same as introduced in the soil influences simulation, the wave travels in mediums with various velocities, the first pair of hyperbolas has the shortest distance between each other since the wave travels the fastest in the air (see Table 3-1).

^⑦ The reason that adjacent utilities are not included is they usually result in continuous responses and the sewer manager can acquire their presence through documents like KLIC melding, which means the adjacent utilities are often expected in the inspection results.

^⑧ The reason that the lower hyperbola of the water void is missing is as explained in ^⑥. There is a strange hyperbola at around 8ns, but its TWTT and shape are not as expected as the lower hyperbola of the water void. There is no exact explanation for this, thus it is regarded as a system error.

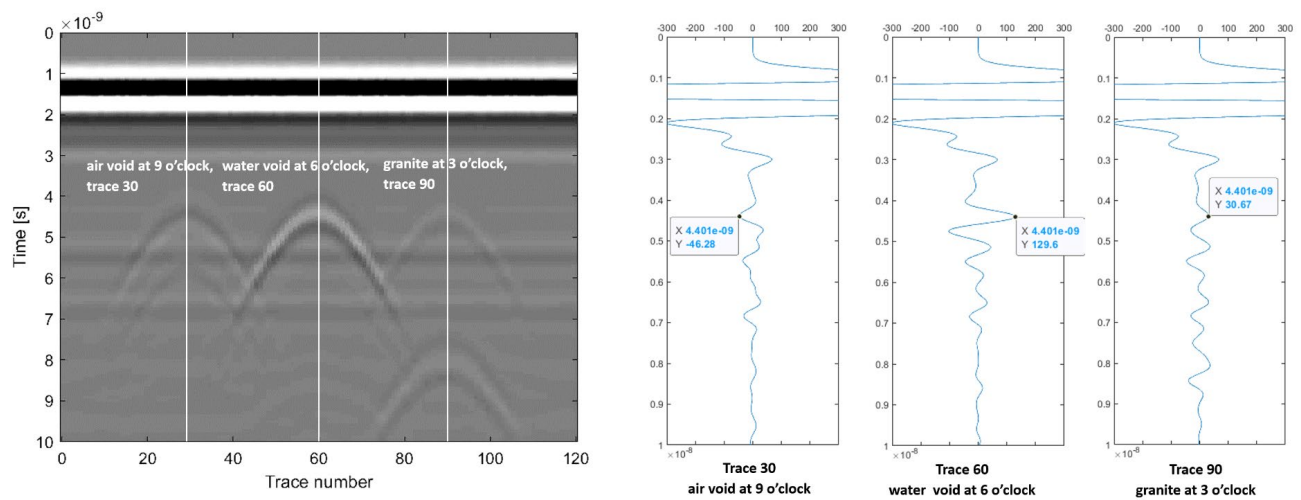


Figure 3-5: In-pipe GPR simulation results of detecting different objects, right: radargram with contrast adjusted; left: A-scans extracted from the center of each detected object.

The above analysis has confirmed that objects of the same size and different materials indeed result in significantly different responses on the radargram, but how to identify the object (e.g., material) based on the information presented in the radargram and A-scans still remains as a question. There are many studies on buried object classification using GPR, for instance, the methods of post-processing the received reflected signals to estimate the electrical properties of the object reviewed in (Li, et al., 2012) and many other buried object identification methods reviewed in (Yoldemir, et al., 2019). Since this thesis focuses on finding the air-filled voids that impose structural threats to the sewer pipe, the method of examining the polarity change in the reflections is discussed[®].

By comparing the reflection polarity with the initial polarity of the transmitted signal, valuable information can be obtained to identify the buried object. The theory behind this is, the polarity of the transmitted wave changes while reflecting on the interface between two mediums, which is the so-called “reflection polarity”. It is a function of the relative permittivity between the two measured mediums, determined by the reflection coefficient R , source from (Gehrig, et al., 2004; Hwang, et al., 2019; van Delft, 2019):

$$R = \frac{\sqrt{\varepsilon_2} - \sqrt{\varepsilon_1}}{\sqrt{\varepsilon_2} + \sqrt{\varepsilon_1}} \quad (3-3)$$

where ε_1 is the relative permittivity of medium one.

ε_2 is the relative permittivity of medium two.

The reflection coefficient has values between $-1 < R < 1$, the magnitude of it determines how much of the transmitted wave is reflected, the sign of it determines whether the reflected wave experiences a reverse in polarity. When the wave propagates from lower permittivity medium to high permittivity medium ($R > 0$, $\varepsilon_2 > \varepsilon_1$), the reflection polarity usually shows a positive amplitude precedes a negative amplitude (if the first strong signal is positive). However, when the wave propagates from a high permittivity medium to a lower permittivity medium ($R < 0$, $\varepsilon_2 < \varepsilon_1$), the reflection polarity shows a reverse, which is usually expressed as a negative amplitude followed by a positive amplitude if the first strong signal is positive (GeoSci, 2019; Gehrig, et al., 2004).

[®] Worth to note, water voids also impose structural threats to the sewer pipe, it is suggested to apply other methods to determine its presence.

Hence the “reversed polarity” then becomes the key to find air voids in the GPR inspections, because except the air-filled voids, there are rarely other materials with a relative permittivity lower than the soil in the subsurface. Be noted this method is not completely applicable in practice (e.g., the high-water content of the soil might increase its relative permittivity), but it is sufficient for the research purpose of this thesis. By calculating R_{air} (-0.26), R_{water} (0.68), and R_{granite} (0.17), this theory is confirmed applicable. More importantly, the A-scans extracted right above the center of the detected objects in Figure 3-5, indicate that indeed only the air void caused a reversed polarity at around 4.4ns compared to the water void and the granite.

In summary, while using GPR to investigate the presence of ground voids under ideal situation (i.e., the soil is homogeneous and its relative permittivity is not very high), a reversed polarity compared to the polarity of the first strong signal, is very possibly indicating the presence of an air void.

3.1.3. Quantifications Analysis of Void

To simulate the in-pipe GPR responses for void detection in the pipe’s exterior environment, the circumferential position, distance to the pipe and the size of the void are considered (see Appendix C). Three scenarios are designed to find out if they can cause significant responses on the radargram and how to obtain meaningful quantitative information about them.

- **Voids at different circumferential positions.** Keep the distance 150mm and the void radius 100 mm, change the circumferential position of the void from 12 o'clock to 9 o'clock, and 6 o'clock, see Figure 3-6a.
- **Voids at different distances.** Keep the void at 9 o'clock and the void radius 100 mm, simulate the detection as the distance is 300mm, 150 and 0 mm from the pipe outer surface to the void surface, see Figure 3-6b.
- **Voids with different sizes.** Keep the void at 6 o'clock and distance 150mm, simulate the detection as the void has a radius of 150mm, 50mm and 100 mm, see Figure 3-6c.

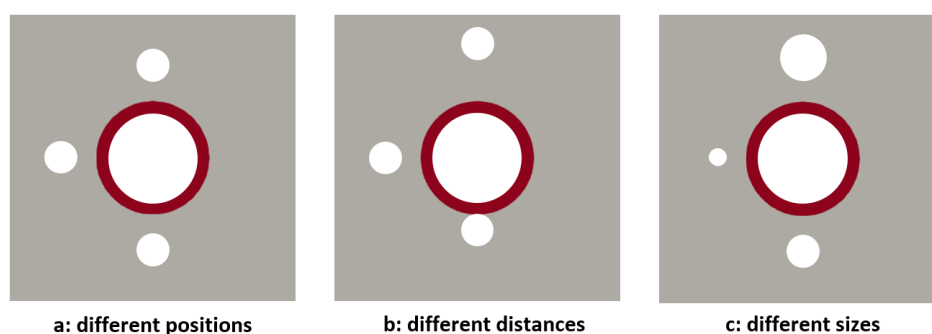


Figure 3-6: In-pipe GPR simulation scenarios for different quantifications of the void.

The aim of the simulations in this subsection is to find out if the pre-defined three quantifications of the void, namely its circumferential position, distance to the pipe as well as the void size, can be interpreted from the in-pipe GPR radargram and whether they can result in a significant difference while changing. For each quantification, three scenarios are set (they were integrated into one simulation for more effective simulation and easier comparison), the simulation results are presented and discussed in the following pages.

Different Circumferential Positions

In this simulation, air voids are set to have a radius of 100mm, located 150mm away from the pipe wall, distributed at 12 o'clock, 9 o'clock and 6 o'clock around the pipe. As seen in Figure 3-7, three pairs of hyperbolas are presented in the radargram. Because the simulation starts at 12 o'clock and the antenna moves around the pipe perimeter anticlockwisely, the peak of the first air void hyperbola is shown at the beginning of the radargram (the other half is at the end of the radargram). The second pair of hyperbolas is shown at trace 30 (9 o'clock), which can be translated as $30 \times 3^\circ = 90^\circ$, moving the antenna from 12 o'clock anticlockwisely by 90° . The same applies to the air void hyperbolas at 6 o'clock (trace 60, the antenna rotated by 180° from 12 o'clock).

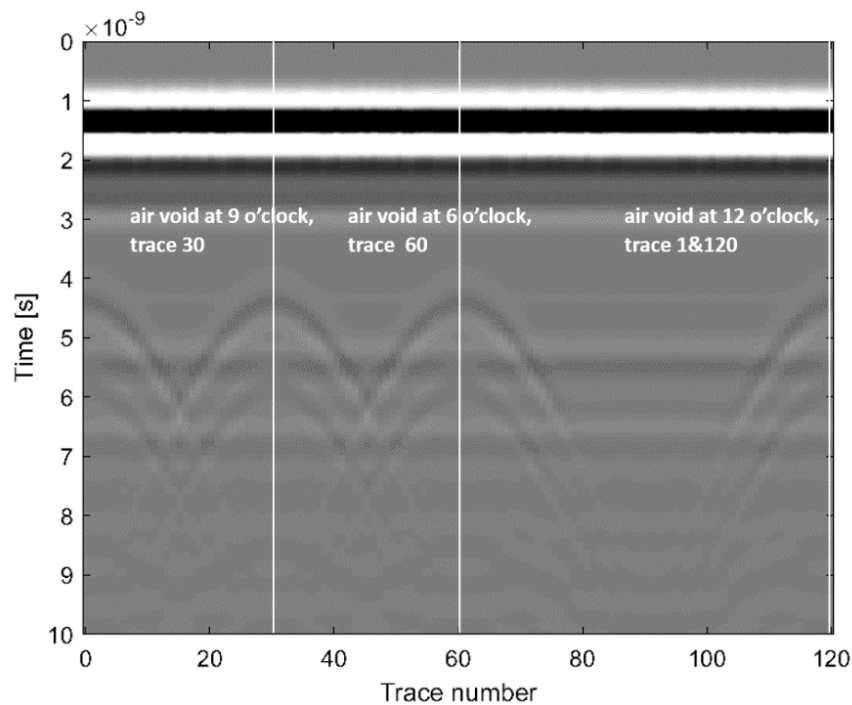


Figure 3-7: Simulation results of detecting voids at different circumferential positions with in-pipe GPR.

After careful comparison, it is found the three pairs of hyperbolas caused by voids at different circumferential positions are identical in both size and shape. The only difference among them is at X-axis, which represents their corresponding circumferential positions, which is expected and their exact circumferential position can be calculated through a simple conversion as mentioned in the paragraph above.

In summary, it can be concluded that voids at different circumferential positions outside the pipe can be easily recognized in the radargram and the information of their circumferential position can be easily calculated and denoted by the clock directions (regarding the pipe cross-section as a clock).

Different Distances to the Pipe

Besides the circumferential position, further information needed to answer the question “where is the void” is its longitudinal location along the pipe length (represented by the z-axis mentioned at the beginning of section 3.1) and the distance between the pipe and the void. The longitudinal location can be obtained directly through the distance measuring system in the in-pipe GPR device as it moves along the pipe. However, the distance (D) between the void and the pipe needs to be interpreted from the radargram, which refers to the “depth” of an object in normal GPR applications, often calculated from the equation below (Reynolds, 2011):

$$D = v_{material} * \frac{\Delta t}{2} = \frac{c}{\sqrt{\epsilon_{material}}} * \frac{\Delta t}{2} \tag{3-4}$$

where $v_{material}$ (mm/ns) is the wave velocity in the soil,

c is the velocity of the electromagnetic wave in a vacuum (299.8 mm/ns).

Δt is the TWTT of the electromagnetic wave, unit in ns.

$\epsilon_{material}$ is the relative permittivity of the soil material, take 3 since sand is used in the in-pipe GPR simulations of the void’s quantifications.

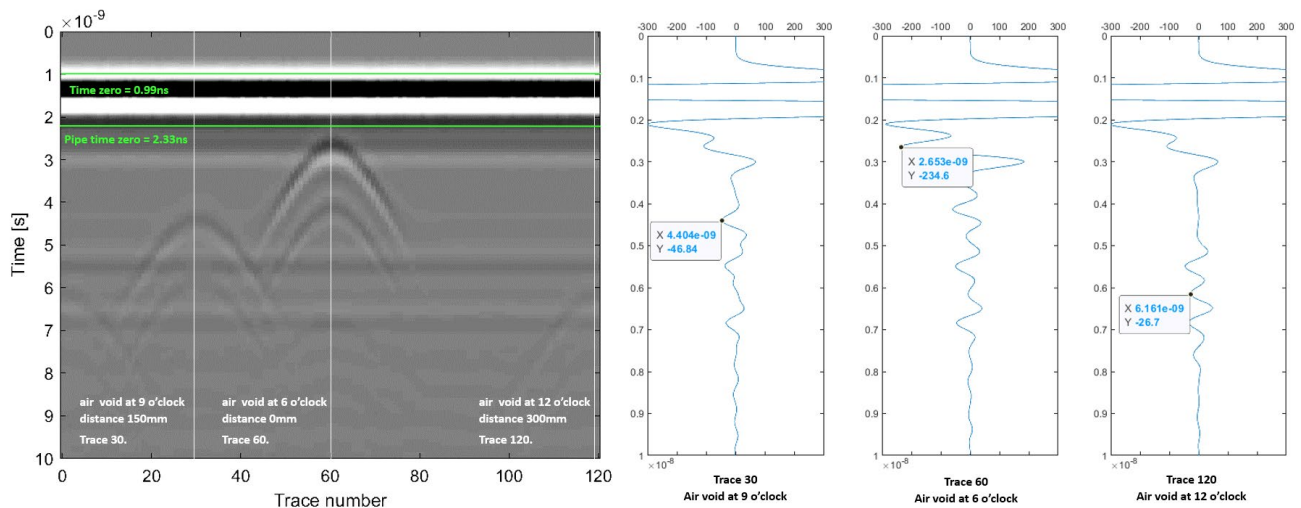


Figure 3-8: Simulation results of detecting voids at different distances with in-pipe GPR (left: radargram with minor contrast adjustment, right: A-scans extracted from the center of each object).

In this simulation, the voids have the same radius 100mm but are located at different distances to the pipe (see the marks in the left radargram in Figure 3-8). As mentioned, the distance calculation of between the pipe and the void is similar to the depth calculation in surface GPR applications, the general way is to apply equation (3-4) and the TZC (Time Zero Correction, see more explanation on page 26). But this equation is not entirely suitable for in-pipe GPR since the wave has to first penetrate the concrete sewer wall before entering the soil, the velocity difference in these two materials will cause a relatively large system error in the distance estimation. Hence, the more suitable method is to consider only the TWTT that the wave is traveling within the soil, which means to set a new time zero at the pipe wall–soil interface, or the so-called “Pipe Time Zero” in this thesis. Theoretically, the pipe time zero equals to TZC plus the TWTT that the wave travels within the pipe wall, calculated as:

$$\text{Pipe Time Zero} = \text{TZC} + \text{TWTT}_{\text{pipe wall}} = 0.99 + \frac{95 * 2}{299.8/(\sqrt{4.5})} = 2.33\text{ns} \quad (3-5)$$

Where 0.99 is the TZC in ns, obtained from MATLAB data processing, see Appendix E.

95mm is the pipe wall thickness, it is multiplied by 2 since the wave travels two ways.

299.8mm/ns is the electromagnetic wave velocity in a vacuum.

4.5 is the relative permeability of concrete.

As also calculated from equation (3-3), the wave reflection coefficient at the pipe wall–soil interface equals to $\frac{\sqrt{3}-\sqrt{4.5}}{\sqrt{3}+\sqrt{4.5}} = -0.1$ (3 and 4.5 are the relative permittivity of concrete and sand respectively). This means the reflection caused by the pipe wall–soil interface is supposed to show a reversed polarity in the A-scans, which can be seen in Figure 3-8. With all three traces in Figure 3-8 showing a reversed polarity at around 2.3ns and the calculation confirming the Pipe Time Zero value of 2.33ns, the validity of the 2.33ns Pipe Time Zero is confirmed. Hence calculations were made to estimate the distance between the pipe and the void, based on equation (3-4) and the Pipe Time Zero. The calculated results are listed below, ranging from the nearest to the furthest:

6 o'clock: $D = \frac{299.8*(2.65-2.33)}{2\sqrt{3}} = 27.7\text{mm}$. the result shows an error of 27.7mm.

9 o'clock: $D = \frac{299.8*(4.4-2.33)}{2\sqrt{3}} = 179.1\text{mm}$. the result shows an error of 29.1mm.

12 o'clock: $D = \frac{299.8*(6.16-2.33)}{2\sqrt{3}} = 331.5\text{mm}$. the result shows an error of 31.5mm.

As seen, the 2.33ns Pipe Time Zero shows an offset around 0.3ns compared to the 2.65ns TWTT of the 6 o'clock void, which is located at exactly the pipe wall-soil interface. Moreover, this offset causes a relatively stable system error (ranges from 27.7 to 31.5mm) in the distance calculation. It is assumed that the offset was caused by the pipe's curvature, the antenna separation as well as the nonvertical wave reflection, together they extended the wave traveling path and consequently increased the TWTT. In this case, this offset is inevitable since the void distance estimation in this thesis neglected these factors for calculation convenience. However, the resulted system error (30mm) is smaller than the pre-defined resolution (43.2mm), which means the error will not impose a significant influence on the detecting result. And if there is a strict requirement on the measurements' accuracy, a minus 30mm correction can be easily made to meet this requirement.

Overall, it can be concluded that voids located at different distances to the pipe can result in significant differences on the radargram (in the TWTT). To estimate the void's distance to the pipe, equation (3-4) and TZC can be used directly but it does not separate the concrete pipe wall from the calculation. Thus it is suggested to use the Pipe Time Zero for more accurate and effective distance estimation (see more about the Time Zero and Pipe Time Zero on page 26).

Different sizes

The void size is another critical quantification for determining its severity, usually refers to its longitudinal length, circumferential width, and thickness (since it is often in an abnormality shape). It is not possible to calculate the void's longitudinal length since the longitudinal movement of the sewer inspection was not considered in the simulation. The proper way to determine the longitudinal length of a void is to find continuous responses in radargrams collected from parallel and closely-spaced sections along the pipe's long axis, calculate the difference of the finishing point and the starting point of the void (but this is out of the scope of this thesis). On the other hand, because the void in the simulation is defined as a sphere, the circumferential width and thickness (actually also the longitudinal length but it is not considered in the later calculation) of the void are then equal to its diameter so when saying void size in the later texts, it refers to the diameter of the void.

Many studies are working on estimating the size of the buried object from the GPR inspection results, such as the curve-fitting procedure in (Shihab, et al., 2005), Gaussian processes regression in (Pasolli, et al., 2009), the ones discussed in (Dolgiy, et al., 2006) and many more. But these are all software-level applications, which require extracting as many data points from the radargram as possible. It is rather complicated and impractical to apply them here, after all, the purpose of this subsection is to reveal the possibility to obtain the void size information. It is ideal to keep the method simple and straightforward. Hence a novel method is introduced in this thesis, which is, the void diameter d is equal to the wave velocity in the air (filled in the void) multiply half of the time that the wave has traveled in the void, defined as the equation below:

$$d = V_{air} * \frac{\Delta t}{2} = V_{air} * \frac{\Delta t_{lower} - \Delta t_{upper}}{2} = 150 * (\Delta t_{lower} - \Delta t_{upper}) \quad (3-6)$$

where V_{air} is the wave traveling velocity in air, 300mm/ns (see Table 3-1).

Δt is the TWTT difference between the upper and lower hyperbolas, unit in ns.

Δt_{lower} is the TWTT of the lower hyperbola, unit in ns.

Δt_{upper} is the TWTT of the upper hyperbola, unit in ns.

Email conversations with a GPR professional were made to consult the feasibility of applying this novel method in this thesis. The GPR professional indicated that there were indeed discussions about this method in the GPR inspection industry before, but it is not recommended for practical uses in surface GPR inspections because there is a high level of variability in the responses of the surface GPR inspection results, e.g., the lower hyperbola caused by the bottom of the target object is often not visible in surface GPR inspection results[®].

However, since both the upper and lower hyperbolas of the target are visible in the simulated results, the novel method is applicable (and also suggested by the GPR professional). By filling the TWTTs read from the radargram and A-scans, calculations based on the novel method were made to estimate the diameter of the voids.

[®] The targets in surface GPR inspections are often metallic objects with a high value of relative permittivity (e.g., cables, metal/reinforced pipes or other utilities). The consequence of this is, majority of the wave might be reflected while entering the top of the target object, which leaves insufficient energy for the reflection of the bottom of the object.

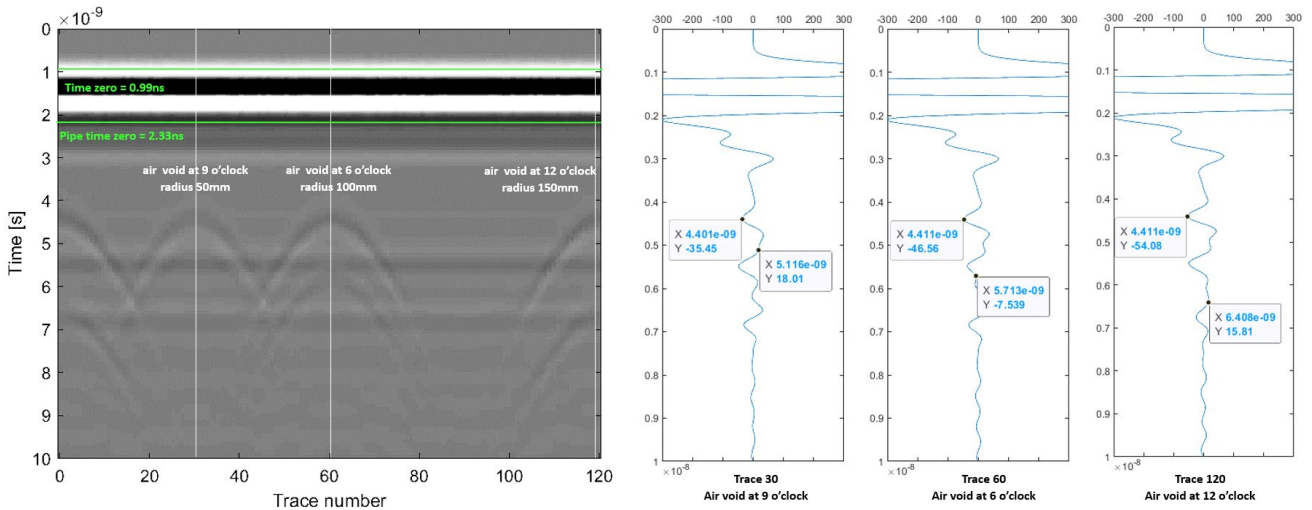


Figure 3-9: Simulation result of detecting voids with different radius with reflection TWTT marked.

$d_{9\text{ o'clock}} = 150 * (5.11 - 4.4) = 106.5\text{mm}$, the pre-defined diameter is 100mm, the error is +6.5mm.

$d_{6\text{ o'clock}} = 150 * (5.71 - 4.41) = 195\text{mm}$, the pre-defined diameter is 200mm, the error is -5mm.

$d_{12\text{ o'clock}} = 150 * (6.4 - 4.41) = 298.5$, the pre-defined is diameter is 300mm, the error is -1.5mm.

As seen from the calculated results, the proposed novel method is very stable in estimating the target's size. When the void size increases, the result seems more prone to the exact void size (error ranges from -1.5mm to +6.5mm).

But there is a difficulty while applying this method, which is about determining the TWTT of the lower hyperbola. As known, the lower hyperbola represents the interface between the air in the void and the soil ($\epsilon_{\text{soil}} > \epsilon_{\text{air}}$, the wave is propagating from lower permittivity medium to high permittivity medium), which means this reflection will not cause a reversed polarity. This makes it inconvenient to find the corresponding peak in the A-scans. Also, the noises generated by the system (e.g., reverberation patterns caused by the opposite pipe wall) might mask the target peak in the A-scans. The way used to determine the TWTT readings of the lower hyperbolas in the above calculation is to closely compare the radargram and the corresponding A-scans, find the most matching TWTT value for the lower hyperbola. It is suggested to develop an algorithm for this purpose if this method is used in practices.

In summary, under the precondition that both the upper and lower hyperbolas of the target object are presented clearly, the novel method of using the TWTT difference between the upper and lower hyperbolas and the wave velocity in the air to estimate the void size is proved accurate and effective. Hence it is recommended to carry out more numerical experiments and calculations to testify the feasibility of this method in a realistic situation since it is indeed a promising method for the development of in-pipe GPR devices.

3.1.4. Standardized In-pipe GPR Data processing & Interpretation Routine

The previous subsections applied certain data processing procedures and techniques for the in-pipe GPR inspection data interpretation process. The aim of this subsection is then to conclude the essential data processing procedures and use a sample inspection data to go through these procedures, finally produce two types of post-processed radargrams as the source data in the developed visualization alternative. The simulation scenario and the generated raw radargram of the sample are presented at right.

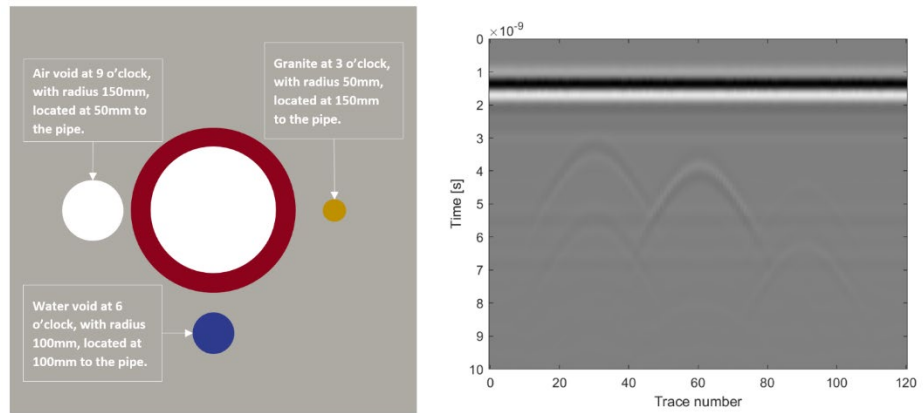


Figure 3-10: Sample data for interpretation and visualization.

By concluding the basic GPR data processing procedures from literature (Cassidy, et al., 2009; Benedetto, et al., 2015) and online tutorials (Bigman, 2017), the flowchart below is proposed as a comprehensive and standardized data processing routine for the interpretation of in-pipe GPR radargrams.

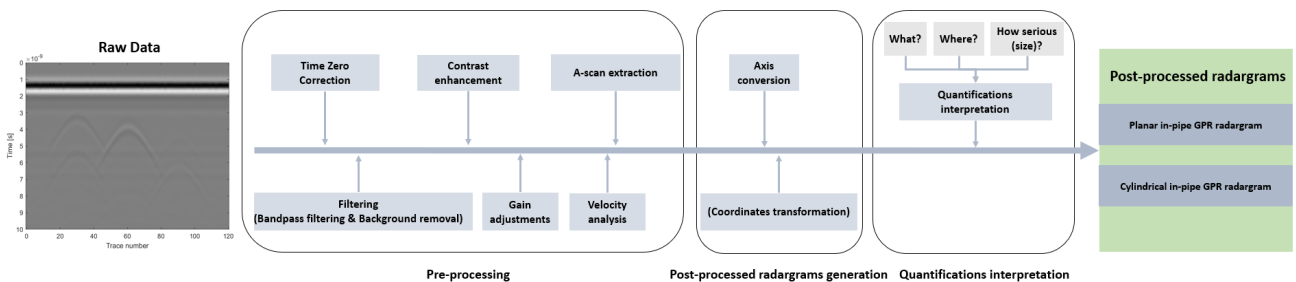


Figure 3-11: Flowchart of the standardized in-pipe GPR radargram data processing and interpretation process.

In general, the in-pipe GPR data processing and interpretation can be divided as the steps below:

- **Pre-processing** improves the quality of raw data through “filtering”, “gain adjustment” and “contrast adjustment”. It also sets up proper parameters for later processing steps through “velocity analysis” and “Time Zero Correction (or Pipe Time Zero Correction)”, see page 26. Moreover, the “A-scan extraction” is performed to extract A-scans of the region of interest (see page 27).
- **Post-processed radargrams Generation** converts the original axes of raw data into clock directions VS. distance, which generates the planar post-processed radargram (see page 28). Moreover, the “coordinates transformation” can be executed to generate the cylindrical post-processed radargram (page 28).
- **Quantifications interpretation** analyzes the hyperbolas in the post-processed radargram and determines the presence and location of the detected object. Moreover, by examining the wave’s polarity changes in the A-scans extracted from the regions of interest, the air-filled void can be identified. Particularly, for an air-filled void, its vertical size can be estimated through its upper and lower hyperbolas (see page 23).

Be noted the GPR data processing and interpretation process is very selective and depends a lot on the quality of raw radargram, usually not all processing procedures are needed to process and interpret one single GPR radargram.

The procedures executed and explained in this subsection for the sample are the ones on the top of the above flowchart plus the “coordinates transformation”. Worth to note, the “filtering” and “gain adjustment” data processing procedures were not applied and discussed in this thesis is that the simulated data is in very good quality. Moreover, the “velocity analysis” is not applied and discussed either because the wave velocity can be directly obtained from Table 3-1 or calculated from the simulation setups based on equation (3-1).

Time Zero Correction (TZC)

Time Zero Correction is often the first step of GPR data processing, which brings up the first reflection (usually caused by ground surface) to zero and allows the operator to accurately measure the depth of the target. This is because there is usually a gap between the antenna and the ground surface that impairs the shallow depth measurements of the target object. There are multiple ways to relocate the time zero, such as correcting it to the first break position, the first negative peak and the zero amplitude point, and more (Pleijssier, 2019; Yelf, 2004).

The method used in this thesis is setting the time zero to the first positive peak of the wave, which is the moment the emitted wave entering the pipe wall (since the gap between the antenna and the pipe wall is set as 0 in the simulations). The position of the first positive peak is different in each trace, that is why TZC calculates the position of the first positive peak for each trace (see Figure 3-12 left). The final time zero of the radargram is equal to the mean of first positive peak positions of all the traces (Pleijssier, 2019; Yelf, 2004). See the middle radargram in Figure 3-12, the Time Zero is plotted at 0.99ns by a green intersecting line. The MATLAB function and codes used to calculate the Time Zero can be seen in Appendix E.

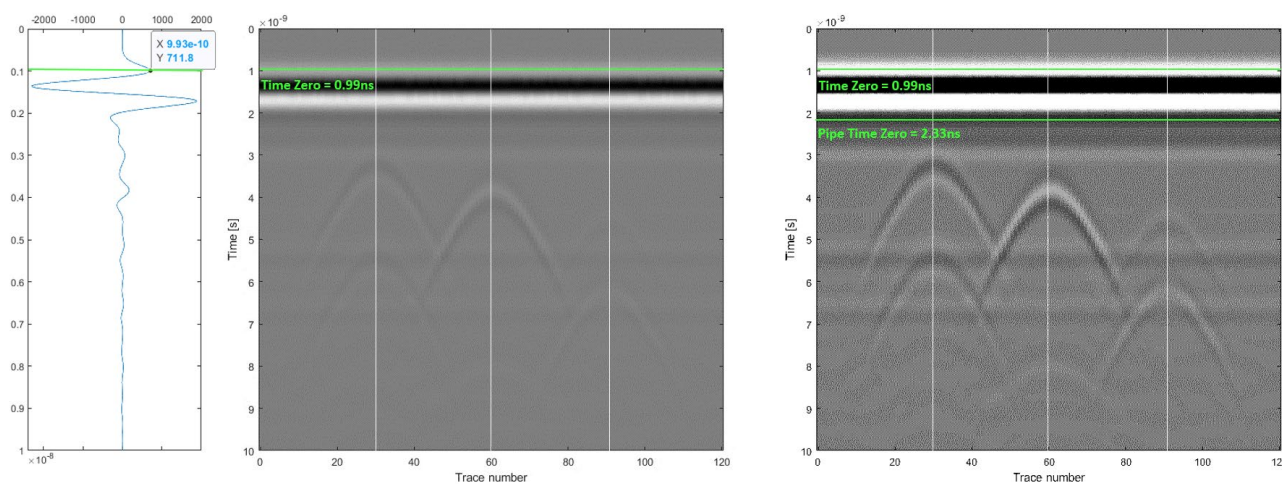


Figure 3-12: left: A-scan of trace 60 with the first positive peak marked; middle: radargram with the time zero plotted; right: radargram with time zero and pipe time zero marked.

The “Pipe Time Zero” mentioned in the analysis of simulation of detecting voids with different distances to the pipe is a special type of TZC, which sets the Time Zero at the moment the wave is propagating through the pipe wall-soil interface. The Pipe Time Zero is very suitable for measuring the distance between the void and the pipe accurately because it removes the pipe wall from the calculation. However, this concept is limited to inspect defects in the pipe exterior environment, it is still suggested to use the conventional TZC if the pipe wall thickness is considered.

Contrast Enhancement

If the absolute reflection coefficient is near zero (i.e., the material of the buried object has a relative permittivity similar to the soil), the resulted reflections (hyperbolas) in the radargram might be very weak or not visible at all. As a basic image processing technique, the contrast enhancement is beneficial and often applied to reveal and enhance the invisible/weak reflections in the radargram (Pleijisier, 2019).

The picture correction tool in Microsoft PowerPoint¹¹ is used to adjust the contrast of the simulated radargram in this thesis, a comparison can be seen in Figure 3-12. The middle radargram is directly generated from the gprMax .out file while the right radargram is the same picture but with 80% of contrast gain. Clearly, the hyperbolas in the right radargram are much more visible than the middle radargram.

A-scan Extraction

While radargrams are more often seen by the users for information such as the location and depth of the buried object, the A-scan provides more precise TWTT readings and polarity changes of the wave, which helps to gain more accurate distance and size calculations, more importantly, the polarity changes can be used to find the air-filled void. Hence it is always suggested to extract the A-scan from data points of interest, three A-scans were then extracted from the centre of each hyperbola in the simulated radargram, see the figure below.

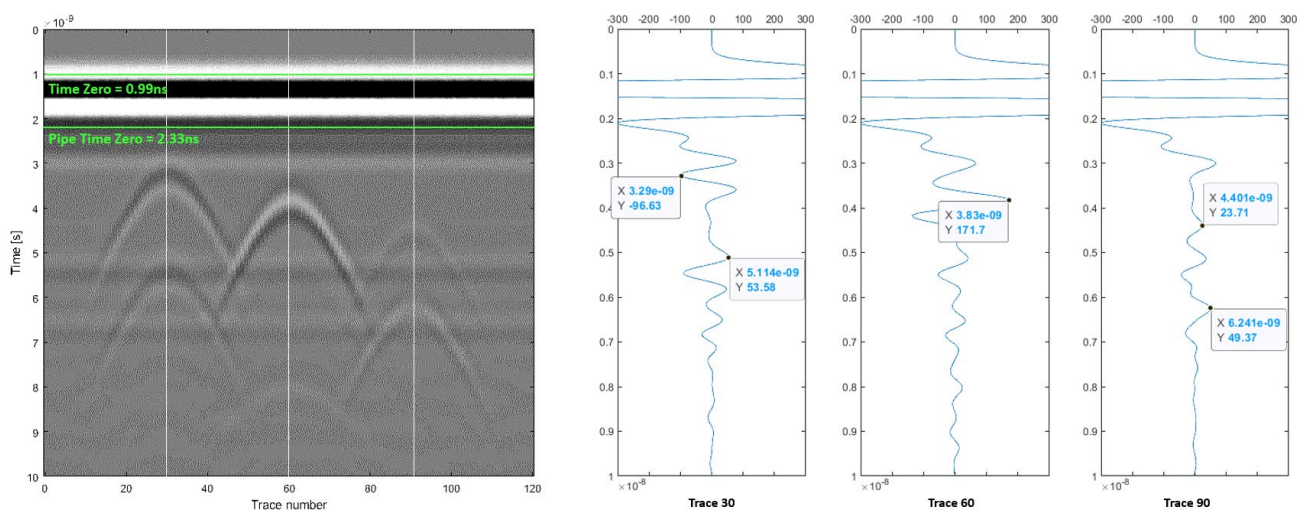


Figure 3-13: Radargram with A-scans extracted from the center of the hyperbolas.

For this sample radargram interpretation, the A-scans were first used to determine the TWTTs of the hyperbolas (see the TWTTs in the A-scans in Figure 3-13). Other than that, It is also found from the A-scans that only the trace 30 shows a reversed polarity after the defined Pipe Time Zero. Hence the conclusion till this step of the sample radargram interpretation process is, the first pair of hyperbolas highly possibly indicated an air-filled void while there were objects detected at trace 60 and 90, but the composition of the detected objects remains unknown.

¹¹ It may sound unprofessional but the fact is, the picture correction tool in Microsoft PowerPoint has more adjustable contrast range (from -100% to +100%) compared to the MATLAB image processing tool that often over-exposes the image, which is inconvenient to use.

Axis Conversion

By converting the XY-axis in the raw radargram into clock directions and distance, the planar post-processed radargram is obtained, see Figure 3-14 below. The hyperbola peaks are manually highlighted with red crescents and A-scans from the center of these hyperbolas are provided at right. Note the distance is converted solely through the wave velocity in the soil, the vertical size cannot be directly calculated by the upper and lower hyperbolas.

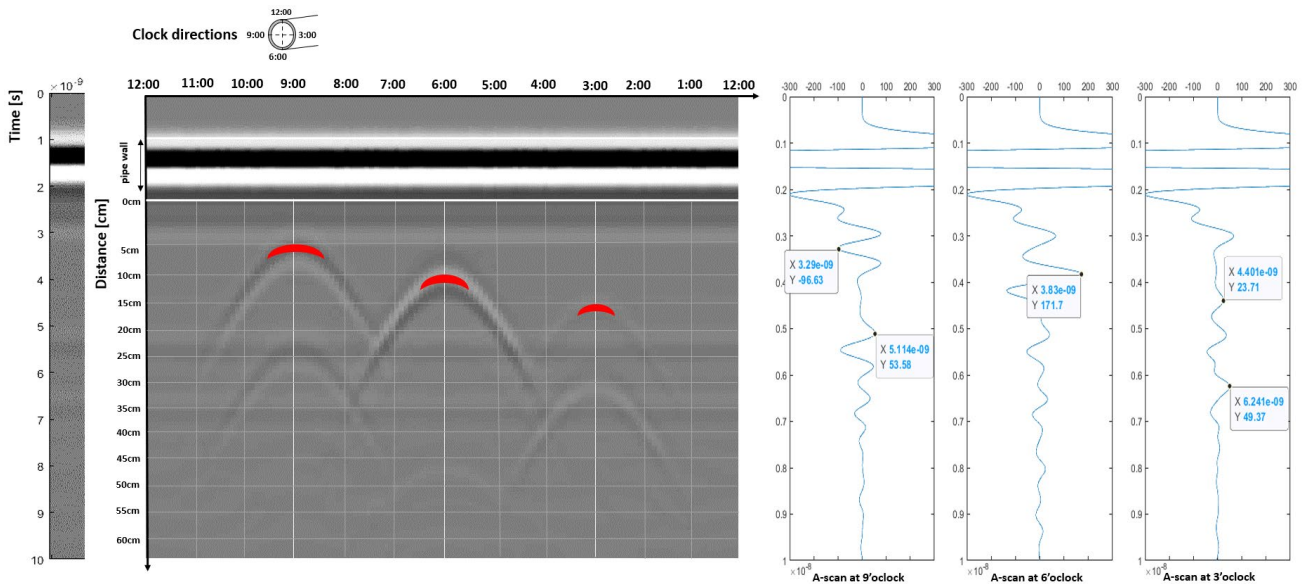


Figure 3-14: Planar post-processed radargram with corresponding A-scans.

Coordinates Transformation

Since the simulated in-pipe GPR inspection was performed by scanning the pipe's circumference, the radargram can be presented in a cylindrical form (see Figure 3-15).

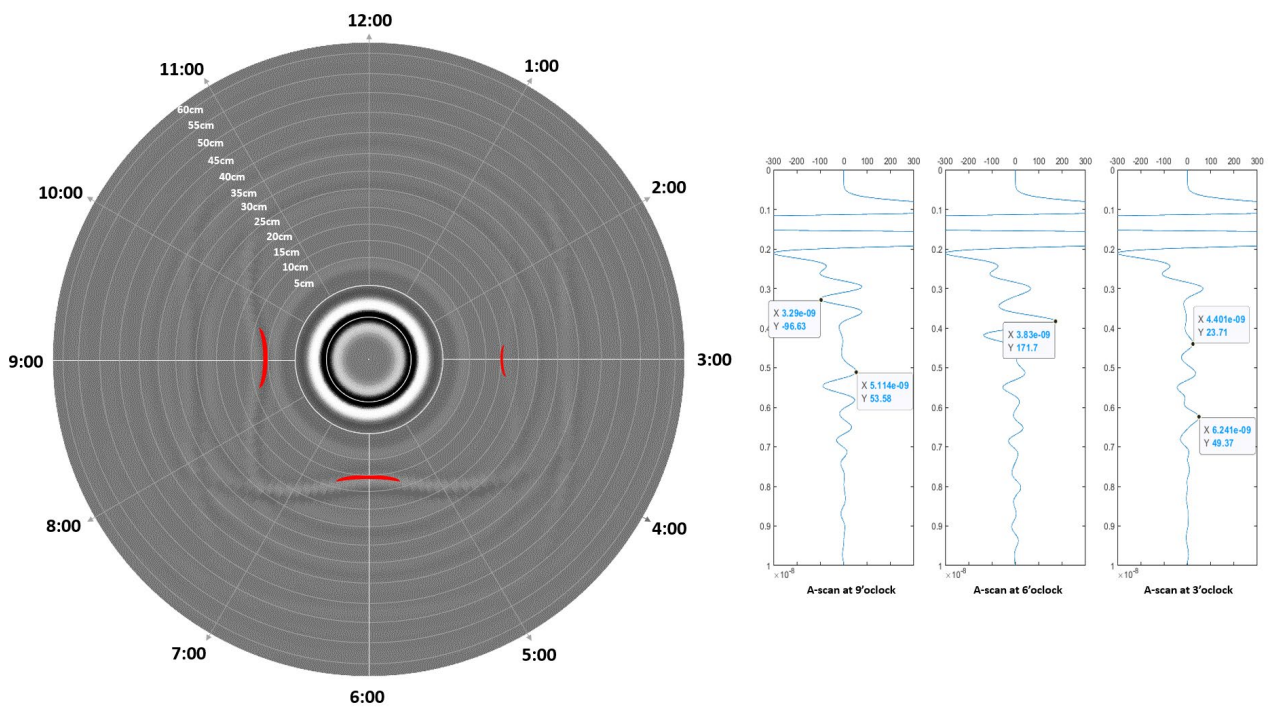


Figure 3-15: Cylindrical post-processed radargram with corresponding A-scans.

The cylindrical radargram in Figure 3-15 was obtained by transforming the cartesian coordinates of the planar radargram into polar coordinates (see the MATLAB function used for the transformation in Appendix F, source from (Islands, 2011), found and provided by Miss. Noshahri for the use of this thesis project). The cylindrical radargram provides users with a pipe cross-section view to easily understand the radargram and locate the defects.

However, the hyperbola in the cylindrical radargram became very wide and flat, which is difficult for users to visually determine its peak, e.g., the hyperbola and its peak at 3 o'clock Figure 3-15 are barely visible. In worst cases, the user could locate the defect in the wrong circumferential position when he/she wrongly determined the hyperbola peak. To avoid such consequences, it is suggested to highlight or preserve¹² the hyperbola peaks during the coordinates transformation (see the manual-marked red crescents in Figure 3-15).

Although there is no extra information added in the cylindrical radargram and the abovementioned disadvantage, it is still more logical to present the in-pipe GPR radargram in a cylindrical form. After all, this is how the inspection performed and it provides a more easy-to-understand data display.

Quantifications Interpretation

By interpreting the post-processed radargrams in Figure 3-14 and Figure 3-15, the condition of the pipe's exterior environment can be assessed. The post-processed radargrams and interpreted results will be used as source data in the final in-pipe GPR data visualization design. Note here the two radargrams are interpreted as real inspection data, the longitudinal location and severity of the defects will be assumed later in the data visualization design.

- **9 o'clock:** An object is detected at around 5cm outside the pipe, which is very possible an air-filled void since a reversed polarity is found in the corresponding A-scan. The vertical size of this air-filled void can be estimated by equation (3-6): $150 * (5.11 - 3.29) = 273\text{mm}$ (see the TWTTs in Figure 3-14 or Figure 3-15). By assuming the object has a circle-shaped cross-section, the unknown horizontal size equals to the vertical size. The way to obtain its longitudinal length can be seen on page 23.
- **6 o'clock:** An object is detected at around 10cm outside the pipe. It is only known that this objective is made of a material with a relative permittivity higher than sand since there is no reversed polarity found in the corresponding A-scan. The lower hyperbola reflected by this object is not shown on the radargram, the reason might (separately or in combination) be: 1). the object has a very large vertical size; 2). the wave velocity within this object is very slow. Either way, the object size cannot be estimated and the object shape remains unknown.
- **3 o'clock:** An object is detected at around 15cm outside the pipe. As no reversed polarity found in the corresponding A-scan, it is only known that this object is made of a material with a relative permittivity higher than sand, the exact material type remains unknown. Because of the unknown material, the vertical size of the object cannot be estimated either, even though the radargram shows the upper and lower hyperbolas reflected by the detected object. Other than that, the shape of the object is also unknown.

¹² As seen, the "highlighting the hyperbola peaks" step in Figure 3-15 was done manually, but Mr. Molegraaf - the external supervisor of this thesis, developed a Python function that could remove the non-peaking points of the hyperbola during the coordinates transformation, which helps to generate a cleaner post-processed radargrams that enables a more efficient and accurate data interpretation. However, this function is out of this thesis's scope, it is expected that Miss. Noshahri (one of the university supervisors of this thesis) could further develop and apply it in her future work.

4. Visualization Method Development

In this chapter, section 4.1 defines “data visualization” in sewer condition assessment and addresses the expected outcome of this thesis. Section 4.2 extracts a series of descriptive aspects from the users’ and system expectations, and formulates specific requirements for the development and assessment of the desired visualization method. Then, a literature review that explores the available inspection data visualization alternatives is provided to enumerates the found alternatives with the descriptive aspects. Further, MCDA criteria are extracted from the descriptive aspects to select the optimal alternative for the desired visualization method. Finally, section 4.3 modifies the selected alternatives into the final visualization method and presents the graphical design of it.

4.1. Data Visualization in Sewer Condition Assessment

According to (FIU, 2018; Tableau, 2020), data visualization is *“the graphical representation of a large set of data that provides an accessible way for the general public to see and understand trends, outliers, and patterns in the data through visual formats like charts, graphs, maps, etc.”* This definition also applies to sewer inspections, as adapted from (Ling, et al., 2014), data visualizations in the sewer condition assessment provide the functions below, and act as a key tool that allows decision-makers to easily pull insights from the overall inspection, make decisions on sewer management activities more timely and accurately:

- enabling large volumes of data (e.g., the inspection data of a regional sewer network) to be processed and organized in a simple, easy-to-use visual format;
- documenting the condition of the inspected sewers (e.g., defects and degradations) and corresponding site activities (e.g., repairing and replacement) through time;
- and allowing information to be readily communicated (e.g., between the sewer manager and contractor);

Conventionally, visualization of sewer inspection data is often integrated into the sewer management software as a subsystem, e.g., CCTV inspection data visualization in **MapKit**. Ideally, the outcome of this thesis is supposed to be designed as such a workable visualization system, but it is impractical to experiment on existing sewer management software or build a new one for this purpose. Hence this thesis turns to provide graphic designs of the interface, essential elements, and particularly the visualization methods of such a visualization system.

Worth to mention, this thesis follows the conventional sewer inspection data visualization approach (see page 2), which visualizes the results interpreted from the raw inspection data (i.e., type, location and severity of defects), whereas the raw (post-processed) data exists only as evidence to defects (this is why Appendix J can still plan for developing visualization methods for the impact echo method without simulation data). The advantages of this visualization approach are **1).** users can understand the sewer condition even without the raw (post-processed) data; **2).** visualization methods developed from this approach are to some extent generic and universal, which are not limited to the type of inspection technology and data, i.e., as long as the visualization purpose is the same and the data is interpreted, the interpreted results can be visualized, (see requirement 13)).

The disadvantage of this visualization approach is that thoroughly human interpretation is always needed before the visualization, which is also why section 3.1 introduced all those procedures for in-pipe GPR inspection data processing and interpretation (see page 25).

4.2. Available & Optimal Visualization Alternative(s) for in-pipe GPR Data

This section aims to find the most suitable visualization alternative that can be applied directly or adapted to visualize the additional sewer condition data collected by in-pipe GPR inspections.

4.2.1. Descriptive Aspects & Requirements Development

The interviewed sewer professionals, who are also sewer asset managers and potential end-users of the desired data visualization method, elaborated that they expect the data visualization of in-pipe GPR to be **generic, readable, shareable, future-proof, and most importantly, compatible with the common-used sewer management software and financially reasonable**¹³. They have also emphasized that the inspected data shall be **presented as detailed and straightforward as possible**, which means **the data of interest (defects) should be easy to identify from the overall visualization**. Lastly, they are very interested to see the additional sewer condition data **presented in 3D** because they think the 3D data visualization is the future trend in the sewer inspection industry (see the full interview results in Appendix B).

Besides the users' expectations, a proper data visualization also requires considerations from a more systematic perspective. Since the functions described in (Ling, et al., 2014) are rather general (see page 30), the concept of "Abstract Tasks" is applied here to enrich the users' expectations from the system perspective. Three¹⁴ of the abstract tasks introduced in section 2.1 are adapted here for such a research purpose, namely: **1). Overview** shows users an overview of the entire collection; **2). Relate** shows relationships among items; **3). History** provides historical data records. See more of these abstract tasks in (Ardito, et al., 2006; Shneiderman, 1996). Because the adapted abstract tasks are introduced from a systematic perspective, they are renamed as "system expectations" to match with the users' expectations in this thesis.

As seen, the users' and system expectations extracted from interviews with the sewer professionals and the Abstract Task method are not very well organized and still with a high level of abstraction. It is not appropriate to evaluate whether a data visualization alternative is suitable for a certain purpose by listing the abstract expectations it has met, a more systematic approach is needed for this process. Therefore, Table 4-1 proposes a series of descriptive aspects to link and categorize these expectations, most importantly, based on these descriptive aspects and the expectations under them, specific requirements are formulated for the development and assessment of the desired final visualization method. The MoSCoW method (Mulder, 2017) is applied in Table 4-1 to prioritize the formulated requirements.

¹³ The abstract word "**financially reasonable**" from the user can be interpreted as the users want the developed visualization methods easy to be integrated with their sewer management software, which can be related to factors such as the difficulty and costs of creating the new visualization methods and integrating it to a sewer management software.

¹⁴ The other four are more about the actual actions/operations that users wish to perform on a visualization system, which is out of the thesis scope.

Table 4-1: Categorizing the expectations and translating them into specific requirements.

Descriptive Aspects	Linked Expectations	Requirements	MoSCoW
Area of application	—	1) The developed visualization must apply to the sewer condition assessment, which means that it should be able to visualize inspection data showing the interior space, exterior environment, or the within-wall space of a pipe. In the case of in-pipe GPR, this particularly means the condition collected from the pipe's exterior environment.	M
Visualized features	—	2) Basic features for sewer condition assessment must be presented, i.e., representation of the inspected pipe and defects, and the coordinate system for ranging pipe's geometry and locating defects. 3) Added-value features such as the pipe registration information and historical inspection data records shall also be presented in the visualization.	M W
Scale	<ul style="list-style-type: none"> • Overview • Straightforward 	4) The scale of the developed visualization must allow it to provide an overview of the entire inspection data collection (e.g., of a pipe segment $\leq 100\text{m}$) that shows all defects collected by (and interpreted from) the inspection technology. 5) The scale of the developed visualization must allow minor defects (and individual data points) to be visibly seen in the above-mentioned visualization overview.	M M
Depiction	<ul style="list-style-type: none"> • Readable • Generic • Relate • History 	6) The visualization overview must fully present the pipe's geometry (i.e., full length and circumference of a complete pipe segment) to represent the pipe space that it intends to visualize. 7) Defects and their characterizations and quantifications such as presence, location, type, size, and severity interpreted from the inspection data must be denoted in and highlighted from the overall visualization. For example, denoting defects with lines, shapes/symbols and 3D objects, whereas highlighting (enhancing) them with colors, codes, (pop-up) annotations, etc. 8) The raw/post-processed inspection data of a certain defect shall be presented to support requirement 6). 9) All units used in the visualization should be metric. 10) The visualization should be complaint with conventional sewer inspection data visualization elements such as the clock directions, severity classes and sewer defect codes. 11) The visualization shall be able to graphically present the spatial relationship between the pipe and defects, i.e., the longitudinal location, circumferential position of a defect and its distance to the pipe. 12) The information related to the inspection can be presented in the visualization, e.g., codes of starting/finishing manholes, local soil information, etc.	M M S S S S W
Compatible data types	—	13) The developed visualization method shall be able to visualize all types of sewer inspection data, as long as it is interpreted and fits the intended visualization purpose, i.e., the type of sensors used (e.g., in-pipe GPR or any other technology) and continuity of the data (and its collection process) should not impose any influence to the visualization. This requirement is in support of requirement 16) ¹⁵ .	S
Viewing perspective	<ul style="list-style-type: none"> • 3D 	14) The viewing perspective must first enable requirement 6). Further, the viewing perspective shall be in a 3D form to fulfill the users' specific expectation of seeing 3D data visualizations (e.g., 3D fixed/rotatable X-ray/transparent view). But there are also many other options, e.g., pipe fold-out view, worm view, etc.	M
Ease of creation	<ul style="list-style-type: none"> • Financially reasonable 	15) The final developed visualization methods should be cost-effective and easy to create and integrate with the users' sewer management software.	W
Future proof	<ul style="list-style-type: none"> • Compatible with sewer management software • Shareable 	16) In terms of being robust for future uses, the developed visualization methods shall first satisfy requirement 13) ¹⁵ . Ideally, certain system requirements shall also be met, e.g., the developed visualization method shall be able to generate sharable visualization files that are compatible with the users' sewer management software. Such requirements reflect certain users' expectations and the other abstract tasks introduced in section 2.1. However, because these requirements are about the actual operations that users wish to perform on a visualization system, they are excluded from the scope of this thesis.	W

Be noted, because there is no solid theoretical reference for framing these descriptive aspects to link and categorize the users' and system expectations, many assumptions were made while creating the above table. The same for the development of the requirements, the requirements are formulated by **1)** expanding, specifying, and translating the descriptive aspects and the users and system expectations into specific questions like the ones listed on the next page; then **2)** setting answers to these questions for the desired visualization methods. Worth to note, the conventional CCTV data visualization method act as a reference of standardization in step **2)** (i.e., generalize the essential elements in this reference and incorporate them into the requirements, e.g., the clock directions, severity classes).

Be noted again, the keywords "**must**" "**shall/should**" and "**can/could**" within the statement of the requirements indicate their importance to the users. But the MoSCoW prioritization addresses the priority of realizing these requirements in the final visualization methods designing phase. Overall, requirements marked with **M (must-haves)**, **S (should-haves)** are supposed to be fully realized in the outcome since they are directly related to the sewer inspection data visualization process. However, the **W (won't-haves)** requirements are involved with extra concerns that are not directly related to the data visualization process and more difficult to consider in this thesis, thus the lowest priority is given to them, meaning they will mainly be discussed and suggested.

¹⁵ An assumption can be made here, requirement 13) partly defines the level of **future proof** of a visualization method, if one visualization method is able to visualize the sewer condition data collected from more than one pipe space, it is then more robust for future uses (assuming no other influences). For example, a visualization method that is developed for integrating sewer condition data collected from all pipe spaces and it fulfills requirement 13). This then indicates that it is applicable to any sewer inspection situation, e.g., visualizing the data collected by any types of inspection technology from any pipe spaces (separately or in combination).

4.2.2. Review of Available Inspection Data Visualization Alternatives

The literature review conducted to find the available data visualization methods and concepts covers inspection practices of several types of infrastructure, namely sewer pipes, underground tunnels, bridge decks, and walls. Other than that, various inspection technologies are also considered, for instance, CCTV, surface/in-pipe GPR, LIDAR, impact echo, ultrasonic, and several multi-sensors inspection systems. Note there might be more choices from other inspection practices (in terms of infrastructure types or inspection technologies), but in this thesis, the scope is limited to these common infrastructure types and inspection technologies.

Table 4-2 in this section categorizes and enumerates (and refers to the specific examples in Table 0-2¹⁶, i.e., clicking the letters in Table 4-2 in to see the examples in Table 0-2 of Appendix G) the data visualization methods and concepts found in the literature based on the developed descriptive aspects, and discusses each categorization through the perspectives of the used descriptive aspects. In this way, Table 4-2 presents an overview of the found available data visualization alternatives in a more taxonomic way and enables a comparison among the alternatives from the perspective of the developed descriptive aspects.

Although the descriptive aspects were already proposed in the previous section, they are more like abstract titles since they were not yet specifically defined. Hence in this section, they are defined by the following questions (established by expanding, specifying, and translating descriptive aspects and the users' expectations under them. In this sense, the process of describing the found visualization alternatives from the perspectives of these descriptive aspects then becomes the process of answering these questions.

- **Area of application:**
 - What is the actual use of this visualization alternative (e.g., condition assessment or others)?
 - Which types of defects are visualized in this visualization alternative and where are they from?
- **Scale:** Does this visualization alternative provide an overview of the entire inspection data collection and show all the individual data points and minor defects?
- **Depiction:** How are the inspected object and data of interest (defects) depicted?
- **Viewing perspective:** What is the angle that users look at the visualization and what do they actually see?

Be noted, the **visualized features** and **compatible data types** descriptive aspects are not shown in Table 4-2 because most alternatives do not differ on these two aspects according to the detailed introduction of them in Appendix G. To be more specific, majority of the found visualization methods and concepts can only provide basic features for condition assessment, and the data being visualized always has to be interpreted in advance (i.e., what is visualized in the visualization is the interpreted result instead of the inspection data itself).

On the other hand, the **ease of creation** and **future proof** are more about the actual and future uses and less related to the data visualization process, which is infeasible and redundant for the main purpose of describing these visualization methods and concepts. Hence, they are not included in Table 4-2 either.

¹⁶ Worth to note, Table 0-2 was actually made first, which comprehensively describes the visualization methods and concepts found in the literature based on the descriptive aspects (except **ease of creation** and **future proof**), and even provided graphical examples for each of them. But due to its large size and the fact it lacks of a categorization of all these available alternatives in Table 0-2, Table 4-2 is created.

Table 4-2: Categorization and enumeration of the found visualization alternatives.

Descriptive Aspects Alternatives	Area of application	Scale	Depiction	Viewing Perspective
1. 2D Pipe fold-out view Examples: A and B in Appendix G	Visualizing sewer defects in/on the pipe inner space/surface (e.g., obstacles and cracks)	Individual data points and minor defects are visible in the visualization overview.	<ul style="list-style-type: none"> ○ Pipe represented by a meshed rectangle (X-axis: length; Y-axis: clock direction) ○ Defects denoted by shapes/symbols, coded colors, pop-up annotations, and sewer defect codes 	Longitudinal top view (unfolded pipe)
2. 2D linear representation of pipe wall condition Example: C in Appendix G	Visualizing pipe wall variations (e.g., thickness changes) and defects within the pipe wall (e.g., voids) but has a (low) potential to visualize defects within to within the pipe	Individual data points and minor defects are visible in the visualization overview (but it needs help from the “zoom in” function when the inspection scale is large, e.g., small thickness loss might be invisible in a very long pipe).	<ul style="list-style-type: none"> ○ Pipe represented by X-axis ○ Pipe wall thickness and rebar configuration are depicted by lines in Y-axis. Meanwhile, defects are denoted by shapes/symbols and coded colors. 	Longitudinal front view (pipe thickness)
3. 2D representation of pipewall- soil interface Examples: D and E in Appendix G	Visualizing defects within/outside the sewer wall (e.g., wall thickness, grout loss and in/external voids)	Individual data points and minor defects are visible in the visualization overview.	<ul style="list-style-type: none"> ○ Pipe and its exterior environment represented by layers with different textures ○ Defects denoted by shapes/symbols, coded colors (for defects), and possibly also pop-up annotations. 	Longitudinal front view (pipe wall – soil interface)
4. 3D pipe with inspection data projected on outer surface Example: F in Appendix G	Originally for visualizing sewer inner surface defects (e.g., corrosion) but has the potential to visualize defects within/outside the pipe	Individual data points and minor defects are visible in the visualization overview (but it needs help from the “rotating” function, e.g. defects out of sight might be invisible from a fixed angle).	<ul style="list-style-type: none"> ○ Pipe represented by a 3D cylindrical surface (no thickness) ○ Defects denoted by coded colors 	Rotatable and zoomable 3D view (3D cylindrical surface)
5. 3D pipe with inspection data projected on inner surface Example: G in Appendix G	Originally for visualizing defects in/on the pipe inner space/surface (e.g., obstacles and cracks) but has the potential to visualize defects within/outside the pipe (similar to alternative 4)	Only able to show defects at a fixed spot/area at a time (defects out the sight of the “worm” view are invisible).	<ul style="list-style-type: none"> ○ Pipe represented by a 3D cylindrical surface (no thickness) ○ Defects denoted by shapes and coded colors 	Immersive inside-pipe “worm” view with the possibility to go back and forth (inside of the 3D cylindrical surface)
6. 2D color-coded defects map Example: H in Appendix G	Visualizing defects on/within the surface of slab-like structures (e.g., thickness losses and voids)	Individual data points and minor defects are visible in the visualization overview (but it need help from the “zoom in” function when the inspection scale is large, e.g., tiny cavities might be invisible in large-scaled inspections).	<ul style="list-style-type: none"> ○ The inspected object is represented by a map that outlines the shape of it. ○ Defects denoted by coded colors 	Top view (a map that outlines the shape of the inspected object)
7. 3D color-coded defects map Example: I in Appendix G	An upgraded version of the above alternative 6	Same as above.	<ul style="list-style-type: none"> ○ The inspected object is represented by a 3D map that outlines the shape of it, and the thickness data is transformed into height. ○ Defects denoted by coded colors and deviations in height 	Rotatable and zoomable 3D view (3D map that outlines the inspected object’ s shape)
8. 3D pipe reconstruction Example: J in Appendix G	Originally for visualizing defects on/within the pipe surfaces (e.g., outer/inner surface damage, rebar configuration) and has great potential to also integrate and visualize defects from all pipe spaces	Individual data points and minor defects are visible in the visualization overview (but it needs help from the “rotating” function, e.g. defects out of sight might be invisible from a fixed angle).	<ul style="list-style-type: none"> ○ pipe represented by 3D pipe model reconstructed from inspection data (3D tube with thickness in a certain form, e.g., transparent, wireframe, X-ray) ○ Defects denoted by 3D objects, coded colors, and annotations 	Rotatable and zoomable 3D view (3D pipe model)
9. 3D point-cloud datasets registration Example: K in Appendix G	Inspecting defective parts (e.g., missing/redundant pieces) in small-scaled industrial assemblies and pipe spool fabrication process (similar to alternative 4 and 5)	Individual data points and minor defects are visible in the visualization overview (but similar to Alternative 4 and 5, it needs help from the “rotating” functions, e.g. defects out of sight might be invisible from a fixed angle).	<ul style="list-style-type: none"> ○ The pipe is represented by two 3D point-cloud datasets. ○ Defects are denoted by coded colors. 	Rotatable and zoomable 3D view (two 3D point-cloud pipe models merging with each other).
10. 3D Immersive VR sewer inspection Example: L in Appendix G	Originally for visualizing small defects in large pipe inner surfaces but has a great potential to present defects from all pipe spaces (similar to alternative 4, 5 and 8)	Only able to show defects at a fixed spot/area at a time (similar to Alternative 5, defects out the sight of the immersive inside-pipe VR view are invisible)	<ul style="list-style-type: none"> ○ pipe represented by a VR environment that depicts the inside-pipe situation (pipe inner surface with patterns and textures) ○ Defects denoted by color-coded 3D objects 	Immersive inside-pipe VR view with the possibility to walk through and look around
11. 3D Stereo AR sewer data visualization Example: M in Appendix G	Originally for asset locating and providing registration information of the utility in-situ but has a similar potential as to alternative 4, 5, 8 and 10	Individual data points and minor defects are visible in the visualization overview (but similar to Alternative 4, 8, and 9, it needs help from the “rotating” function, e.g. defects out of sight might be invisible from a fixed angle).	<ul style="list-style-type: none"> ○ Pipe represented by a real-size 3D AR model in a certain form (e.g., transparent, wireframe, X-ray) in-situ ○ Defects denoted by color-coded 3D objects 	3D zoomable view (3D AR pipe model in-situ and with the possibility to walk around

4.2.3. Selecting the Optimal Data Visualization Alternative

As indicated in Figure 2-1, after categorizing and enumerating the found visualization alternatives, the following step is to compare them and select the most suitable ones as the final visualization alternative for the researched in-pipe GPR sewer inspection application in this thesis. In total there are eleven visualization alternatives available, but not all of them are suitable for sewers, hence a pre-selection is first executed to reduce the number of choices for the later MCDA comparison and selection.

Two mandatory considerations based on the **area of application** and **scale** descriptive aspects¹⁷ can be formulated for the pre-selection: **1).** the desired visualization must be able to visualize the inspection data showing the interior, exterior or the within-wall space of a pipe; **2).** the scale of the desired visualizations has to be able to present the individual data points and minor defects on its visualization overview (e.g., thickness at a single point of the pipe wall, or a tiny crack should be readable from the visualization overview that presents the overall condition of a complete pipe segment). By taking these two considerations into account, alternatives below are excluded:

- **5. 3D pipe with inspection data projected on inner surface & 10. 3D Immersive VR sewer inspection**

These two methods are excluded because they failed to meet the consideration **2).** The immersive inside-pipe viewing perspective is inherently unable to provide a visualization overview that presents all defects found in a pipe, users need to literally “walk” through the pipe to see each of the defects. Such visualizations are more suitable for inspectors to operate the inspection equipment in-situ and precisely interpret the collected data instead of being presented as a visualization to decision-makers for the overall sewer condition assessment.

- **7. 3D color-coded defects map**

This method is excluded for a reason that relates to consideration **1).** This method is an upgraded version of alternative 6 by innovatively converting thickness data into 3D height, which is very suitable for slab-like structures. But for visualizing the thickness of a sewer pipe, this then means the pipe needs to be unfolded into a 3D slab that allows height information to be easily comparable on the same plane, which is illogical and unnecessary when a 3D pipe can be modeled directly. One might argue that this method can be adjusted to using the pipe’s thickness data to form up a 3D pipe model, which is certainly possible. But this then drifts away from its original visualization idea and somehow overlaps with the “3D reconstruction” idea of Alternative 8, which is still a reason to exclude it from the list of choices in the later MCDA.

- **9. 3D point-cloud datasets registration**

This method is excluded because it does not meet consideration **1).** This method can only visualize defects that do not require complex data processing and interpretation procedures to identify and analyze (e.g., obvious redundant/missing pieces). In this way, this method to some extent integrates the data collection and visualization into one process since there is no need to interpret the data in advance. These are not suitable for the visualization purpose of the researched in-pipe GPR application, i.e., visualizing the condition in the pipe's exterior environment. Meanwhile, human analysis (i.e., data processing and interpretation) is still inevitable for the researched in-pipe GPR sewer inspection method.

¹⁷ These two aspects are selected because they refer to relatively fixed and strict requirements, which can easily exclude unsuitable alternatives.

After the pre-selection, seven alternatives are left for the MCDA comparison and selection. By following the procedures introduced in section 2.1, the MCDA objective is first determined as **“to select the most suitable data visualization alternative for the in-pipe GPR sewer inspection method”**.

The next steps are to define and weight the criteria to be used in the MCDA. The four descriptive aspects used in Table 4-2 are perfect criteria for measuring the performance of each visualization alternative from different perspectives. Moreover, the **ease of creation** and **future proof** descriptive aspects are also considered here since they to some extent represent the feasibility of implementing these alternatives and their future uses¹⁸. See the reason why **visualized features** and **compatible data types** are not used here on page 33.

These selected criteria are quantified into three levels (bad, fair, and good with scores 0-2 for later ratings in the MCDA (this is done by setting ranges for the performance of each visualization alternative towards fulfilling the requirements defined in Table 4-1).

- **Area of application:** This criterion considers two factors, the inspection technology that the alternative was specially designed for and its visualization purpose/capability (i.e., the applicability of a visualization alternative as to a specific inspection technology is dependent on its visualization capability and the pipe space assigned to this technology). For example, the **2D representation of pipe wall- soil interface (3)** can be rated as “good” on this criterion since it is specially designed for in-pipe GPR applications and it can visualize the condition of the pipe’s exterior environment. Take this as an example, the other alternatives are rated as “good/fair/bad”.
- **Scale:** This criterion measures whether the alternative can perfectly present all individual data points and minor defects in one view. For example, the **2D pipe fold-out view (1)** can be rated as “good” on this criterion. Other than that, for those alternatives that need help (e.g., rotating) to achieve this intention, they are rated as “fair”.
- **Depiction:** This criterion measures whether users can easily answer the “where”, “what”, “how serious” questions about a defect by looking at the visualized information. For example, the **2D pipe fold-out view (1)** and **3D pipe reconstruction (8)** can be rated as “good”, whereas **2D Pipe wall condition linear representation (2)** **2D representation of pipe wall- soil interface (3)** can be rated as “fair” because they only present the condition of the pipe wall or pipe’s exterior environment at one or several certain circumferential positions instead of all.
- **Viewing perspective:** As known from the interview results, the users are eager to see 3D sewer inspection data visualizations. Hence all 3D visualization alternatives are rated as “good” while the 2D visualization alternatives are rated as “fair”.
- **Ease of creation:** This criterion considers two factors, the difficulty, and the costs of creating the visualization and integrating it into a sewer management system. For example, it is common sense that 3D visualizations are more costly and difficult to create than the 2D visualizations. Hence the 3D Stereo AR sewer data visualization (11) can be rated as performing “bad” on this criterion since it requires much more effort than normal 3D modeling (e.g., AR modeling, real-time locating, etc.). Take this as an example, the ordinary 3D alternatives can be rated as “fair” while the 2D alternatives can be rated “good” on this criterion.

¹⁸ Be noted, indeed the requirements under these two criteria are prioritized as **won’t have** in Table 4-1, but that is mainly for the development of the final developed visualization methods, here they can still be used to roughly compare the performance of the visualization alternatives.

- Future proof:** In Table 4-1, the future proof of a visualization alternative is defined by its compatibility and shareability (see requirement 16)), but these two factors are unavailable to measure before they were actually in use. Hence, the assumption “if one visualization alternative is able to visualize the sewer condition data collected from more than one pipe space it is more robust for future uses” from requirement 16) is applied here. In short, here this future proof criterion considers whether the alternative can visualize sewer condition data collected from more than one pipe space (e.g., in/within/outside the pipe). For example, **3D pipe reconstruction (8)** and **3D Stereo AR sewer data visualization (11)** can be rated as performing “good” on this criterion since they have the potential to visualize defects from all pipe spaces. On the other hand, the alternative is rated as “fair” if it is only able to visualize defects collected from one pipe space.

After the criteria were quantified, they are weighted by comparing with each other in Table 4-3. The “+” means this criterion is more important than the other while “0” and “-” means the criterion is equally important or less important than the other. Through this comparison, each criterion takes a percentage from 100% as its weight (i.e., assuming “0” represents a basic weight of 5% while “+” means a 5% that it should add, all six weights should add up to 100%). Note there is no solid theoretical reference to prove one criterion is more important than another, the comparison below is solely based on the author’s understanding of users’ and system expectations. The weights can be adjusted for more practical considerations.

Table 4-3: MCDA criteria weighting.

	Area of application	Scaling	Depiction	Viewing perspective	Future proof	Ease of creation	Weight
Area of application	0	+	+	+	+	+	30%
Scaling	-	0	+	+	+	+	25%
Depiction	-	-	0	0	+	+	15%
Viewing perspective	-	-	0	0	+	+	15%
Future proof	-	-	-	-	0	+	10%
Ease of creation	-	-	-	-	-	0	5%

While the alternatives and criteria are ready, rating and calculations in the MCDA table below are made to find the most suitable data visualization alternatives. Note the scores (0-2) rate the bad/fair/good performance of the alternative on this criterion, particularly, the “-” means this alternative is not suitable for this visualization purpose.

Table 4-4: MCDA of comparison and selection of the optimal visualization alternative for in-pipe GPR sewer inspection, the “0” means the alternative is not specifically suitable for the inspection range of the researched in-pipe GPR application in this thesis.

Alternatives	Criteria	Area of application	Scaling	Depiction	Ease of creation	Future proof	Viewing perspective	Final Scores
		(30%)	(25%)	(15%)	(15%)	(10%)	(5%)	
3. 2D representation of pipewall- soil interface		2	2	1	2	2	1	1.8
2. 2D Pipe wall condition linear representation		0	2	1	2	1	1	1.1
1. 2D pipe fold-out view		0	2	2	2	1	1	1.25
6. 2D color-coded defects map		0	2	2	2	1	1	1.25
4. 3D pipe with inspection data projected on outer surface		1	1	1	1	1	2	1.05
8. 3D pipe reconstruction		1	1	2	1	2	2	1.3
11. 3D Stereo AR sewer data visualization		1	1	2	0	2	2	1.15

As seen from the highlighted items in the above table, the **2D representation of sewer pipe wall- soil interface (3)** is selected as the final visualization alternative for visualizing the sewer condition data of the pipe’s exterior environment collected by in-pipe GPR inspections. The following briefs the major reasons for this alternative’s highest ranking, and elaborate on the main limitations/imperfections they still own, which need to be modified/improved in the later design phase. Be noted, the alternatives rated “0” in the **area of application** criteria are not suitable for visualizing sewer condition data collected from the pipe’s exterior environment, but they are very promising for visualizing condition data of the sewer pipe wall (i.e., defects on/within the pipe wall). This means they might be very useful for the data visualization of technologies that excel at inspecting anomalies within structures (e.g., impact echo), this thesis explores the possible use of them in Appendix K and M.

Optimal Alternative for In-pipe GPR data visualization: 2D representation of pipewall- soil interface (3)

This is the only 2D alternative for visualizing condition data of the pipe’s exterior environment collected by in-pipe GPR, which is easy to create and has developed to a relatively mature level. There are also several 3D alternatives with the potential to visualize defects outside the sewer, but they have an inherent deficiency that cannot directly present all defects in one view (e.g., defects in the back of the 3D pipe model are invisible to users without rotating).

Although selected as the final visualization alternative of choice, this alternative currently can only provide condition information of the pipe’s exterior environment at several circumferential positions instead of all (see example D and E). Thus it needs a customized solution to allow users to see the pipe’s exterior environment around its full circumference, which relates to the pre-defined requirement 6).

Other than the abovementioned limitations/imperfections that the selected alternative still owns, it also needs to fulfill several design requirements, e.g., the sewer defects codes, source data for certain defects, information related to the inspection process, and the inspected object/environment, are still missing in the selected alternative. Moreover, the interface of the selected visualization alternative is still not standardized and user-friendly when compared to the CCTV data visualization. These all need modifications and improvements in the later phase.

4.3. Designing the In-Pipe GPR Sewer Inspection Data Visualization Method

The visualization alternative selected for visualizing the condition data of the pipe’s exterior environment collected by the in-pipe GPR method is originally from the **2D representation of sewer pipe wall- soil interface (3)**. As denoted on page 37 and compared to the design requirements, three major limitations remained to solve for the intended visualization purpose: **1)** it does not present the condition of the exterior environment around the pipe’s full circumference; **2)** the sewer defect codes are not yet incorporated in this alternative; **3)** the source data of defects are not provided. These limitations are solved in this section, see the graphical designs below.

Be noted, the design below visualizes the interpreted results and simulation data from section 3.1.4 as a practical example of this modified in-pipe GPR sewer inspection data visualization method. This example assumes an in-pipe GPR inspection has been executed to a real sewer pipe in the Landmansweg of Hengelo, which is 13m long and has the same geometry as used in the in-pipe GPR simulations (see section 3.1.1). According to the data processing and interpreting process in section 3.1.4, three defects were detected (the longitudinal location and severity of the defects presented in the design are assumed).

There are possibilities to add more profiles to the **2D representation of sewer pipe wall- soil interface (3)** or replace the profiles with a pipe fold-out view to show the exterior condition of the pipe’s full circumference. But they either make the visualization redundant (i.e., at least twelve profiles are needed) or cannot comprehensively indicate the spatial relationship between the defects and pipe. Therefore, this section overcame this limitation by combining these two solutions. The combination of these two solutions is designed into two versions, the pop-up version and the pipe-roller version (see figures below).

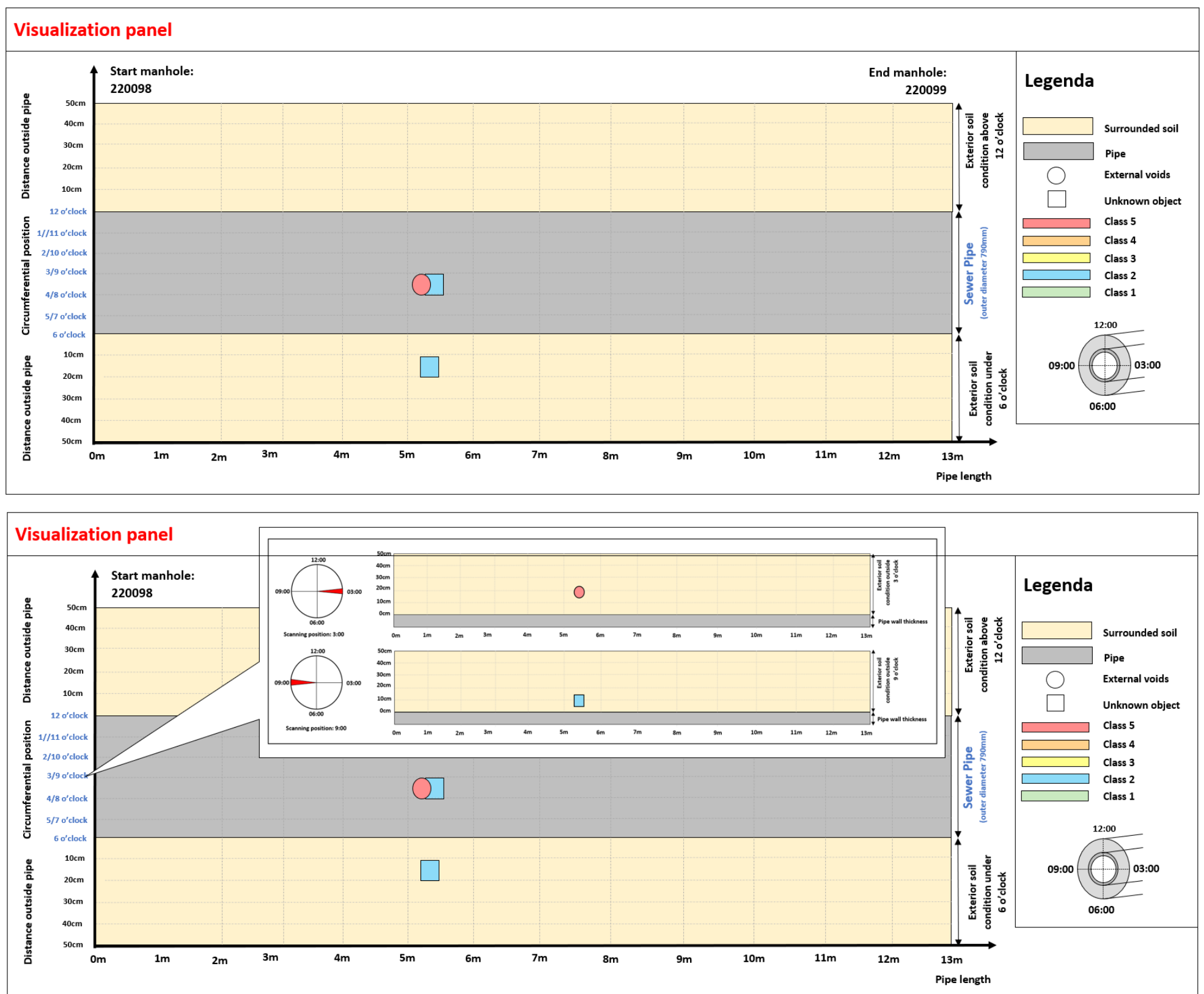


Figure 4-1: Visualization panel of the modified in-pipe GPR sewer inspection data visualization method (pop-up version).

Figure 4-1 above presents the visualization panel of the pop-up version of the modified visualization method, which mainly shows a front view of the pipe and 50cm¹⁹ of its upper and lower exterior environment. The X-axis represents the pipe length (the arrow indicates the direction of the inspection). The upper and lower exterior conditions are visualized by two in-pipe GPR inspection profiles at 12 o'clock and 6 o'clock respectively²⁰, the Y-axis represents 50cm of the exterior environment, starting from the pipe's outer surface. The defects (i.e., voids and unknown objects) are represented by predefined 2D shapes (i.e., circles and squares). The color of the circles and squares indicates their severity (see the legenda at the right of Figure 4-1). Be aware, the size of circles and squares are not necessarily reflecting the actual size of a defect since the shape of defects is often not ideal, this then also ensures the realization of requirement 5).

Besides that, defects found in other circumferential positions can be registered on the pipe's front view. The pipe's front view contains ten²¹ profiles collected from the other circumferential positions, here the Y-axis represents the circumferential positions (denoted by clock directions). However, on the pipe's front view, only the type, longitudinal location, and severity class of the defect can be seen directly. To visualize more details of them (e.g., distance to the pipe and size), the clock directions in the Y-axis are made clickable, by clicking them, the corresponding profiles can pop up, see the second part of Figure 4-1 as an example.

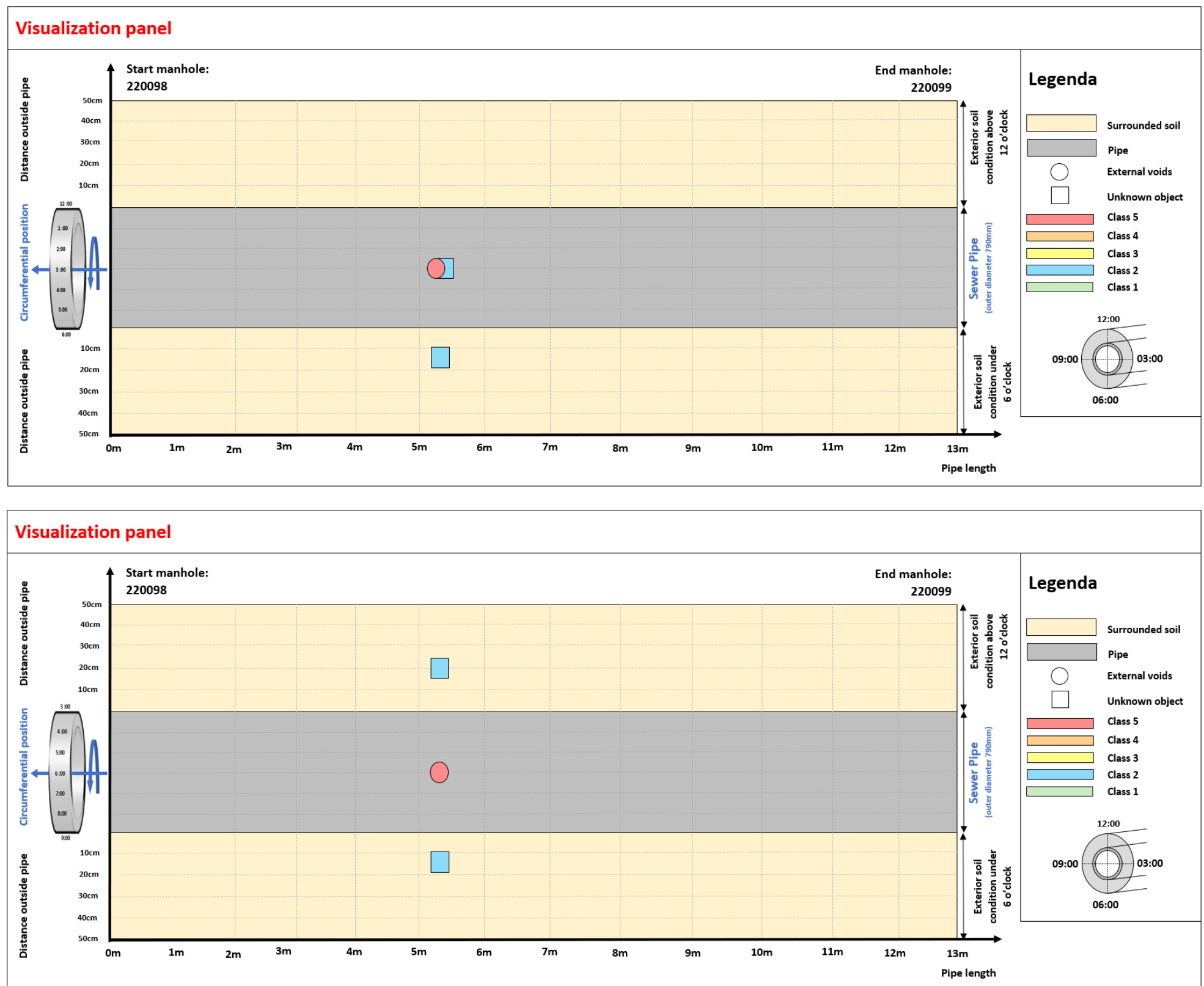


Figure 4-2: Visualization panel of the modified in-pipe GPR sewer inspection data visualization method (pipe-roller version).

Figure 4-2 above presents a slightly different design as in Figure 4-1. Instead of popping up the profiles at circumferential positions other than 12 o'clock and 6 o'clock, the pipe's front view is designed scrollable (see the small pipe-roller icon at left). While rolling the pipe-roller icon, profiles from the other ten circumferential positions will replace the 12 o'clock and 6 o'clock profiles, hence more details of the defects from the other circumferential positions can be visualized. This is a very innovative design, it keeps the visualization panel simple and clean, hence this version of in-pipe GPR data visualization is more recommended. With the pop-up and pipe-roller versions of in-pipe GPR data visualization designs, the remained limitation 1) is solved.

Besides, the interface layout of *MapKit* is used in the design to make the proposed visualization method more standardized and user-friendly. Thus, the added-value features such as the "pipe registration information" and "inspection history" are added. Note the "local soil information" is suggested as a new feature to store and present the electromagnetic properties of the local soil for future in-pipe GPR inspections. See the complete designs on the next page, which solved the remained limitations 2) and 3).

¹⁹ Default detecting range set in this thesis, the simulated defects are all within this range. This range can be freely adjusted according to users' needs.

²⁰ These two profiles are presented in the main visualization panel because defects above and under the pipe impose more serious threats than defects at other circumferential positions, hence it is better to emphasize them.

²¹ It is assumed that in total twelve profiles are sufficient to represent the full circumference of the pipe, more profiles can be added if needed.

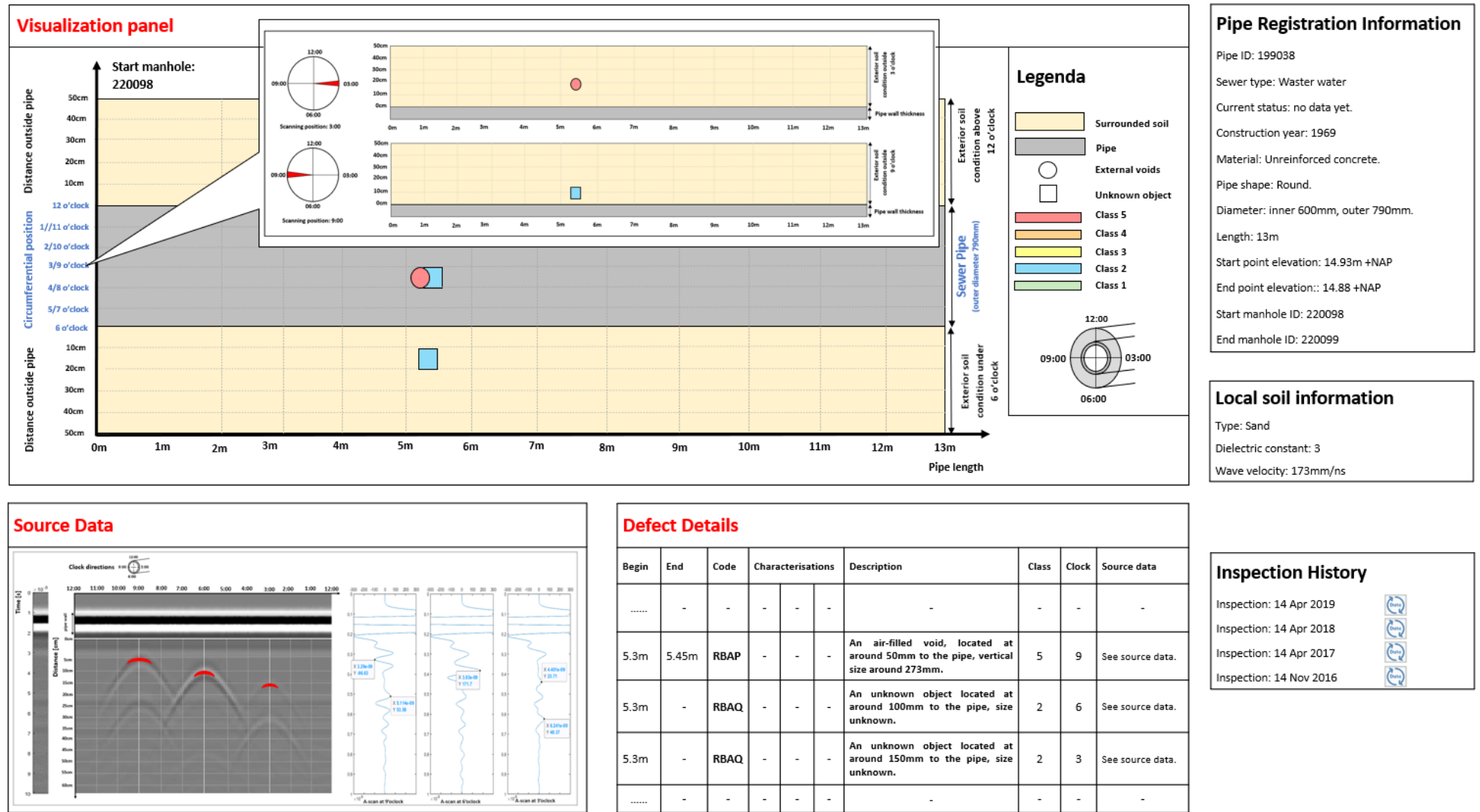


Figure 4-3: The complete interface of the modified in-pipe GPR sewer inspection data visualization with the simulation data presented (pop-up version + planar radargram).

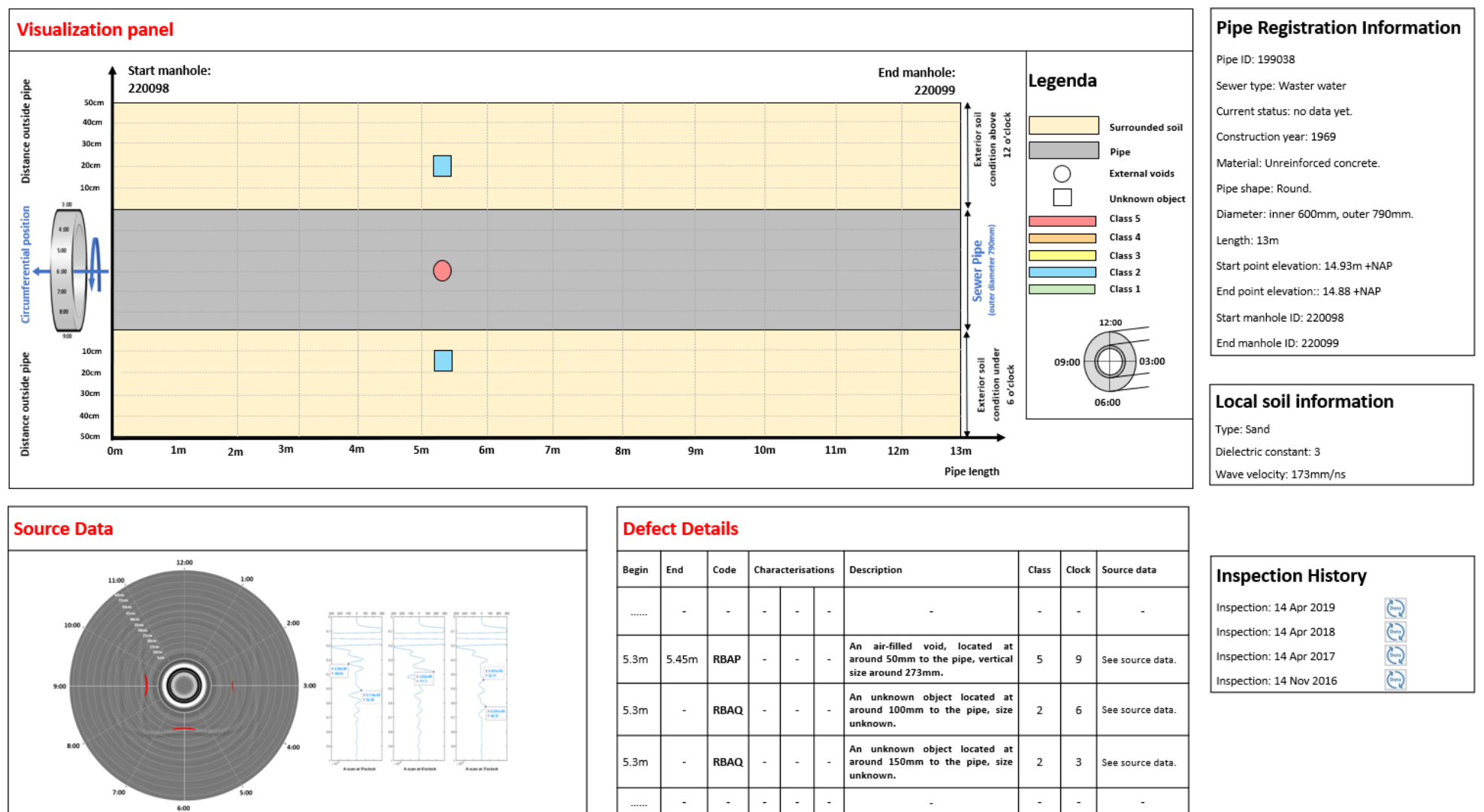


Figure 4-4: The complete interface of the modified in-pipe GPR sewer inspection data visualization with the simulation data presented (pipe-roller version + cylindrical radargram).

As seen from the figures above, the post-processed (planar/cylindrical) radargrams are provided as the source data for the interpreted defects. Moreover, the newly developed additional sewer defect codes (see Appendix L) are used to classify and summarize the defects and their detailed condition information. It is suggested to link the defect shapes in the visualization panel with the corresponding defect codes, i.e., when selecting the defect shape in the visualization panel, the corresponding code is also selected (highlighted), which shows all information related to the defect directly. This suggestion is adapted from *MapKit*, which could save users' effort to actually read the information from the visualization panel. These then solved the remained limitation 2) and 3) of the original 2D representation of sewer pipe wall- soil interface (3).

In summary, the innovative content of "visualization panel", "defect details", "source data" and even the "local soil information" presented in the above graphical designs comprehensively solved the limitations of the originally selected data visualization alternative for visualizing the in-pipe GPR sewer inspection data.

5. Verifying the Developed Visualization Method

The new visualization method developed in section 4.3 needs to be assessed through the verification and validation processes. The validation process requires interaction with users to ensure that their expectations have been fully reflected in the design. However, the intended validation was limited due to the limited availability of users during this thesis project. As a consequence, this thesis cannot make any judgments about the validation of the design.

Therefore, this chapter only evaluates the developed in-pipe GPR sewer inspection data visualization method by verification of the requirements from section 4.2.1. This ensures that each of the requirements formulated and prioritized in Table 4-1 has been fully (reasonably) realized by the proposed visualization method.

Below the requirements from Table 4-1 are listed, the numbering refers to their orders in Table 4-1). For each requirement, an explanation is given to motivate why and how it is verified by the proposed visualization method. To explain how the features and elements as listed in the requirements are addressed, Figure 4-1, Figure 4-2, Figure 4-3 and Figure 4-4 will be referred to. Further, considering the requirements (except requirements 1) and 14)) were formulated based on the conventional CCTV data visualization method, these requirements are regarded as fulfilled by the CCTV data visualization method (see Figure 1-2) by default. Therefore, if the developed visualization performs equivalently on a requirement (i.e., copying the visualization approach, elements and features), the requirement is also regarded as fulfilled by the developed method.

1) *The developed data visualization method must be **applicable** to sewer condition assessment. This specifically means the developed in-pipe GPR data visualization method must be able to visualize the condition data collected from the sewer pipe's exterior environment (**must-haves**).*

This is a general requirement supported by requirements 2), 6) and 7), which provide different elements and features needed for this requirement. This requirement is realized as long as requirements 2), 6) and 7) are realized. A simple verification of this requirement is that the examples of visualizing the defects in the pipe's exterior environment (i.e., objects behind the pipe wall) in Figure 4-1 and Figure 1-2.

2) *Basic **features** for sewer condition assessment must be presented, i.e., representation of the inspected pipe and defects, the coordinate system for ranging pipe's geometry and locating defects (**must-haves**).*

This requirement is realized because, as seen from the example of the proposed visualization method in Figure 4-1, the inspected pipe is represented by its longitudinal front view; defects are represented by the predefined 2D shapes (see the legenda in Figure 4-1, also be noted that although the proposed method only considered defects of voids and unknown objects behind the pipe wall, more can be added to this list depending on the needs of sewer asset manager); and the coordinate system is built based on the length and circumference of the pipe as well as a vertical axis that denotes a certain range of the pipe's exterior environment.

- 4) *The **scale** of the developed visualization must allow it to provide an overview of the entire inspection data collection that shows all defects collected by (and interpreted from) the inspection technology (**must-haves**).*

This requirement is realized because the developed visualization method presents the visualization overview in a longitudinal front view of the pipe and its upper and lower exterior environment, see Figure 4-1 and Figure 4-2. Although the figures only provide defects in one pipe cross-section instead of the entire data collection (i.e., all pipe cross-sections), it can be assumed that the in-pipe GPR data collected at other pipe cross-sections shows no defects. On the contrary, if there were defects detected, they can be registered on the visualization overview in a similar fashion as in the standard CCTV data visualization presented in Figure 1-2.

- 5) *The **scale** of the visualization must allow minor defects (and individual data points) to be visibly seen in the above-mentioned visualization overview(**must-haves**).*

This requirement is realized because the developed visualization represents defects interpreted from the raw in-pipe GPR inspection data with predefined 2D shapes (see the legenda in Figure 4-1). Particularly, the size of these 2D shapes does not necessarily reflect defects' actual size in the visualization (e.g., defects presented in Figure 4-1 are not in similar size but the 2D shapes for representing them are). Thus, as long as the defect is interpreted, it can be registered on the visualization overview to be visibly seen, no matter how small it is.

- 6) *The visualization overview must fully present the pipe's geometry (i.e., full length and circumference of a complete pipe segment) to represent the pipe space that it intends to visualize (**must-haves**).*

As verified in requirement 2) and 0, the overview (including the representation of the inspected pipe) of the developed visualization method presents in its longitudinal front view and its exterior environment at 12 o'clock and 6 o'clock. The pipe's longitudinal front view (contains ten profiles collected from the other circumferential positions) happens to already present the pipe's full length. With that, the "pop-up" window is proposed to pop up corresponding profiles by clicking the clock directions (design clickable) in the Y-axis of the pipe's longitudinal front view (see Figure 4-1), whereas the "pipe-roller" view is proposed to roll the pipe's longitudinal front view (designed scrollable) and replaces the 12 o'clock and 6 o'clock profiles with the other ten profiles (see Figure 4-2). These together represent the pipe space that the in-pipe GPR inspects – the exterior environment of the full circumference and length of the pipe, hence this requirement is realized.

- 7) *Defects and their characterizations and quantifications (e.g., presence, location, type, size and severity) interpreted from the raw data must be denoted in and highlighted from the overall visualization (**must-haves**).*

As verified in requirement 2), the developed visualization method represents defects with 2D shapes, but this only indicates their presence and types. This requirement 7) requires more information about defects, it is realized in the developed visualization method by highlighting the defects from the visualization overview with coded-colors (see the legenda in Figure 4-1), which also indicates their severity; annotating defects' size in the defect details (see Figure 4-3 and Figure 4-4); locating the defect's location is denoted by the coordinate system introduced in requirement 2), which is verified in more details in requirement 11).

8) *The raw/post-processed inspection data of a certain defect shall be presented (**must-haves**).*

This requirement is realized because the developed visualization provided the planar and cylindrical post-processed in-pipe GPR radargrams, see in the source data of Figure 4-3 and Figure 4-4.

9) *All units used in the visualization should be metric (**must-haves**).*

This requirement is realized because, for instance, the pipe's length is ranged in meters (m), see the visualization panel in Figure 4-1; whereas the pipe's diameter and defects' distance to the pipe are measured in millimeters (mm), see the pipe registration information and defect details in Figure 4-3 and Figure 4-4.

10) *The developed visualization must be compliant with the conventional sewer inspection data visualization elements such as the clock directions, severity classes and sewer defect codes (**must-haves**).*

This requirement is realized because the developed visualization **1).** uses clock directions to range the full circumference of the pipe; **2).** indicates the five severity classes with coded-colors; and **3).** provided options to incorporate additional sewer defect codes (for defects (e.g., voids and unknown object) behind the pipe wall; see Figure 4-3 and Figure 4-4. These all are presented in a similar fashion as in the standard CCTV data visualization, which is compliant with the conventional sewer inspection data visualization elements.

11) *The visualization shall be able to graphically present the spatial relationship between defects and the pipe (**should-haves**).*

This requirement is realized by the coordinate system introduced in requirement 2), which locates the defect based on its spatial relationship with the pipe. Specifically, the longitudinal location of defects is denoted in the pipe's full length; the circumferential position of defects is denoted by the twelve clock directions; the distance between defects and the pipe is denoted by the vertical axis that denotes a certain range of the pipe's exterior environment; see Figure 4-1 and Figure 4-2.

13) *The developed visualization method shall **be able to visualize all types of sewer inspection data**, as long as it is interpreted and fits the intended visualization purpose (**should-haves**).*

This requirement is realized because the developed visualization follows the conventional visualization approach from the standard CCTV data visualization. Specifically, it mainly visualizes the sewer condition information (i.e., defects) interpreted from the raw in-pipe GPR inspection data while the raw/processed inspection only acts as the evidence to defects. This means, if a technology different than in-pipe GPR is used to inspect the pipe's exterior environment, the developed visualization method is also able to present the results interpreted from the data collected by this new technology. The type of sensors used and the continuity of the data and its collection process (e.g., continuous data like CCTV videos, discontinuous data like in-pipe GPR radargrams collected from pipe's cross-sections at intervals) will not impose any influence to the visualization.

The following requirement is not fully realized in the developed visualization:

14) The **viewing perspective must first enable requirement 6) and should be in “3D” (must-haves)**.

This requirement is partly realized by enabling requirement 6), see the verification above. The reason for not developing the desired in-pipe GPR sewer inspection data visualization method in 3D is because the alternative **2D representation of pipewall- soil interface (3)** ranked the highest in the MCDA, which is specifically designed for in-pipe GPR and the pipe space it inspects. Although the developed visualization method is not in 3D, it provides a rotatable “pipe-roller” view, which to some extent reflects the 3D features. Further, this thesis suggested a 3D integrated sewer inspection data visualization method that can also visualize the pipe exterior condition, see Appendix N.

In summary, the verification of the in-pipe GPR sewer inspection data visualization method developed in this thesis turned out positive since it successfully realized eleven out of twelve requirements that were prioritized as **must-haves and should-haves**, whereas only requirement 14) was not fully realized as expected. Hence, it is concluded that the developed visualization method was fairly designed, and they are able to visualize the additional sewer condition data, as was formulated (or expected by the users) in the requirements.

Furthermore, the demonstration of the proposed method proves its capability to present sufficient sewer condition information in sewer pipe’s exterior environment to decision-makers for sewer condition assessment in a similar fashion as in the standard CCTV data visualization method (except the way of presenting the full-range pipe’s exterior environment with the “pop-up” window and “pipe-roller” view). Moreover, compared to the original **2D representation of pipewall- soil interface (3)** found in the literature (see Table 4-2), the proposed method extended its visualization range and provided options to include the post-processed in-pipe GPR radargrams and additional sewer defect codes.

During the verification process, it was found there are still several limitations within the process of developing the desired visualization method, i.e., **1).** the design requirements extracted from interviews were not yet confirmed by users; **2).** the users’ specific expectation of seeing 3D visualization was not fulfilled. These limitations will be addressed in the following chapter and recommendations will be suggested to future research to overcome them.

6. Discussion

In this chapter, section 6.1 elaborates on the major contributions of this thesis. Section 6.2 addresses the limitations and provides recommendations for future research to overcome them.

6.1. Contribution

The major contributions of this thesis research are that **1)** it provided a literature review of inspection data visualization methods and concepts within the infrastructure asset industry. This laid a brick to fill up the gaps of missing approaches to visualize the additional sewer condition data collected from non-conventional sewer inspection technologies such as in-pipe GPR; **2)** it developed a new visualization method particularly for in-pipe GPR sewer inspections based on users' expectations and comparison among the available and potential visualization alternatives found in the literature.

In reference to the first contribution, existing literature does not provide such a review specifically about sewer inspections. Further, only a few cases reported in grey literature (Ekes, et al., 2011; Ekes, et al., 2014; Ékes, et al., 2012) provide visualizations of in-pipe GPR data. This was, however, not reported in detail, nor was it based on a prior review of visualization concepts. The visualization proposed in this thesis adds to this by extending its visualization range and included the option to visualize post-processed data and annotated defect codes.

6.2. Limitations & Recommendations

First, this thesis assumed that the assessment of the structural conditions of a sewer takes place by assessing the presence, characterizations, and quantifications of certain defects. However, this thesis did not provide solid references to support this assumption. Thus, it will be interesting for future research to explore the factors that determine the sewer wall's remaining quality and the pipe's exterior condition to verify or refine this assumption. Based on that, future research can also make suggestions on the additional sewer condition data that users should collect and visualize to improve the current sewer condition assessment.

Second, the data used for exploring the in -pipe GPR sewer inspection data processing and interpretation process in this thesis was from simulations. These ideal data presentations do not represent the variability and background noise of data coming from real-life in-pipe GPR sewer inspections. Therefore, if the future research has access to practical in-pipe GPR devices, this thesis suggests researchers reproduce the data processing and interpretation process presented in this thesis with real (or more realistic) sewer inspection data (e.g., collected from in-situ inspections or experiments), to verify if the standardized in-pipe GPR sewer inspection data processing routine proposed in section 3.1.4 is sufficient and comprehensive.

Third, the requirements for developing the final in-pipe GPR sewer inspection data visualization method were formulated by specifying and interpreting users' expectations extracted from interviews (see Table 4-1). The final visualization method developed in this thesis was not validated by end-users for its intended uses, which makes it difficult to conclude about its workability and implementation feasibility. Thus, this thesis suggests future research

to obtain their users' opinions about the extent to which the design complies with their expectations. This may also help to refine the requirements in terms.

A final path for future research could be to experiment with the original **3D pipe reconstruction** visualization concept during in-pipe GPR sewer inspections (i.e., visualizing the sewer condition data while collecting them), and let this serve as the central platform that integrates the sewer condition data from multiple sources (i.e., collected by different technologies from other pipe spaces). Appendix N provided an attempt on this (i.e., an integrated sewer inspection data visualization method was suggested), whereas Appendixes L and M provide other potential elements, data sources that could be input and contributed to this (i.e., the additional sewer defect codes and the impact echo sewer inspection data visualization method were suggested).

7. Conclusion

This chapter first answers research questions in a Q&A form, then provides a general conclusion for the core work and main results of this thesis.

1) *What are users' data needs regarding the current CCTV-led sewer condition assessment?*

The emerging users' data needs arose from the limited detection range of the conventional CCTV inspection, which can only inspect the interior of the sewer pipe. However, the users have developed interests in the pipe wall's remaining quality and condition of the pipe's exterior environment. By assuming the condition of these two pipe spaces are partly defined by the presence, characterizations, and quantifications of certain defects, this thesis translated users' data needs into the needs to collect such information for pipe wall losses, voids, delamination and cracks of/within/on the pipe wall and voids in the pipe's exterior environment (see page 3).

2) *As the complementary sewer inspection technology, what is the state of the in-pipe GPR method in terms of its data interpretation and visualization?*

Although the in-pipe GPR sewer inspection has reached the TRL of Deployment 8: a few recorded implementations. Data processing and interpretation remain complicated. There is a lack of suitable visualization methods to present both raw and interpreted in-pipe GPR sewer inspection data to decision-makers for the condition assessment purpose, which needs particular developments.

3) *Which essential data processing procedures should be taken for interpreting raw in-pipe GPR inspection data into meaningful sewer condition information?*

The in-pipe GPR data processing and interpretation process discussed in section 3.1 suggested that there are three essential steps to take, which are **1). Pre-processing** that improves the quality of raw data, sets up parameters such as wave velocity and (Pipe) Time Zero Correction, and extracts A-scans from defective regions; **2). Post-processed radargrams generation** that produces planar post-processed radargrams by converting the axes of raw data into clock directions VS. distance (or cylindrical post-processed radargrams through coordinates transformation); and **3). Quantifications interpretation** that analyzes the post-processed

radargram and A-scans to roughly identify the detected object, determine its circumferential position, estimate its distance to the pipe and its vertical size (see page 29 for an example interpretation).

4) *What are users' expectations of visualizing the sewer condition information interpreted from the in-pipe GPR inspection data?*

The users' expectations extracted from the interviews with sewer management professionals were, however, ambiguous and incomprehensive. Thus, this thesis amended them with three system expectations from literature about the Abstract Task method. The expectations were restructured and categorized by eight descriptive aspects. These descriptive aspects are **area of application, visualized features, scale, depiction, compatible data types, viewing perspective, ease of creation and future proof**. These descriptive aspects were translated into specific requirements to represent the users' expectations on the desired visualization method in a more comprehensive and systematic perspective (see Table 4-1). Four important requirements are:

1. The visualization must be applicable to sewer condition assessment practice. This means that it should be able to visualize inspection data showing the interior space, wall and exterior environment of a pipe.
2. The visualization must contain the basic features of full-range pipe representation, defect representation, and a coordinate system that ranges the geometry of the pipe and locates the defects.
3. The visualization must be able to show an overview of all data collected from one inspection (of one pipe), which includes identified minor defects (and individual data points).
4. The visualization must include written characters to denote the characterizations and quantifications of defects (i.e., presence, location, type, size and severity).

5) *Among all the available inspection data visualization methods and concepts, which is the most suitable one for visualizing the sewer condition information interpreted from the in-pipe GPR inspection data?*

The literature review led to the identification of eleven visualization alternatives (e.g., **2D Pipe fold-out view (1); 2D linear representation of pipe wall condition (2); 2D representation of pipewall- soil interface (3); 3D pipe with inspection data projected on outer surface (4); 3D Stereo AR sewer data visualization (11); 2D color-coded defects map (6) and 3D pipe reconstruction (8)**). See Table 4-2 for a detailed overview.

Quantitative ranking through an MCDA (see Table 4-4) resulted in the most promising visualization alternative - **2D representation of pipewall- soil interface (3)** for in-pipe GPR. The features and elements from this visualization alternative were integrated into the graphical design of the final visualization method (see section 4.3). The final developed in-pipe GPR sewer inspection data visualization shows the front view of a buried pipe and its upper and lower exterior condition as the visualization overview (see Figure 4-1 and Figure 4-2). Defects such as voids and unknown objects behind the pipe wall are registered on this overview by predefined 2D shapes based on their longitudinal location and circumferential position. The detailed exterior condition at other pipe circumferential positions are presented through the "pop-up" window (see Figure 4-1) or the "pipe-roller" (see Figure 4-2).

6) *What is the feasibility of the final developed in-pipe GPR sewer inspection data visualization method?*

The final developed visualization method was verified by thoroughly examining whether the proposed visualization method has met the requirements formulated with respect to users' expectations (see Chapter 5). Although the verification result suggested that the developed visualization method successfully fulfilled eleven out of twelve highly prioritized requirements while only one requirement was partly realized. The important requirements 1 and 2 were realized by providing a longitudinal front view of the pipe and its upper and lower exterior environment and by including the "pop-up" window and "pipe-roller" view, whereas 3 and 4 were mainly realized by presenting defects in a similar fashion as in the conventional CCTV data visualization. The partly realized requirement is about developing the final visualization method in 3D (see requirement 14)), which is partially realized by providing 3D features through the "pipe-roller" view.

However, due to the lack of validation with end-users' and the difficulty of validating the proposed visualization method in a static graphical form, it is not yet feasible to conclude the workability and implementation feasibility of the developed method. A workable visualization system is needed for this matter.

In summary, this thesis mainly provided a verified visualization method that shows both the post-processed in-pipe GPR sewer inspection data and the corresponding interpreted results to help sewer asset managers from municipalities and asset management organizations assess defects such as air-filled voids and unknown objects behind the pipe wall. The core contributions of this thesis are this proposed visualization method together with the review of existing and potential visualization alternatives for infrastructure inspections.

Limitations relate to the lack of real in-pipe GPR data as a basis for the design of this visualization method, and the lack of end-users' involvement to validate the proposed visualization. Future research should target these weaknesses by **1).** collecting real (or more realistic) in-pipe GPR sewer inspection data to reproduce and testify the standardized in-pipe GPR data processing; and **2).** implementing the proposed visualization method into a workable sewer condition data visualization system for future validation.

Finally, as observed in this project, the "comprehensive sewer condition assessment" based on multiple data sources is promising for the industry. This study thus recommends asset management companies to incorporate the proposed in-pipe GPR sewer inspection data visualization method into their sewer management system, and to consider the side-products suggested in Appendixes K, M and N (i.e., additional sewer defect codes, impact echo and integrated sewer inspection data visualization methods).

Appendixes

A. Interview Setups and Questions

Table 0-1: Contacts of interviewee arranged for interviews

Interviewed Person	Function/organization	Email address	Note
Mr. Patrick Zwerink	Sewer manager Hengelo	p.zwerink@hengelo.nl	
Mr. Freddy Verhoeven	Van der Velden Rioleringbeheer Manager	Freddy.Verhoeven@vandervelden.com	

Needs to improve CCTV inspection (mainly on the visualization)

- 1) Which sewer GIS software are you currently using to register/show the sewer health condition?
- 2) Are you familiar with the CCTV data visualization? How is a defect determined as severe or not (judged by the inspector based on NEN)? Isn't this subjective?
- 3) Is the CCTV inspection result sufficient for making decisions on sewer management work as you think? Considering the CCTV can not see outside the pipe and it cannot evaluate the remaining strength of the pipe.
- 4) If not, what is a complete and comprehensive sewer inspection for you? Also considering the costs, what is your priority on knowing the condition of a sewer?
- 5) What do you think shall be improved in terms of current CCTV inspection? What data do you think is missing for better, predictive decisions? (e.g., do you feel it's necessary to add the inspection of voids outside the pipe?)

Opinions on the new technologies

- 1) Have you thought about applying other inspection technologies to make the sewer condition more accurate and comprehensive? Why and why not?
- 2) Do you know in-pipe GPR and impact echo (GPR can find objects in the soil and impact is widely used in concrete evaluation)? In my thesis I attempt to use in-GPR to find voids outside the pipe and impact echo to find thickness reduction of the pipe, voids, delimitations within pipe wall and cracks on the pipe outer surface)?
Do you think they can complement CCTV in terms of data collection and visualization?
- 3) How do you prefer inspection outputs from these new technologies to be presented (considering raw data as well as interpreted results)? How do you want to see them? Presented like CCTV results?
- 4) For voids around the pipe, do you have a severity classification yet (e.g., in terms of size, depth and distance to the pipe)? If a new code is needed for this defect, how do you determine its severity (classify it from 1-5)?

Data integration and visualization

- 1) CCTV, in-pipe GPR and impact echo together make sewer inspection more complete. If we have such a multi-sensor system, can you imagine how the data will be integrated and presented together?
- 2) How do you see the possibility of the integration of these data with CCTV by following ideas such as pipe 3D reconstruction and extended CCTV visualization method, do you have any suggestions?
- 3) As a potential user, what are your expectations or requirements on such an integrated sewer condition data visualization tool that I am going to develop?

B. Interview Results

Hengelo municipality

The sewer managers from the Hengelo municipality, Mr. Patrick and Mr. Broens, have shown great interest to know more condition information of the sewer through additional technologies like in-pipe GPR and impact echo. They think this could bring more accurate repair and replacement suggestions to their sewer maintenance work. As they introduced, Hengelo currently only inspects the sewer with CCTV (usually 10% of the total pipes per year), process and make use of the inspected data in accordance with the NEN regulations.

The often-seen sewer defects are cracking (BAB), surface damage (BAF) and so on. When observed from CCTV footage, they will be visualized and classified (done by the CCTV inspectors) in the Kikker software that uses the same visualization method as introduced in Figure 1-2. The sewer managers have also explained that making in time sewer management decisions requires them to know exactly where, when, and how a pipe should be repaired or replaced, it is all about prioritizing. In addition to the defect severity, prioritizing also needs to take factors such as house connections, traffic concerns, economical influences, and costs into account (which is a complicated process done by the Rolsch software – Rasmariant). Based on that, the Hengelo municipality makes short-term (5 years) and long-term (5-10 years) plans to rehabilitate their pipes.

They think the current CCTV inspection cannot provide information about the pipe thickness and remaining strength. They have also looked for new inspection technologies such as laser scanning, but it is not yet practical to be applied in pipes. After knowing such information can be collected through impact echo and in-pipe GPR, they wish the data output from them to be generic, readable, shareable and future-proof, and most importantly, financially reasonable. While responding to the question of providing suggestions to the final data integration and visualization tool, they are very interested to see the 3D pipe reconstruction. They think this could be the future trend and can be further developed to include the road condition above the pipe.

Almelo CCTV inspection team

Mr. Verhoeven and Mr. Kropman, as the managers of the Almelo sewer CCTV inspection team - Van der Velden Rioleringsbeheer B.V., took the interview through a questionnaire. Mr. Verhoeven and Mr. Kropman gave answers to the questionnaire on behalf of CCTV operators and inspectors who are direct users that involve in CCTV inspection operation, data processing, interpretation, and registration.

Very important news from Van der Velden is that a new standard will be applied in the Netherlands from 2020, whereby classification of the defect's severity is left for sewer managers to decide, the CCTV inspector only needs to register all measured values of the defect that he/she has observed (the measured values are determined based on measurements with laser points in tenths of millimetres). This issue is confirmed by one of the examination committee members – Mr. Molegraaf and the Hengelo sewer managers. The Hengelo sewer manager, Mr. Patrick has also pointed out that the measured values of defects in a sewer pipe are recorded in a “.ribx” file, which will be imported into the sewer management system of the municipality. Because the system has incorporated the agreements (the upper and lower limits can be adjusted by the local sewer manager, thus it might be different in each municipality) about classifying the defect severity, it can determine and assign specific classes of severity to certain defects by matching the agreements with the measured values. In this way, the influence on the sewer management decision-making brought by the CCTV inspectors' subjective opinion can be reduced.

As a CCTV inspection team, Van der Velden thinks the CCTV-led sewer condition assessment is already sufficient for sewer managers to make effective decisions on the following maintenance work because most of the sewer damages happen inside the pipe. But on the other hand, they have also realized that more information about the problem might be needed in terms of events like subsidence or visible cavities (possibly this is not visible from inside the pipe). For such events, they usually advise the sewer managers to take additional research to find out the cause or extent of the problem, expressions of such additional research can often refer to open-cut trench excavation along the pipe. Instead of in-pipe GPR or impact echo, Van der Velden is interested in an innovative sewer drone inspection technique, which flies a drone into confined pipe space caused by high water level, large obstacles, or severe collapses that restricts conventional CCTV platform to drive through. With such an inspection technology, they aim to keep focusing on inspecting the internal pipe condition visually, increase the inspection range and productivity. Moreover, the 3D pipe reconstruction method of sewer drone attracts a lot of their attention, which further proves the 3D data visualization method is an expected ideal data visualization method for the users.

While explaining their needs on knowing more condition information of the sewer, Van der Velden requires to present the inspected data as detailed and straightforward as possible. This can be mainly related to the location and extent of certain damage (also the elevation/depth if necessary), for example, the pipe wall thickness, besides providing the measured numbers, they suggested to also use different colors to highlight the reduced pipe wall thickness. More importantly, the file with the visualization and the registered data must be compatible with the inspection software that is currently being used.

C. Translating Users' Additional Sewer Condition Data Needs into Specific Defects

As mentioned in section 1.1, the additional sewer condition data that users desired to know is either from the pipe exterior environment or within the pipe wall. More importantly, they were translated into specific defects. In this section, each of these defects is introduced in detail, including how they are formed, why they are important to the sewer structural integrity and so on. Among that the most important part is, characteristics and quantifications of each defect are defined in this section, which helps to quantify the judgment of the severity of the defects (used in the development of the additional sewer defect codes in Appendix L).

Voids behind the pipe wall

External voids could form from reasons like design errors, inappropriate construction operations (e.g., wrong bedding/backfill material) and soil erosion (Balkaya, et al., 2012; Moore, 2008). An example of the void formed from soil erosion and its consequence is presented in Figure 0-1. The void comes into existence because the soil leaks into the sewer through a small fracture. When the soil enters the pipe, the flowing wastewater moves them away, the more soil enters the pipe and gets flushed away, the bigger the void develops. When the soil between the ground surface and the pipe is all gone, the ground will sink and the pipe will collapse directly (Boven, 2019).

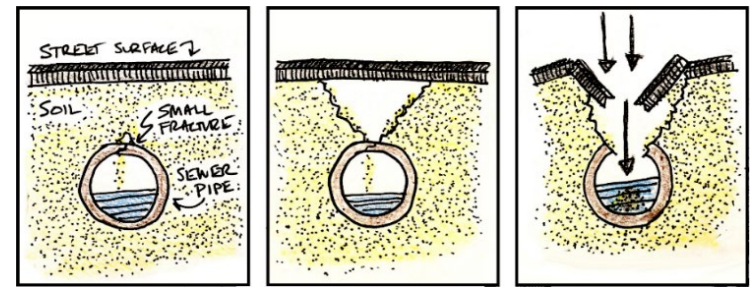


Figure 0-1: Voids formed because of pipe cracking and erosion (Boven, 2019).

Even on a less severe extent, the voids outside the sewer could result in pipe vertical/horizontal misalignment (see Figure 0-2) since a considerable part of the bearing capacity has to deal with the increased local bending over the void (Balkaya, et al., 2012). If the deterioration of soil support is not fixed in time, it could result in undermining of the overlying structure (as the sinkhole in Figure 0-1 shows).

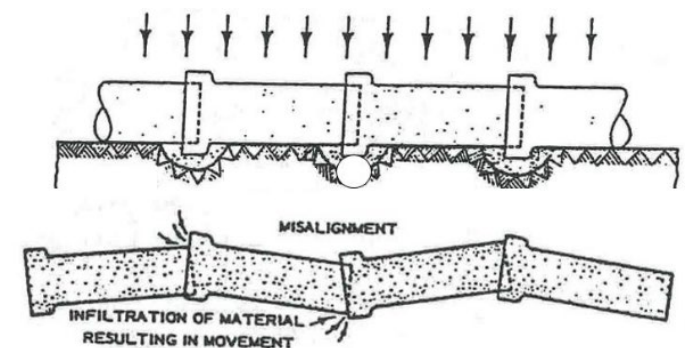


Figure 0-2: Misalignment caused by voids (NYSDOT, 2018).

The consequence of pipe failures caused by external voids does not only include collapses of the sewer itself, but also the damages to the above infrastructures (which might cause fatal traffic accidents) and the pollutions brought by the escaped wastewater. Such consequences are difficult and costly to remedy and some are even impossible to be restored (e.g., deaths) (NYSDOT, 2018). To prevent such events from happening, it is important to determine the void's severity and take measurements to deal with it accordingly. Hence, the following information is suggested to collect for further describing and classifying the severity of an external void:

- **Location of the void.** According to (Balkaya, et al., 2012; Kamel, et al., 2008), the minimum safety factor of a pipe decreases as the void gets closer to the joint (longitudinally) while the vertical displacement increases as the void move from the pipe crown to the invert (circumferentially).
- **If the void was observed in the vicinity of other defects that may cause soil erosion.** See Figure 0-1, soil erosion could accelerate void development.
- **Void type.** Both air void and water void could impose threats to the pipe's structural integrity, but only air void is studied in this thesis.
- **Distance to the pipe.** Usually, a void caused by soil erosion is in close contact with the pipe (see Figure 0-1). But it is also possible that a void is in a distance to the pipe. The smaller the distance is, the larger threat it brings to the pipe.
- **The void size** refers to its longitudinal length, depth and circumferential width. Any aspect of these three increases could increase the probability of pipe failure (Kamel, et al., 2008).

Pipe wall thickness reduction

Changes in sewer pipe wall thickness are often expressed as thickness reduction, which can usually be explained by surface damages. The surface damages are either caused by chemicals (e.g., corrosion) or mechanical actions. Besides that, if the inner lining is damaged or detached from the pipe wall, it can also play a role in reducing pipe wall thickness (see Figure 0-7 as an example). The part where pipe wall thickness often reduces is the lower part of the pipe since it is below the waterline and has the most chemical/mechanical contacts with the wastewater flow.

The collected thickness information can act as an indicator of the pipe remaining strength (if the pipe wall thickness reduces, the load-bearing capacity of the pipe is reduced too). It can also be used to verify the CCTV inspection results, for example, if there is a surface damaged (e.g., chemical erosion) on the pipe wall but it is not observed in the CCTV results, the thickness reduction known from impact echo can provide a notification to the sewer manager, then she/he can check the CCTV video again and find the erosion. By any means, gaining the knowledge about changes in pipe thickness and further to determine the extent of other defects can greatly help to determine the remaining lifespan of the sewer (Pleijssier, 2019). The thickness reduction can be measured by **reduced thickness in mm** or **the ratio between the reduced thickness and the total pipe wall thickness**, the **size of the area with thickness reduced** should also be measured.

Internal voids

Inside any concrete structure, voids are inevitable due to the use of chemical admixtures or improper vibration during the casting, there is no difference for concrete pipes. Air voids can often be seen on the surface of the concrete structure (see Figure 0-3) or exist inside the concrete. The size of these voids varies from smaller than 1mm fine/entrained air voids to larger coarse/entrapped voids (assuming the void is a sphere).

Though the manufacturer has the responsibility to ensure all produced concrete pipes are void-free, it is still possible the installed sewer pipe has internal voids in it, which could reduce the bending resistance and strength. Even when the voids are relatively small, they can act as storage to keep the reinforcement being corroded once hairline cracks occur and create accesses for corrosive wastewater to contact the steel reinforcement, which



Figure 0-3: Concrete surface voids, source from Google.

weakens the concrete-steel interface and results in premature failures. The following information is suggested to collect for further describing and classifying the severity of an internal void:

- **Void location.** The longitudinal location and circumferential position of the void should be recorded.
- **The void size** refers to its longitudinal length, depth, and circumferential width. Any aspect of these three increases could increase the probability of pipe failure (Kamel, et al., 2008). E.g., the void with a diameter that reaches the reinforcement could increase the probability of delamination and debonding of the reinforcement.

Surface cracks

Cracking of concrete structures generally occurs at points when tensile stress exceeds tensile (Tran, et al., 2018), which can often be seen in load-bearing infrastructures like pavements and sewer pipes. The examination of cracking is usually visual-based, however, this can be troubling in a sewer pipe. Because the in-pipe environment often lacks lighting and the pipe inner surface is often patterned with complex textures and other spurious features (Browne, et al., 2007). Very possibly the minor cracks on the pipe inner surface are not detected (imagine Figure 0-4 left is a used sewer) or the cracks on the outer surface of pipe are completely ignored (see Figure 0-4 right, the cracks are outside the pipe and the pipe inner surface is still intact).

Cracks on the pipe surface can be in longitudinal, circumferential, or other complex orientations, whichever could reduce the pipe strength and bring negative impacts to the pipe structural integrity. Even when the cracks are minor, they can increase in size and numbers over time and eventually lead to severe problems like delamination, in/exfiltration, erosion voids, or pipe collapses. It is mentioned in (BS_EN_13508-2:2003+A1, 2011), the main criterion used to determine the severity of a crack is its **width**, other criteria such as its **depth** into the pipe thickness and **longitudinal/circumferential length** can also be considered. In this thesis, it is suggested to follow the sewer coding system from (BS_EN_13508-2:2003+A1, 2011).



Figure 0-4: inner pipe cracks (left) and outer pipe cracks (right).

Delamination

Because of the steel cylinder/rebar or prestressed cables inside the commonly used sewer pipe, it can be divided into several layers, bounded by different interfaces (see the cross-section view in Figure 0-5). With such a composite structure and harsh conditions like continuous heavy traffic impact and exposure to wastewater, delamination of the composite structure could occur and comprise the integrity of the pipe.

The delamination often discussed are mechanical delamination, which describes the physical separation between layers, such as interior splitting of concrete, debonding of the concrete-steel interface, and long-term corrosion (Garcia, et al., 2017). As shown in Figure 0-6, delamination often starts from (hairline) cracks. The crack allows water to get in, erode and damage the reinforcement, finally loosen the bonding between layers and cause delamination and further pipe structural issues (see Figure 0-7, the concrete lining at the pipe lower part is washed away because of delamination).

It is found both the **size** and **depth** of the delamination are critical indicators to classify the health condition of the concrete structure (Garcia, et al., 2017). It is also mentioned in the introduction to Figure 0-28, that the relative flaw size has significant effects on the impact echo response, therefore the WTDR (width-to-depth ratio, $\frac{d}{T}$) can be an ideal quantification to integrate all related indicators and determine the delamination severity, if all parameters needed can be collected by impact echo. Note the delamination size (d) means the circumferential dimension of the pipe, and the depth (T) means the wall thickness minus the distance from the pipe inner surface to the top of the delamination.

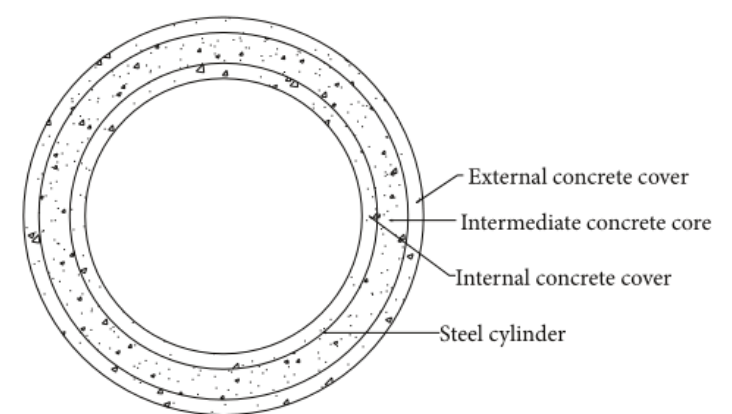


Figure 0-5: Cross-section of a reinforced concrete pipe (Gong, et al., 2015).

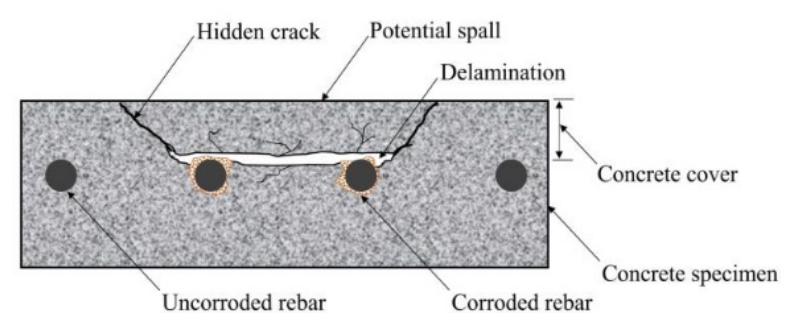


Figure 0-6: Delamination formation, from (Mac, et al., 2019).



Figure 0-7: Delamination at the pipe bottom, source from Google.

D. Technology Readiness Level Scale

Phase	TRL	Hardware	Software
Research	1	Basic principles	
	2	Concept and application formulation	
	3	Concept validation	
Development	4	Experimental pilot	
	5	Demonstration pilot	
	6	Industrial pilot	
Deployment	7	First implementation	Industrialization detailed scope
	8	A few records of implementation	Release version
	9	Extensive implementation	

Figure 0-8: TRL (Technology Readiness Level) scale, source from (Blanc, et al., 2017).

E. Time Zero Correction

As shown in the Figure below, a plain radargram was first generated by reading the gprMax .out file and cut off its white margin. With this plain radargram (without XY-axis and margin), the first positive peak of each trace in the radargram was read, then a mean time zero is calculated (see the workspace, the timeZero is at pixel 52.8713 in total 536 pixels (representing the 10ns time window) along the Y-direction of the radargram. By converting the pixel number into time, Time Zero = 1ns was obtained. The calculation of Pipe Time Zero was as presented in the distance simulation data analysis (see page 22). Both Time Zero and Pipe Time Zero were plotted on the radargram by a green line, figure 3 in the figure above shows the radargram with the data before Time Zero cut off.

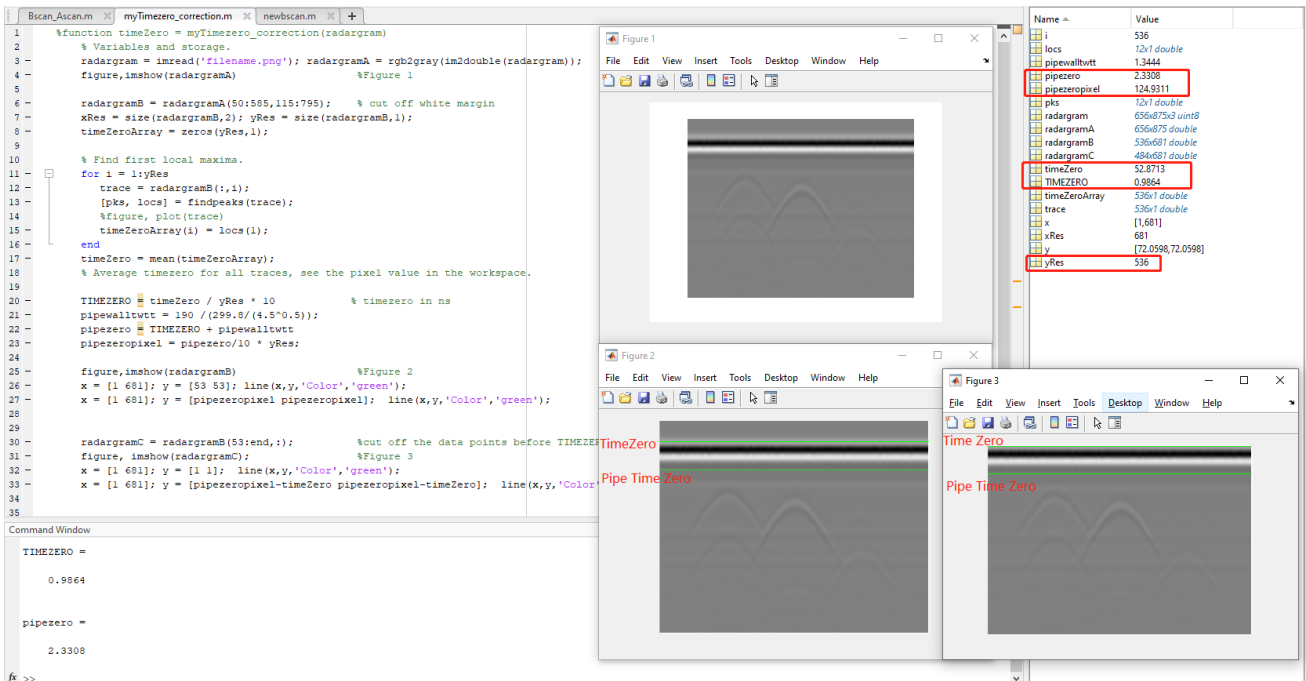


Figure 0-9: Calculating and plotting Time Zero and Pipe Time Zero, screenshot from MATLAB.

F. Coordinates Transformation

The coordinates transformation is rather simple since it is an image processing procedure after all, there is no need to manipulate the source data. As seen in the screenshot below, a planar radargram is first imported as the input file (figure 1 in the screenshot below). After simple cropping, the white margin of the input image was removed. Then the *imagecartesian2polar* function was used to transform the planar radargram into a cylindrical radargram.

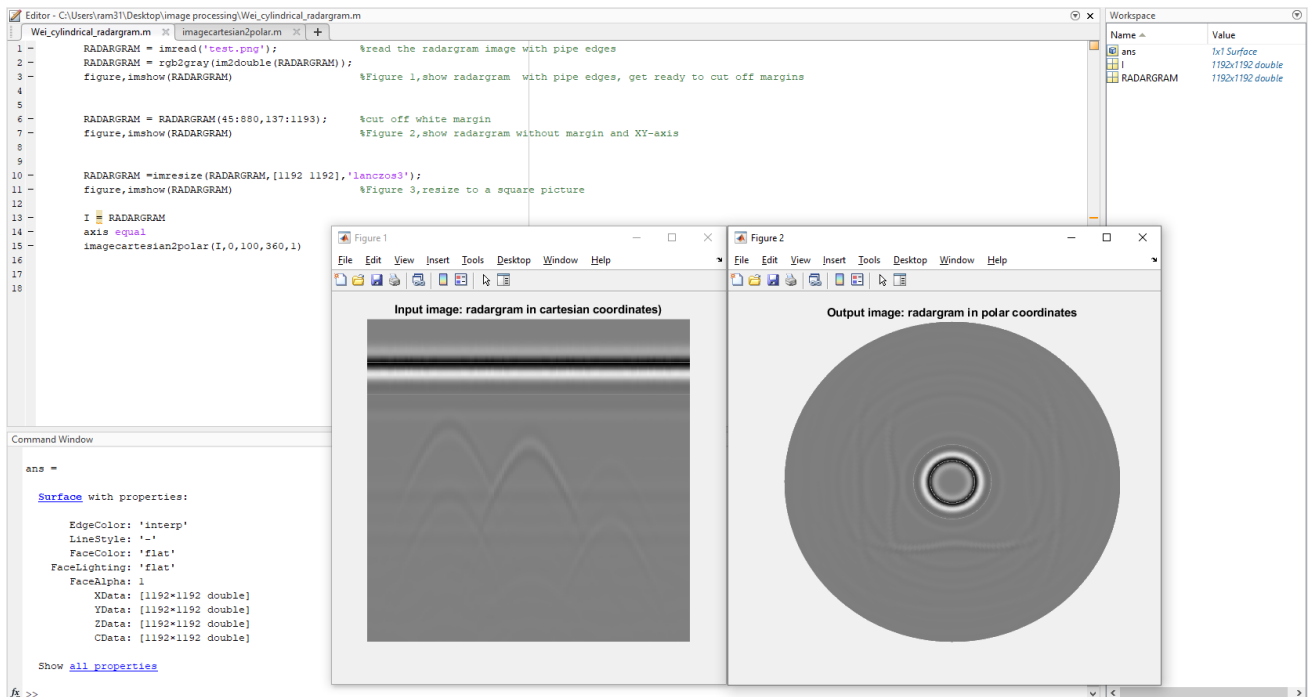


Figure 0-10: Transforming the planar radargram into a cylindrical radargram, screenshot from MATLAB.

See the codes of the *imagecartesian2polar* function in below, source from (Islands, 2011):

```
function [H]=imagecartesian2polar(I,radius_min,radius_max,angle,make_square)
% IMAGECARTESIAN2POLAR converts a given bidimensional gray color image from cartesian coordinates to polar coordinates according to usually B-
mode ultrasounds image representation.
%The input image, I(i,j), is mapped (rows->columns) to (double) polar coordinates (xx,yy) and then represented as a surface (I(xx,yy))
% Input:
%   I:          bidimensional graycolor image
%   radius_min : min radius length (by default 0)
%               accepted values: min_radius>=0
%   radius_max : max radius length {max_radius>min_radius} ( by default 100)
%               accepted values: max_radius>min_radius
%   angle:      # of angles to be considered for decomposition (by default 60)
%               (degrees). The polar representation spans the interval
%               [-angle/2,angle/2]
%               accepted values: 0<=angle<=360
%   make_square: option to transform the input non-square image to a square MxM or NxN image (the biggest one).
```

```

        %To accomplish that, the image is resized. The purpose of this is only to force always the output image to show the
        appearance to the normally seen on echographic systems. This option accepts a value (by default 0):

%           0: the input image is not resized
%           1: the input image is resized

clc; close all;

% Check the argument data
if (nargin < 1)
    error('Error in the number of arguments (it should be >0). Use: I,radius_min,radius_max,angle,make_square');
end

% Check if there are some arguments by default

if exist('radius_min','var') == 0
    radius_min = 0;
end

if exist('radius_max','var') == 0
    radius_max = 100;
end

if exist('angle','var') == 0
    angle = 60;
end

if exist('make_square','var') == 0
    make_square=0;
end

% Check if the input argument data are valid
if (radius_min < 0)
    error('radius_min sholud be >=0')
end

if (radius_max <= radius_min)
    error('radius_max sholud be >radius_min')
end

if (angle<0 && angle>360)
    error('angle sholud be 0<=angle<=360')
end

if (make_square ~= 0 && make_square ~= 1)
    error('make_square sholud be either 0, or, 1')
end

% Plot the input image (rectangular coordinates)
figure(1) %I=imadjust(I); %activate if needed
imshow((I)); title('Input image: radargram in cartesian coordinates')
[M N]=size(I);

% If the option make_square==1, the input image is resized
if make_square==1
    if(M>N) dim=M;
    else dim=N;
end

```

```

end

I=imresize(I,[dim dim]);

[M N]=size(I);

end

% We rotate pi/2 the input image to have the desired view
I=imrotate(I,90);

% The mapping from cartesian to polar coordinates
theta_max=angle;
step_theta=theta_max/(N-1);
step_r=(radius_max-radius_min)/(M-1);
[r,theta] = meshgrid(radius_min:step_r:radius_max, -theta_max/2:step_theta:theta_max/2);
xx=-r.*cos(theta*pi/180)-radius_min;
yy=-r.*sin(theta*pi/180)-radius_min;

% Map the input image I to the polar coordinates xx, yy and represent as
figure(2);
H=surface(yy,xx,im2double(I),'edgecolor','interp');
colormap(gray)
view(0,90)
axis off
title('Output image: radargram in polar coordinates')

%%%%%%%%%%%%%%%%%%%%%%%%%%%%%%%%%%%%%%%%%%%%%%%%%%%%%%%%%%%%%%%%%%%%%%%%
% Author: Luis Gomez Deniz, Nov. 2011
% CTIM (Image Technology Center), University of Las Palmas Gran Canaria
% the Canary Islands, SPAIN
% lgomez@ctim.es
%%%%%%%%%%%%%%%%%%%%%%%%%%%%%%%%%%%%%%%%%%%%%%%%%%%%%%%%%%%%%%%%%%%%%%%%

```

G. Detailed Visualization Alternatives Found in Literature

Table 0-2: A systematic literature review on possible inspection data visualization methods and concepts

Visualization methods/concepts	Description	Visualized features	Graphical examples
--------------------------------	-------------	---------------------	--------------------

A. 2D CCTV pipe fold-out view

- This visualization is specifically designed to visualize sewer condition data collected by CCTV and other visual inspection techniques, it presents defects from the pipe inner space and surface (e.g., obstacles and cracks).
- The raw data is usually visual-based (e.g., videos and images captured by the CCTV camera), which is collected continuously along the pipe. Sometimes simple data pre-processing procedures (e.g., filter out invalid data, enhance image quality) are needed to get the raw data ready for interpretation if the data quality is not good. Besides that, the raw data always needs to be visually observed by certified inspectors and interpreted into presentable sewer condition information before visualizing.
- Depiction methods used in this visualization are various. First, a meshed rectangle is used to represent the pipe itself; then defects are marked by small circles, rectangles and pop-up annotations on the meshed pipe rectangle according to their location and continuity; coded colors are used to indicate the damage severity of each defect.; last but not the least, sewer defect codes are used to enhance the defects' interpretation.
- The unfolded pipe is presented in a 2D planar view while users look at it from the top.
- The scale of this visualization is fixed at a level that allows all defects to be visible compared to the entire visualization (as long as they are interpreted and registered).

- The main visualized items are:**
- The unfolded pipe sketched as a long meshed rectangle.
 - Defects inside/on the pipe and their condition information are denoted by shapes and colors as well as annotations (pop-up).
 - Defect codes.
 - Defects' source data (raw images and videos).
 - Coordinate system (X-axis represents the pipe length while Y-axis represents the clock direction).
 - Pipe registration information.
 - Historical inspection data records.

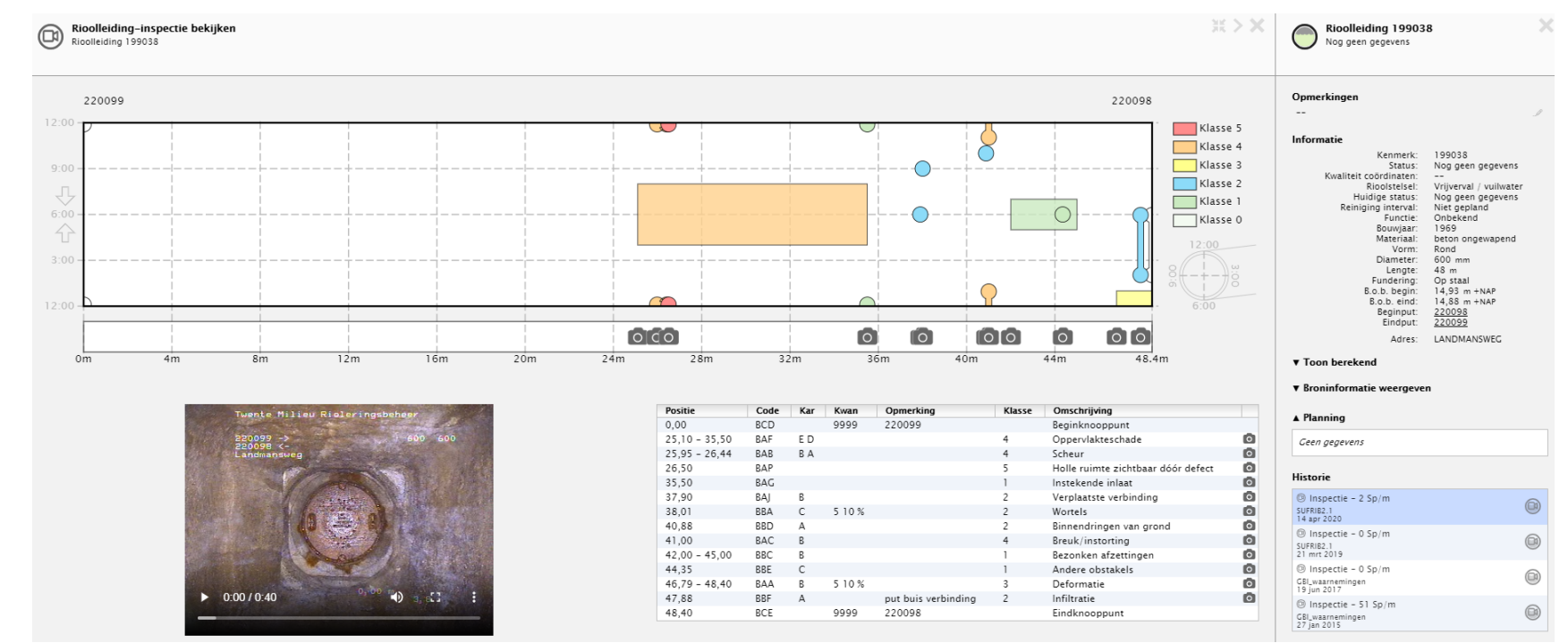


Figure 0-11: Example of the CCTV inspection data visualization: CCTV pipe fold-out view, source from the screenshot of MapKit.

B. 2D Full-range pipe fold-out image

- This visualization is designed for sewer condition data collected by continuous scanning inspection techniques like SSET (Sewer Scanner and Evaluation Technology), LIDAR scanning, etc. It is particularly suitable for visualizing pipe inner surface damages like holes, cracks, loss of pieces, erosions and even intruding roots.
- Data types compatible with this method are various, but to generate a full-range image of the pipe inner surface, the data must be collected continuously (or technique like image stitching can be used). If the collected data is visual-based and the resolution is sufficiently high, pre-processing is usually very simple like the pre-processing in **Visualization A** or not even needed (because the interpretation is directly performed on the visualization). If the data is collected by other sensors, e.g., LIDAR scanning, certain data pre-processing procedures are needed to get the raw data ready for interpretation, which might require experts' skills and specially designed data processing tools.
- As seen in the example at right, defects can be visually observed from the image directly, even without interpretation. The main depiction method used here is annotating the defects at corresponding locations on the image, coded colors and shapes can also be used to enhance the data interpretation.
- The visualization is presented in a 2D planar view while users look at it from the top.
- In essence, this data visualization is a high-resolution image of the pipe inner surface. As also seen in the example, the visualized pipe is either long or large, thus minimal defects are all visible, especially after they were interpreted and annotated.

- The main visualized items are:**
- A digitized computer image that shows the inner surface of the sewer pipe is a fold-out view.
 - Defects in/on the pipe inner space/surface and their condition information, which are mainly denoted by annotations.
 - Defects' source data. The visualization itself is made of raw data. But bear in mind, it is not a "visualization" until it is interpreted.
 - The coordinate system used is not introduced in the literature, assuming it uses the same coordinate system as the CCTV pipe fold-out view.

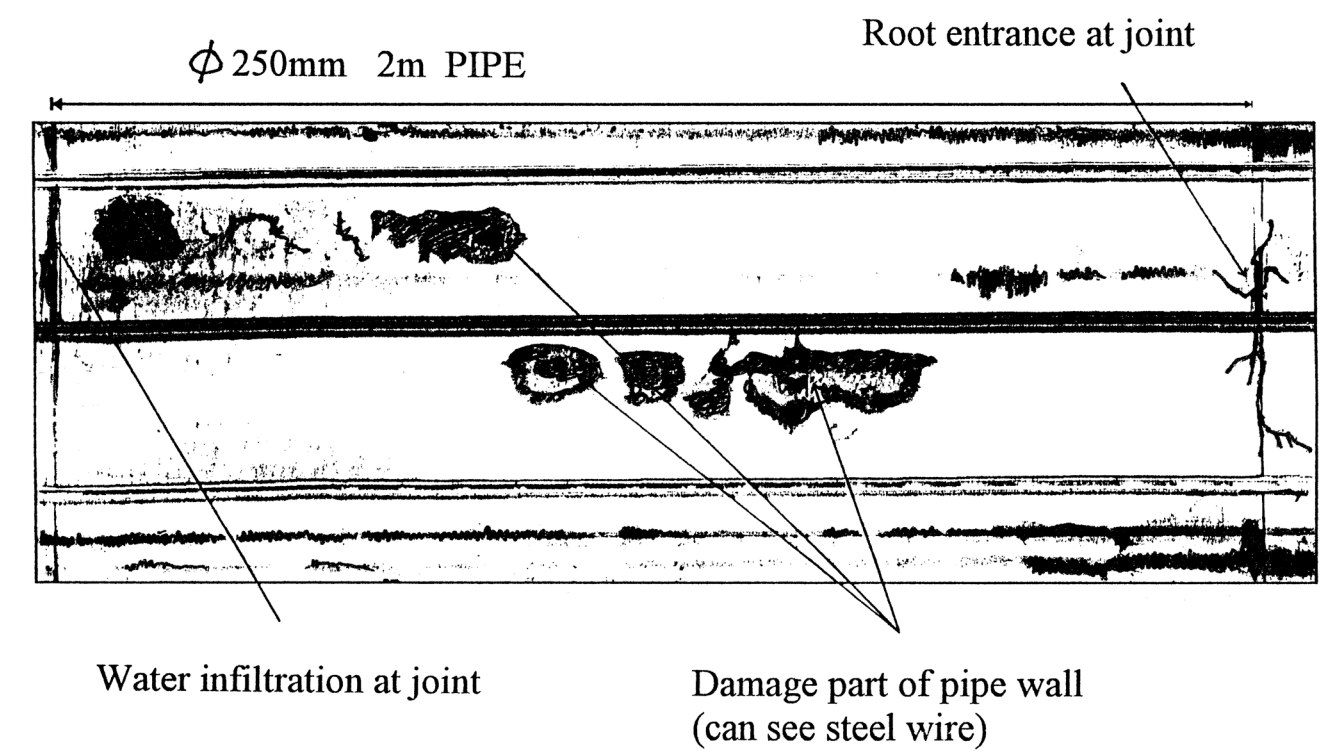


Figure 0-12: Sample image of the sewer pipe SSET system, source from (Wirahadikusumah, et al., 1998), similar examples can also be found in (Kirkham, et al., 2000).

C. SewerVUE – 2D Linear representation of pipe wall thickness and rebar configuration

- This visualization is designed to visualize condition data collected for the sewer pipe wall, particularly for the pipe wall thickness information and condition within the pipe wall.
- In the example, the collected raw data is the basic GPR data (wiggly traces and radargrams), which is collected along the pipe in small intervals. The data needs certain pre-processing procedures (e.g., filtering, background removal, etc.) to get the data ready for interpretation. The pre-processing and interpretation usually requires experts' skills and specially designed data processing algorithms or software.
- As seen in the example, the pipe wall thickness is represented by a continuous black line while rebar cover variations are represented by bar graphs. Besides that, the red dots mark the average rebar cover of a small interval, internal defects such as voids are denoted by small yellow rectangles.
- The visualization is presented in a 2D planar view, but it actually represents a front cross-section view of the pipe (imagine unfold the pipe and look through its thickness along the pipe length). **The limitation of this view is, it only provides the pipe thickness information of one certain circumferential position instead of all.**
- As seen in the example, the visualized pipeline is often very long, which might cause minimal data points (e.g., minor thickness loss) invisible in the visualization overview. This can be easily solved by a "zoom in" function.

- The main visualized items are:**
- The pipe that is represented by the X-axis (including the location of manholes).
 - Pipe condition information such as variation of the pipe wall thickness, variation of the rebar configurations (i.e., the thickness of the rebar cover) and defects within the pipe wall and their location (e.g., voids). **Note the circumferential position of this information remains unknown.**
 - Defects' source data. The lines are made of raw data.
 - Coordinate system (X-axis represents the pipe length while Y-axis represents the pipe wall thickness).

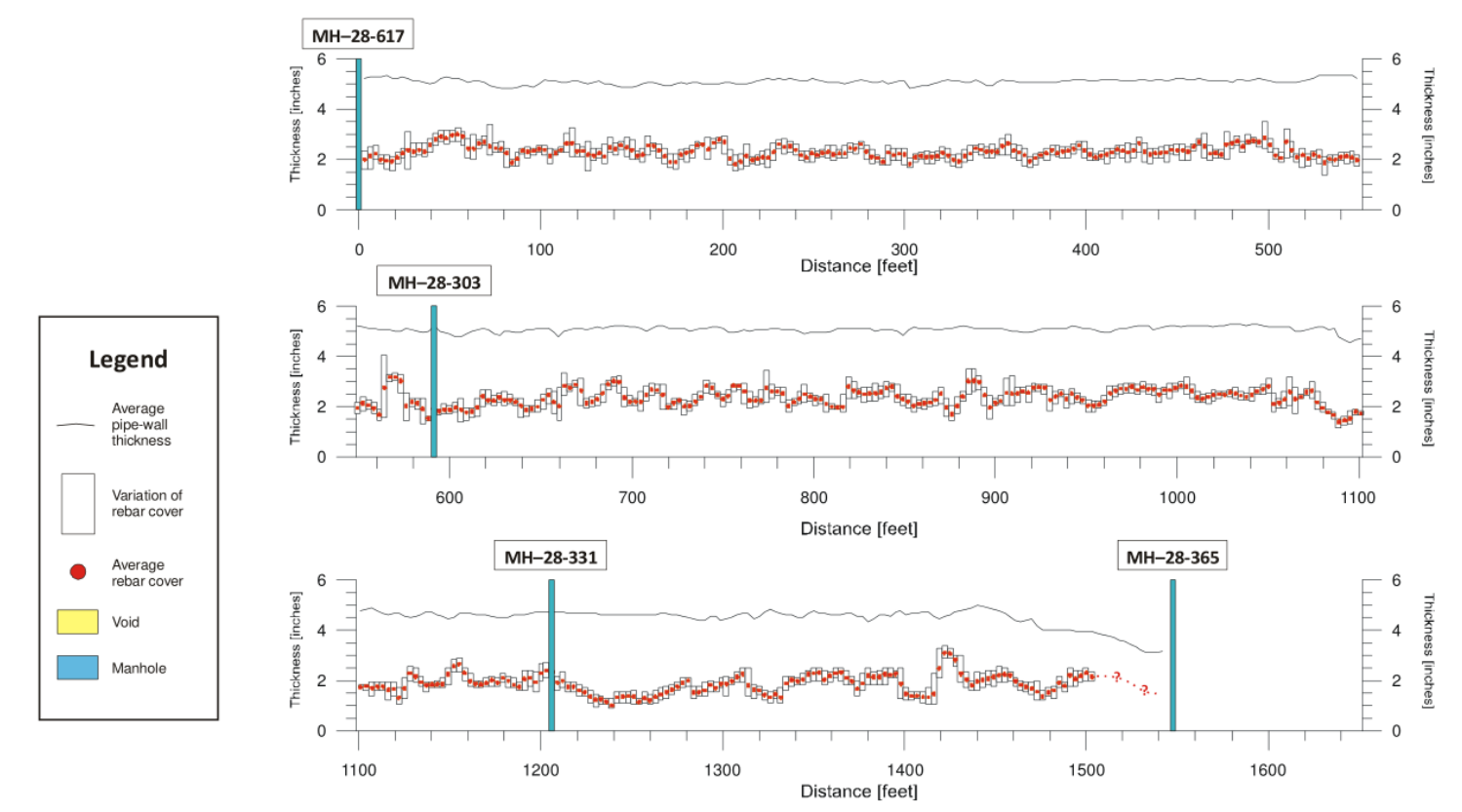


Figure 0-13: Example of the SewerVUE – Linear representation of pipe wall thickness and rebar configuration, source from (Ekes, et al., 2014).

D. SewerVUE integrated – 2D presentation of pipewall-soil interface

- 1) This visualization is designed to visualize the condition data within and outside the sewer wall, particularly for the pipe wall thickness information and condition within/outside the pipe wall.
- 2) In the example, the collected raw data is the basic GPR data (wiggly traces and radargrams), which is collected along the pipe in small intervals. The data needs certain pre-processing procedures (e.g., filtering, background removal, etc.) to get the data ready for interpretation. The pre-processing and interpretation usually requires experts' skills and specially designed data processing algorithms or software.
- 3) The interpreted results are superimposed on the actual depth profiles versus distance, see the top of Figure 0-14A, four individual in-pipe GPR profiles with corresponding clock positions are presented. The green layer represents the pipe wall while above the green layer is the pipe external environment. Anomalies and other notable features are denoted by shapes and highlighted by coded colors, the vertical dashed lines denote their longitudinal location.
- 4) This visualization presents multiple views. First, a front cross-section view is used to present the condition within and outside the sewer wall along its length. Then a CCTV fold-out view (Figure 0-14A bottom) is used to denote the profile positions, other than that, a combination of the CCTV fold-out view and several left cross-section views (Figure 0-14B) is used to denote the longitudinal location and circumferential position of the defects.
- 5) The scale of this visualization is similar to **Visualization C** but the pipe length is reduced significantly, which makes it easy to show all small defects, e.g., the pipe wall thickness at any point can now be read directly.

The main visualized items are:

- 1) The pipe wall-soil interface is represented by two-layer profiles (essentially two rectangles).
- 2) Pipe condition information such as variation of the pipe wall thickness, rebar configuration (red lines), and defects within and outside the pipe wall, e.g., voids.
- 3) Coordinate system, X-axis represents the pipe length while Y-axis is the pipe wall thickness and depth into the pipe external environment.

Note this visualization has a limitation similar to the one in Visualization C, compared to that, this visualization presents more information around the pipe's perimeter but still not all.

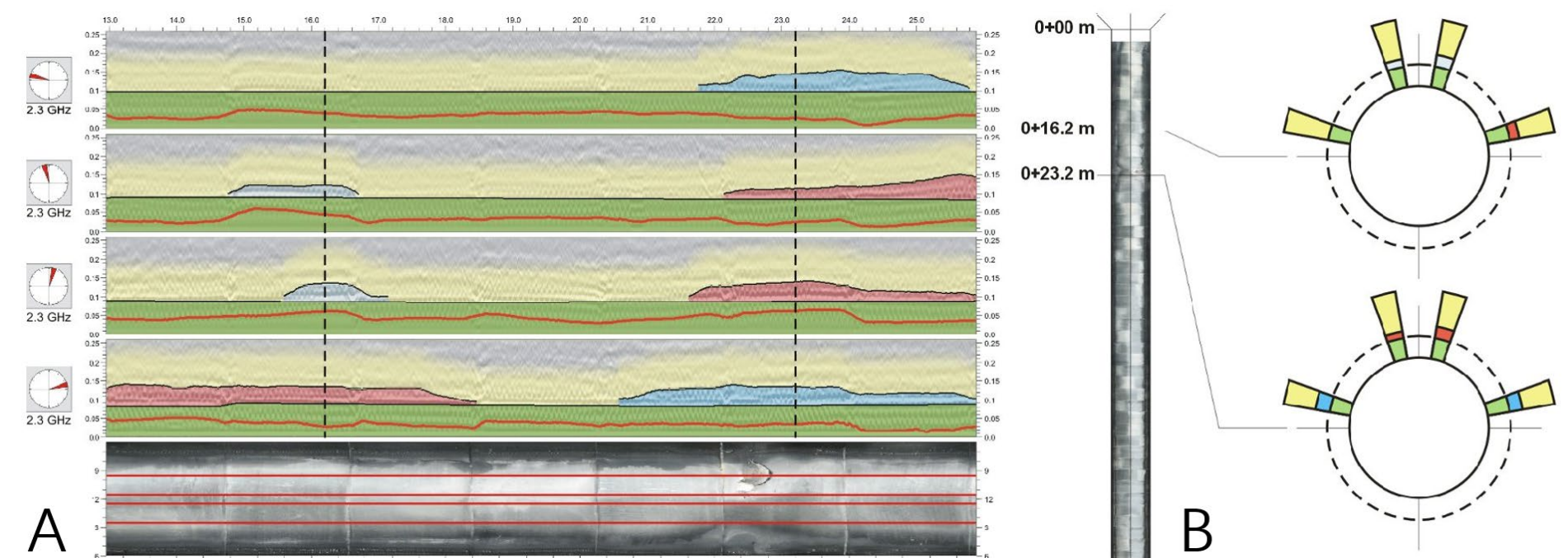


Figure 0-14: Example of SewerVUE integrated – 2D representation of pipewall-soil interface;

A: the longitudinal front view of the pipe-wall interface showing in-pipe GPR profiles at multiple clock positions with corresponding CCTV fold-out view of a reinforced concrete sewer pipe; **B:** left cross-section views combined with corresponding CCTV fold-out view showing the circumferential position and longitudinal location of the defects, source from (Ekes, et al., 2011).

E. SewerVUE integrated – Sewer condition within & outside pipe wall + LIDAR scanning

This method is essentially a **Visualization D** added a **Visualization B** (a full-range LIDAR scanning of the pipe inner surface).

Besides the same elements used in visualization D, this visualization added the following elements:

- 1) A legend that indicates all symbols used.
- 2) Grout of the pipe outer surface is also considered (see the dark green layer in the example).
- 3) A pipe condition bar running under the pipe wall wall-soil profiles, which uses coded colors to state the general condition of the pipe segment (green indicates acceptable pipe conditions, yellow indicates potential problem areas while red marks areas where immediate attention is needed).
- 4) The LIDAR scanning is visualized in a pipe fold-out view, which also uses coded colors to present the inspection results (needs a high level of pre-processing and interpretation), white marks no corrosion while yellow and red mark increasing amounts of corrosion (corrosion is the main defect found in the example).

The main visualized items are:

The same as the visualization features in Visualization D but without the left-cross-section views, and added the LIDAR inspection data in a pipe fold-out view (defects are color-coded in raw data).

Note this integrated visualization has the same limitation (at part the wall-soil profiles) as to the one mentioned in Visualization D.

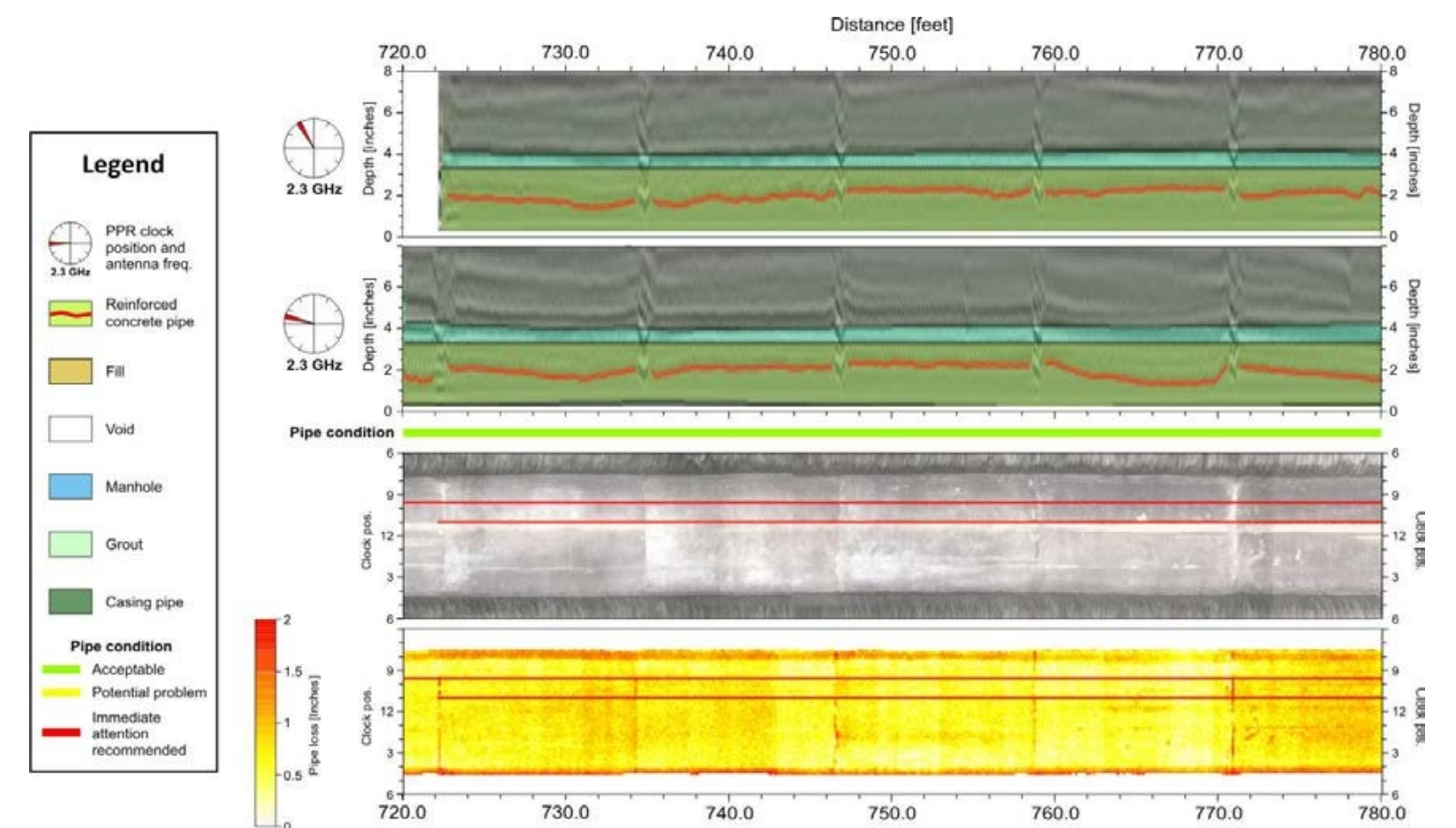


Figure 0-15: Example of the SewerVUE integrated – Sewer condition within & outside pipe wall (integrated with LIDAR inspection results), source from (Ekes, et al., 2012).

F. 3D pipe with LIDAR scanning data projected on outer surface

This is an upgraded version of the fold-out LIDAR scanning data visualization in **Visualization E**.

- 1) This visualization is designed to visualize the sewer condition data collected from LIDAR inspections, mainly for pipe inner surface damages, like the corrosion.
- 2) The raw data is continuously collected along the pipe via LIDAR scanning, which needs certain pre-processing and interpretation procedures to get translated into the corresponding pipe condition information (e.g., pipe wall loss). This often requires experts' skills and specially designed data processing algorithms or software.
- 3) The pipe is represented by a simple 3D pipe model, coded colors are used to denote the difference in the data collection (white marks no corrosion, yellow and red mark increasing amounts of corrosion). The color-coded pipe wall loss is projected to the outer surface of the 3D pipe model to form up a 3D image.
- 4) The visualization is presented in a perspective view of the 3D model, which is "wearing" the 3D image. It is assumed the 3D pipe model also allows users to rotate and zoom in/out.
- 5) This visualization is mainly a scaled-down 3D model of the real pipe, whether minimal data points were visible is dependent on its dimension and severity (e.g., the damaged it might be not easy to distinguish from the entire visualization if it is too small or not very severe). But overall, with the rotating and zooming functions, this visualization shall be able to present all small defects.

The main visualized items are:

- 1) A simple 3D pipe model.
- 2) Defects on the pipe inner surface that are projected on the outer surface of the 3D pipe model with coded colors.
- 3) Defects' source data. The data projection is made from raw data.
- 4) The coordinate system used is not introduced in the literature, it is assumed the long axis of the pipe (length) and the clock directions are used.



Figure 0-16: Example of the 3D pipe model with LIDAR data projection (left, A); 3D CCTV image as a comparison (middle, B); Right: summarized inner pipe-wall geometry based on LIDAR data, the black line represents the original pipe diameter, source from (Ekes, et al., 2012).

One noticing point here is, the projected data is originally from the pipe inner surface, but it is projected on the pipe outer surface so that as many data points can be visible from a certain angle. This is exactly the opposite of **Visualization G**.

G. Ultrasound color-coded discretized Voronoi diagram

- 1) The visualization is designed to visualize the sewer condition data in/on the pipe inner space/surface, the data in the example was collected by ultrasound sewer inspections (in-pipe version).
- 2) In the example, the raw data was collected via ultrasonic scanning in small intervals/grids (but the data is continuous). The raw data needs certain pre-processing and interpretation procedures to get translated into corresponding pipe condition information, which often requires experts' skills and specially designed data processing algorithms or software.
- 3) As seen in the example at right, a 3D pipe model is first constructed to represent the pipe's inner space and surface, individual data points are represented by small ellipses coded with different colors (dark blue means normal). Deviation (representing defects caused by height difference) from the ideal pipe surface is shown in green, yellow, or red.
- 4) The visualization is presented in an (immersive) "worm" view, which means the user has to follow the robot's vision to actually go through the entire pipe to obtain an overall condition of the pipe.
- 5) Due to the scale of the immersive "worm" view, this visualization cannot present all defects in an overview directly. But in essence, all defects are visible when they are within the range of the "worm's" vision.

The main visualized items are:

- 1) A simple 3D pipe model.
- 2) Defects denoted by coded colors (mainly defects caused by height difference to the ideal pipe model, such as obstacles and surface damages).
- 3) Defects' source data. The data projection is made from raw data.
- 4) The coordinate system used is not clearly introduced in the literature but it is assumed the long axis of the pipe (length) and the clock directions are used.

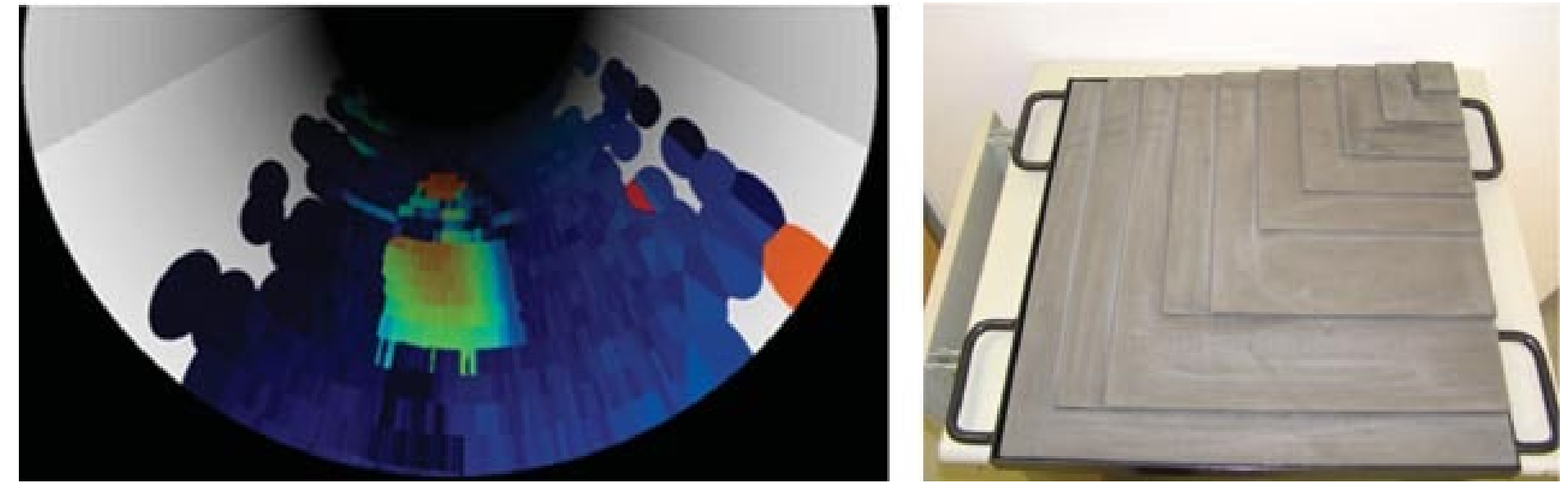


Figure 0-17: Example of the Ultrasound color-coded discretized Voronoi diagram;

(right) color-coded diagram of individual ultrasound measurements in relation to an ideal pipe cylinder showing the pyramid test object (left) that represents a pile of gravel, source from (Walter, et al., 2012).

As mentioned, this visualization is the opposite of Visualisation F, except the "worm" view, there are other ways to see the defects, e.g., making the model transparent, wireframe, X-ray, and so on.

H. 2D color-coded defects map

- 1) The visualization is designed to visualize inspection data collected in plate-like concrete structures (e.g., bridge decks, large concrete slabs or walls) by technologies such as surface GPR and impact echo. Mainly used to discover anomalies within the concrete plate, such as voids and delaminations.
- 2) Reflected electromagnetic or acoustic signals are collected along the inspected concrete structure in small intervals/grids. The collected raw data needs a high level of pre-processing and interpretation to convert it into thickness and defects related information, which often requires experts' skills and specially designed data processing algorithms or software.
- 3) As seen in the examples at right, the outline of the inspected plate is mapped in a planar view, coded colors are used to represent the thickness of and defect information within the inspected object (the outline of the defect can also be visualized if the data is collected in a high resolution). The color coding can be complex because thickness changes in such plate-like structures can be either normal or caused by defects.
- 4) These visualizations are typically presented as a 2D map while users look at it from the top.
- 5) The visualization is a scaled-down planar representation of the inspected object, visibility of the minimal data of interest is dependent on the inspection resolution. For large-scale inspections (e.g., Figure 0-18) with low resolution, small thickness losses, or voids may be invisible compared to the overall visualization. But if the inspection resolution is high enough, small defects can be seen with a "zoom in" function.

The main visualized items are:

- 1) Map representation of the inspected plate-like structure.
- 2) Defects denoted by coded colors (mainly thickness losses, voids, delaminations, discontinuity of reinforcement, and so on).
- 3) Defects' source data. The data map is made from the raw data.
- 4) Coordinate system (X-axis represents the length of the plate-like concrete structure while the Y-axis represents its width).

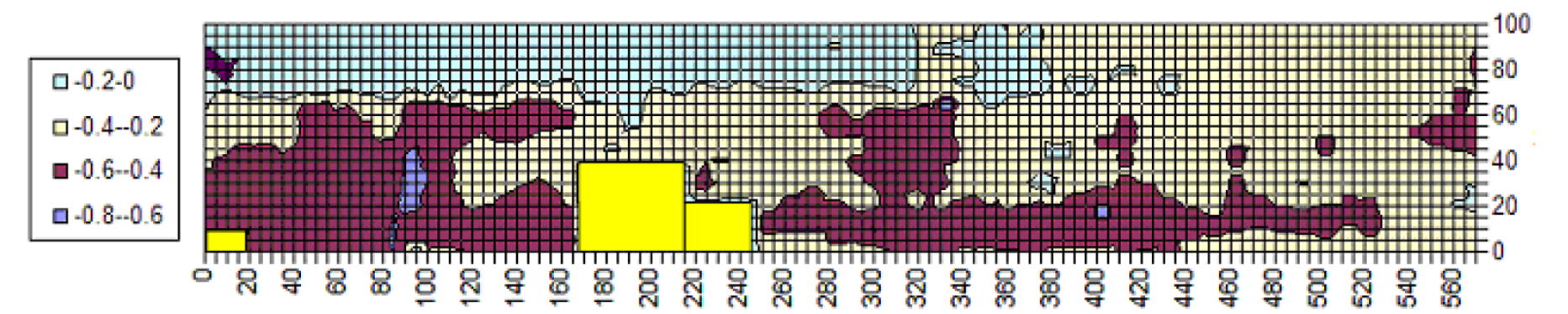


Figure 0-18: The example of surface GPR colored-coded void map for a warehouse, yellow represents the offices while the darker outlines indicate the void area, source from (radarviewllc, 2020)

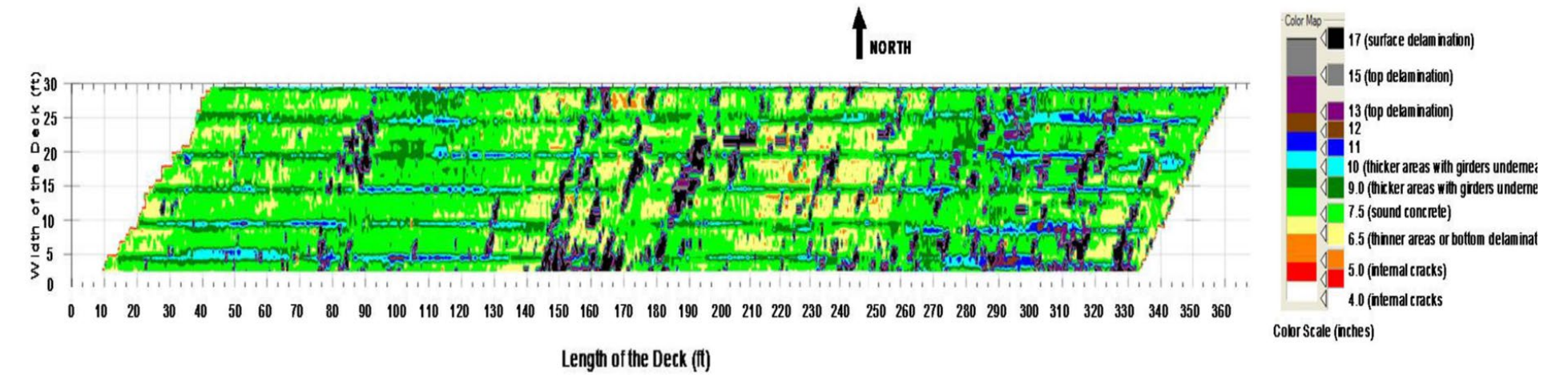


Figure 0-19: The example of impact echo color-coded thickness tomogram of a bridge deck (full range), source from (Olson, et al., 2011).

I. 3D color-coded defects map

This visualization is an upgraded version of Visualization H, while the thickness is not only coded with different colors but also translated into 3D height.

Basically, this visualization presents the same features as Visualization H, only in the depiction method, the thickness is not only coded with different colors but also transformed into 3D height.

The main visualized items are:

This visualization has the same features as Visualization H, but there is a height dimension added, then the coordinate system became the standard Cartesian 3D coordinate system.

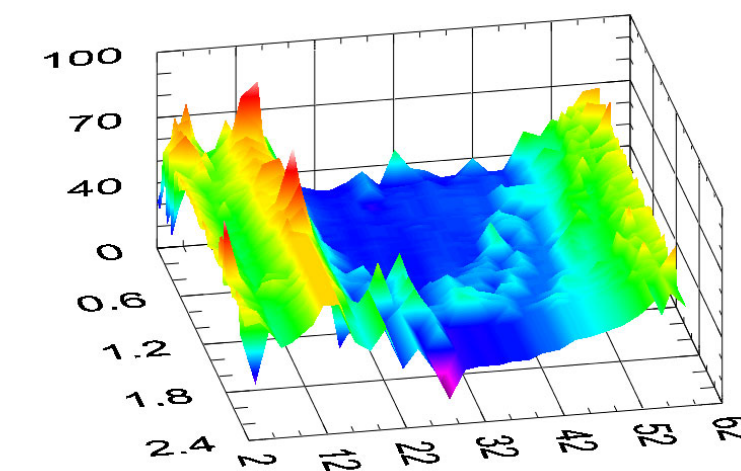


Figure 0-20: 3D Impact Echo Scan Display showing the thickness of a 2.4m-wide wall over its 2-62m length (scale of 1m), source from (Olson, et al., 2011).

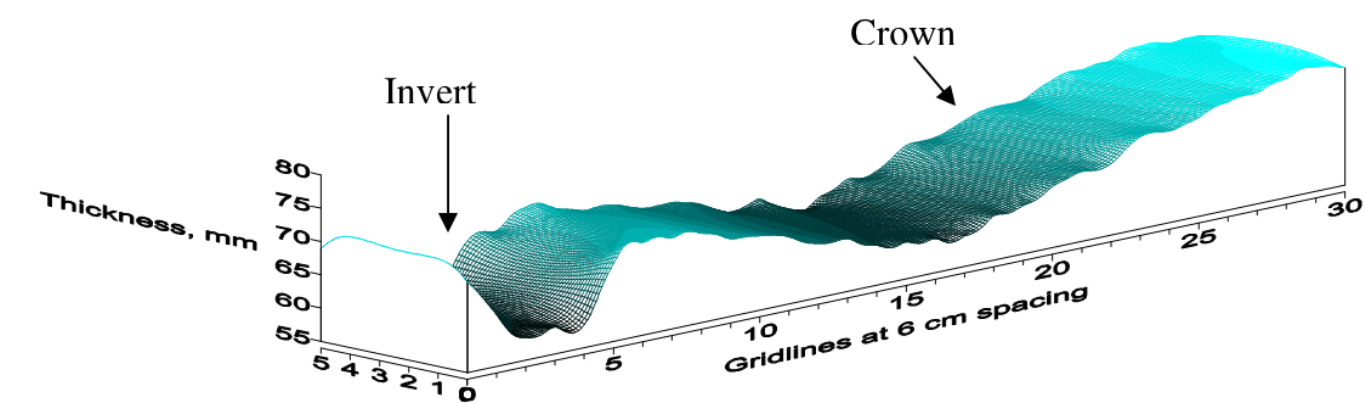


Figure 0-21: Application of this method for visualizing the thickness change of a pipe, source from (Kommireddi, et al., 2004)

J. Sewer inspection data visualization: 3D pipe reconstruction.

Note this technique is still under-development since the automation of reconstructing the pipe and recognizing features and defects with the inspection data is very complicated, especially for non-visual inspection technologies like in-pipe GPR.

- 1) This visualization is originally designed to visualize the sewer condition of the pipe itself (e.g., surface damages, rebar configurations). Although external deteriorations (e.g., voids) are not yet included, this method has great potential to visualize all types of defects, no matter they are from the inside/outside of the pipe or within the pipe wall. Two multi-sensor sewer inspection systems ("SewerVUE surveyor" and "intelligent PIG (pipeline inspection gauge)") were found developing such a visualization method.
- 2) Data types compatible with this method are various, e.g., the left figure in the example was constructed from an inside tunnel GPR inspection, the middle figure was generated from a SewerVUE in-pipe GPR inspection, and the right figure was constructed from the posture data estimated from the IMU (Inertial Measurement Unit) sensors of the "intelligent PIG". The data is not necessarily collected continuously but needs a high level of pre-processing and interpretation to be translated into presentable condition information, which requires experts' skills or specially designed algorithms or data processing software.
- 3) A constructed 3D pipe can be viewed in a variety of ways to allow users to see both inside and outside the pipe (Daniels, 2000), e.g., solid block, wireframe, and transparent 3D objects. Features and defects found in the pipe, such as pipe wall thickness reduction and rebar configuration, can be denoted by predefined 3D objects and colors (see the middle and right figures in the example).
- 4) The visualization can be viewed in many 3D forms, e.g., transparent, wireframe, X-ray. It is also supposed to be rotatable and allow users to zoom in/out to see more details.
- 5) Ideally, this visualization is a scaled-down model of the actual object, defects shall all be visible to users (if they were registered). A limitation is, this visualization cannot provide an overview that shows all defects in one screen directly, but this can be easily solved by the rotating and zooming functions.

The main visualized items are:

- 1) A 3D pipe model that represents the real pipe (and possibly also the pipe exterior environment, see the left in the example).
- 2) Defects (inside/outside of the pipe or within the pipe wall) denoted by coded colors, 3D objects, and annotations.
- 3) The coordinate system used in the visualization is not introduced in the literature, it is assumed that the long axis of the pipe (length) and the clock directions are used.
- 4) Defects' source data, the visualization itself is constructed from the raw data.

GPR-SLICE@V7.0 Vector 3D Navigation Formats complete tunnel imaging + any randomized geometry

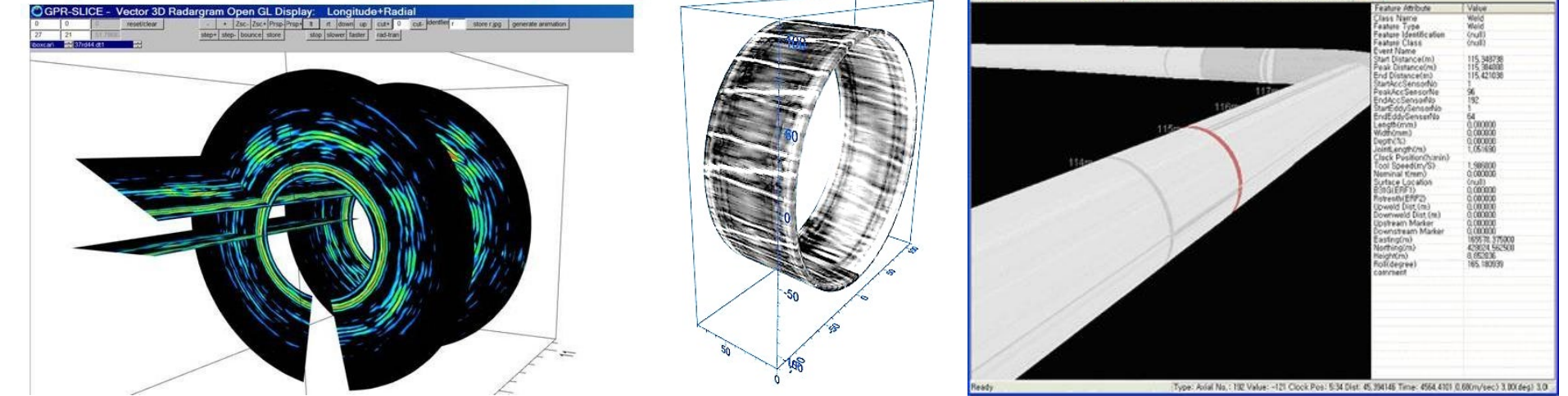


Figure 0-22: Example of 3D pipe reconstruction; Left: in-pipe GPR inspection profiles (longitudinal and radial B-scans) making up a 3D tunnel (GPR-SLICE, 2020);

Middle: circumferential 3D view of a pipe joint, white bands and lines represent rebar (Ékes, et al., 2014; Ékes, et al., 2012; Ekes, et al., 2011); Right: outside view of a 3D constructed pipeline (Han, et al., 2007).

Interestingly, the 3D pipe reconstruction data visualization for GPR applications could use a lot of theories from the literature, such as obtaining cylindrical radargram in (Donazzolo, et al., 2010) and assembling multiple B-scans to form up a 3D image (Duman, et al., 2015) and so on.

K. Registering 3D point-cloud inspection dataset with a designed CAD point-cloud dataset

- 1) This visualization is part of the inspection tool designed in (Nahangi, et al., 2014), which is used to find defective spools in the industrial assemblies and pipe spool fabrication process.
- 2) The raw inspection data is collected through LIDAR scanning, which is continuously collected all over the pipe spool. The data needs a high level of pre-processing before registration (e.g., removing noises), which is often done by specially designed data processing software or experts.
- 3) A 3D CAD model is first constructed and converted into 3D point-cloud format to represent the design state of the pipe spool, the as-built status of the pipe spool is then indicated by the 3D LIDAR scanning (also in point-cloud format). By registering the two sets of point-cloud data (coded in different colors) in the same coordinate system, defective parts can be observed from differences in the results (see the part b in the example).
- 4) The visualization is presented in a 3D view, assuming the model is rotatable and allows users to zoom in/out to see more details.
- 5) Objects visualized by this visualization are usually not large, hence the scale of this visualization is fully able to show all minimal data points. But the same limitation as mentioned in Visualization J also occurs here, this visualization cannot provide an overview that shows all defects in one screen directly even though they can be seen through the rotating and zooming functions.

The main visualized items are:

- 1) Two sets of point-cloud data (in different colors) that represent the designed state and as-built status of the inspected pipe spool merging with each other.
- 2) Defects denoted by 3D objects and coded colors.
- 3) Defects' source data, half of the visualization is made of the inspection data.
- 4) The coordinate system used in the visualization is not introduced in the literature, it is assumed the standard Cartesian 3D coordinate system is used.

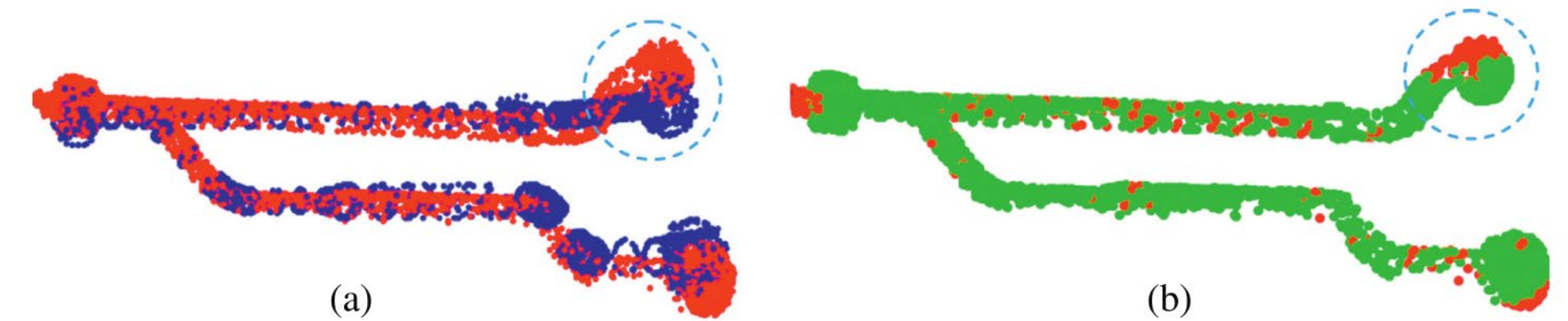


Figure 0-23: (a) Registration results of a wrongly fabricated pipe spool. (Blue: 3D CAD model in point-cloud format, Red: laser-scanned data); (b) Deviation analysis results to detect the defective parts (green means well fabricated, red means incurred defects), source from (Nahangi, et al., 2014).

L. Immersive VR sewer inspection

Note the VR and AR are both immersive visualizations, which highly depend on the 3D reconstruction technology and the device used. There is currently no specific AR application found for visualizing sewer inspection data but there is one VR application found for the sewer inspection purpose, see the example at right.

- 1) This visualization method was initially developed to visualize small damages in large sewer pipes (e.g., pipe diameter larger than 1m), the example here is from the ARSI project (ARSI, 2017).
- 2) The raw data used to construct the VR environment in this example is visual data, collected by a CCTV camera. It is possible to use other types of inspection data, but it must be collected continuously to build a continuous virtual pipe environment. A complicated process is needed to reconstruct the pipe with the raw inspection data, which requires highly support from experts and specially designed algorithms or software.
- 3) The depiction methods used in this visualization are various, the most important one is the 3D reconstruction of the virtual pipe environment. The preferred way is extracting textures/patterns and other information from the inspection data to generate the pipe inner space and surface and form up a VR model automatically. As seen in the example, the pipe inner surface, structure, and defective parts are represented by graphical/heatmap/wireframe surfaces. Besides being highlighted by code-colors, defective parts are also denoted by virtual primitives (which are pre-defined 3D objects).
- 4) Similar to but more advanced than Visualization G, the VR sewer inspection provides an immersive "worm" view for users to move forward/backward and zoom in/out freely inside the pipe. **But this also brings the same limitation, the user has to walk through the entire pipe and look around to see all the defects.**
- 5) Since this visualization is meant to present small defects in large pipe surfaces, it should allow the users to see all minimal data points (through moving back and forth and zooming in the virtual pipe). **However, a small limitation here is, this visualization cannot provide an overview that shows all defects in one screen directly.**

The main visualized items are:

- 1) A VR environment that represents the inner space, surface, and structure of the sewer pipe. A virtual cursor that can be used much as a computer mouse except it can move in 3D.
- 2) Defects denoted by virtual primitives and highlighted by coded-colors. The virtual primitives are extensions of the virtual cursor, which allow the inspector to construct and fit simple 3D objects to features of interest (see the transparent spheres in the example).
- 3) Defects' source data, which made up the VR environment.
- 4) The coordinate system used is not introduced, it is assumed the long axis of the pipe (length) and the clock directions are used.

More of this visualization method can be seen in the webpage of the ARSI project and papers of (Saenz, et al., 2010; Lawson, et al., 1998; Lawson, et al., 2002).

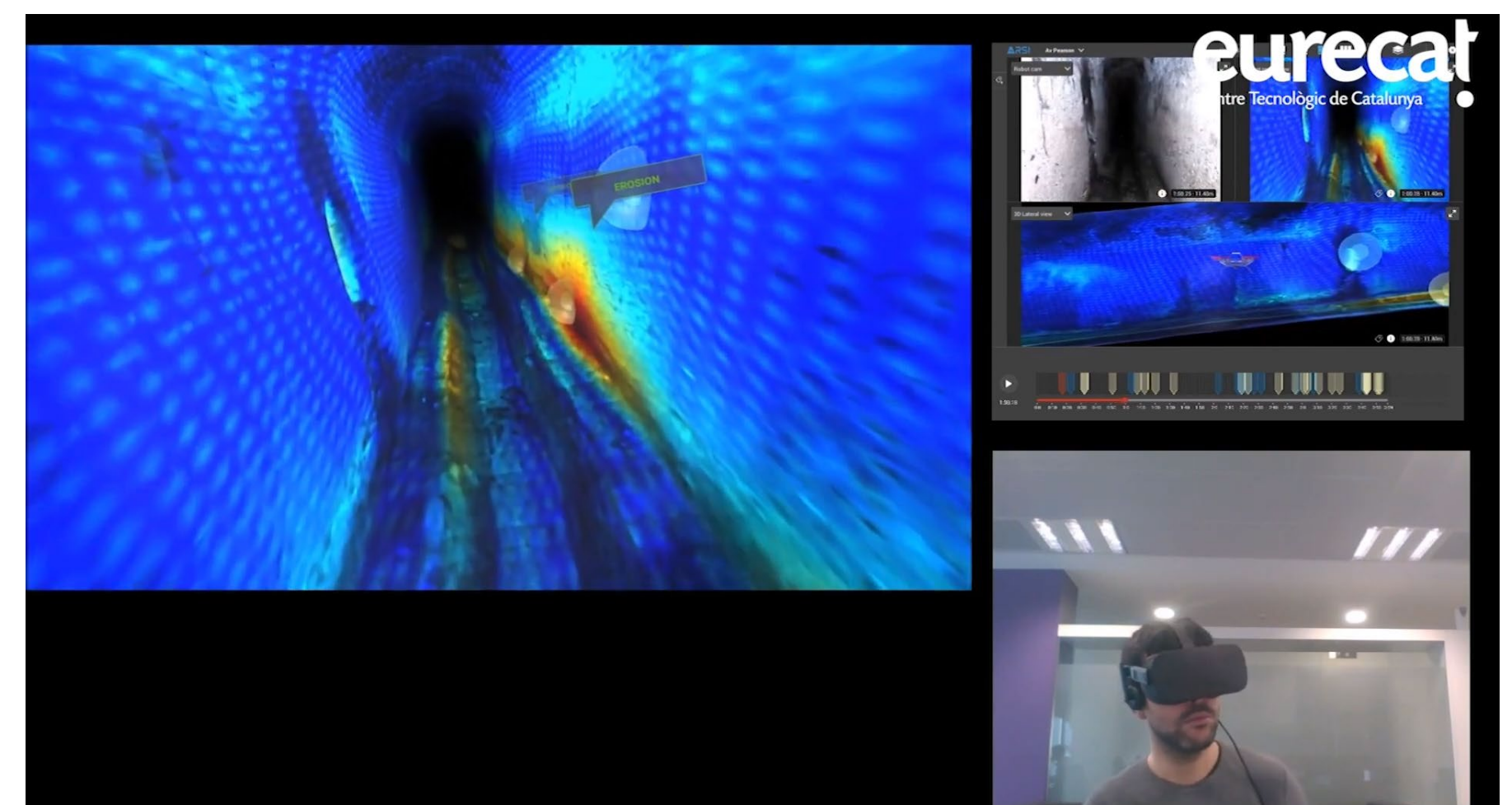


Figure 0-24: Example of the immersive VR sewer inspection data visualization, source from the ARSI project (ARSI, 2017).

- 1) This visualization was originally developed for asset workers to locate the buried utilities and their adjacent utilities, as well as obtain the registration information of them in-situ more easily. The idea of using it to visualize sewer inspection data is rather new, a simple description is, scanning and locating the street through a smart device with camera (e.g., smartphones), a 3D model of the sewer network overlaid to the real-world street can be seen in the device screen, with all kinds of information related to the pipe presented.
- 2) Data types compatible with this visualization are various since it is a matter of interpretation and registration. As long as the collected data can be interpreted into presentable sewer condition information (e.g., features, defects), they can be registered to the 3D AR model. It does not matter if the data was visual or other types, or was it collected continuously or not. Although pipe exterior deteriorations (e.g., voids) and defects within the pipe wall has not yet been included in this concept, this visualization has great potential to integrate all these inspected defects. In essence, whatever the data type is, it needs a high level of processing and interpreting before visualizing because what is presented in the visualization is only the interpreted sewer condition information.
- 3) There is not yet an actual application of this visualization, it is assumed the depiction methods of this visualization will be similar to **Visualization F, G, and J**, which registers interpreted defects onto a designed 3D model, assuming coded-colors and virtual primitives (pre-defined 3D objects) will be used to represent the defects.
- 4) The visualization is presented in an immersive 3D side view. The 3D pipes are overlaid to the street view (in-situ or in a city model). It is assumed that this 3D model also allows users to walk around and zoom in to see the details of the pipe (see the example at right, the reason for using wireframe is to allow the users to see the condition inside the pipe).
- 5) Ideally, the 3D model shall be designed in a 1:1 scale to the real object, and with the zoom-in function, users shall be able to walk around the AR model and see all the minimal data points (as long as they are registered). **Similar to other 3D visualizations, this visualization cannot provide a pipe condition overview that shows all defects in one screen directly.**

The main visualized items are:

- 1) A 3D pipe model overlaid to the street view. A visual cursor that can be used much as a computer mouse except it can move in 3D.
- 2) Defects denoted by 3D virtual shapes and possibly coded colors.
- 3) The coordinate system (for the inspection data) used is not introduced, it is assumed the long axis of the pipe (length) and the clock directions are used.

M. Stereo 3D AR sewer data visualization

To avoid confusion between AR and VR in this research, they are simply distinguished by the viewing perspective. It is regarded the inspector needs to enter the virtual pipe environment for the VR visualization while for AR visualization the inspector only needs to look at it in a 3D side view.

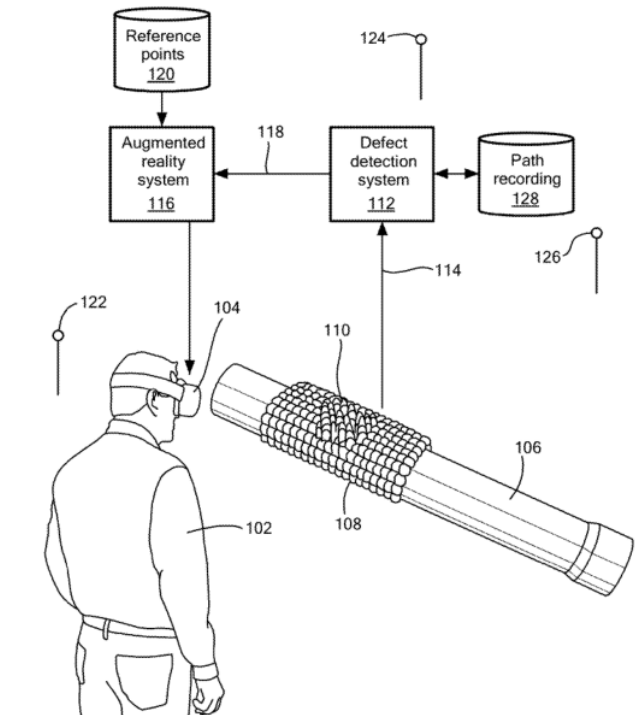
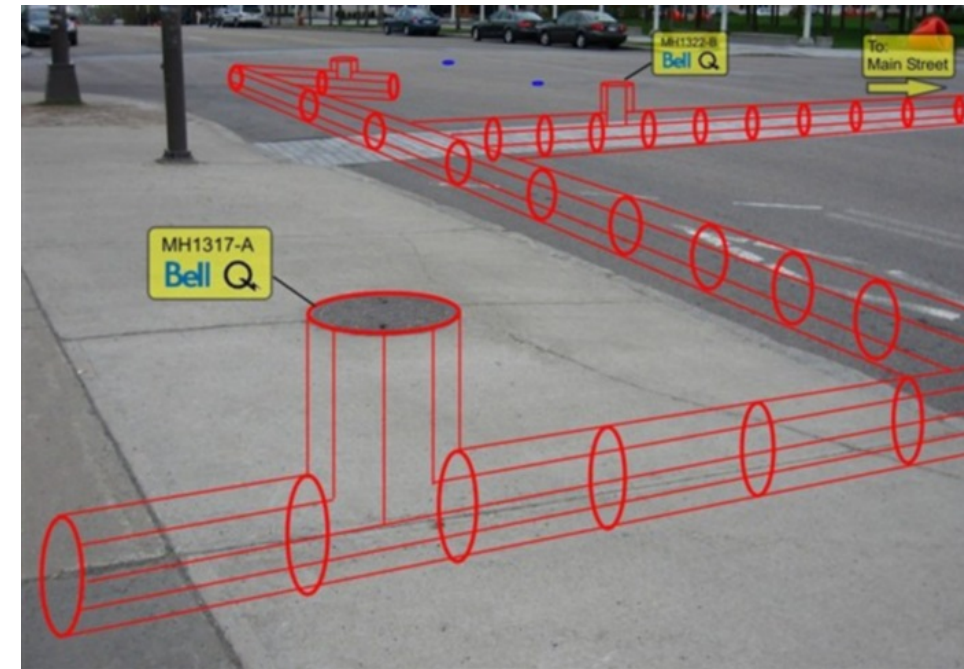


Figure 0-25: Example of the stereo AR sewer inspection data visualization;
 Left: the stereo AR sewer inspection data visualization overlaid in a real-world street view in a wireframe format, source from Google;
 Right: patent of this visualization concept to be used for pipe inspection, source from (Babcock IV, et al., 2020).

H. European Sewer Defects Coding System

As shortly mentioned in the CCTV visualization method (section 1.1), the sewer defects coding system introduced in the European norm (BS_EN_13508-2:2003+A1, 2011) is the documentation of the CCTV inspected sewer defects (Caradot, et al., 2018), which covers more than 25 types of visual defects that can be observed through CCTV inspections. The defect codes are divided into four groups:

- **Codes relating to the fabrics of the pipeline** mainly describe defects from the structural domain. The defects assigned to impact echo (thickness reduction, internal void, delamination, and surface cracks) can be categorized into this group. For the convenience of the research, it is also suggested to categorize the defect assigned to in-pipe GPR (external voids) into this group even though it is from the external environment domain. Sewer defect codes in this group start with “BA...”.
- **Codes relating to the operation of the pipeline** mainly describe hydraulic defects (e.g., obstacles) and some defects that could reduce the pipe’s structural integrity (e.g., roots and exfiltration).
- **Inventory codes** describe the general sewer situation.
- **Other codes** describe problems that could happen during the inspection.

See the figures below for an overview of all the sewer defect codes. a: all codes and the related sewer defect types and their possible severity classes; b: an example code of the “fissure” defect.

Aspect	Characterisations 1 and 2	Classification
Fabric		
BAA	Deformation flexible pipes	A or B
BAB	Fissure	A, B, C or D
BAC	Break/collapse	1, 2, 3, 4 or 5
BAD	Defective brickwork or masonry	1, 2, 3, 4 or 5
BAE	Missing mortar	1, 2, 3, 4 or 5
BAF	Surface damage	1, 2, 3, 4 or 5
BAG	Intruding connection	1, 2 or 3
BAH	Defective connection	1, 2, 3, 4 or 5
BAI	Intruding sealing material	A or Z
BAJ	Displaced joint	A, B or C
BAK	Lining defect	A, B or C
BAL	Defective repair	1, 2, 3 or 5
BAM	Weld failure	1, 2, 3 or 5
BAN	Porous pipe	1 or 5
BAO	Soil visible through defect	1 or 5
BAP	Void visible through defect	1 or 5
Operation		
BBA	Roots	A, B or C
BBB	Attached deposits	A, B, C or Z
BBC	Settled deposits	A, B, C or Z
BBD	Ingress of soil	A, B, C, D or Z
BBE	Other obstacles	A, B, C, D, E, F, G, H or Z
BBF	Infiltration	1, 2, 3, 4 or 5
BBG	Exfiltration	1 or 5
BBH	Vermin	1 or 5
Inventory		
BCA	Connection	A, B, C, D, E, F, G or Z; A or B
BCB	Local repair	A, B, C, D, E or Z
BCC	Curvature of sewer	A or B; A or B
BCD	Start node	A, B, C, D, E, F or Z
BCE	Finish node	A, B, C, D, E, F or Z
Other		
BDA	General photograph	
BDB	General remark	
BDC	Inspection abandoned	A, B, C or Z
BDD	Water level	1, 2, 3, 4 or 5
BDE	Flow in incoming pipe	A or B
BDF	Atmosphere within the pipeline	A, B, C or Z
	Loss of vision	A, B, C or Z

a

Fissure	
BAB	
Characterisation 1	The nature of the fissure : — surface crack (A) – a crack only in the surface; — crack (B) – crack lines visible on the pipe wall, pieces still in place; — fracture (C) – crack visibly open in a pipe wall, pieces still in place.
Characterisation 2	The orientation of the fissure: — longitudinal (A) – A crack or fracture which is mainly parallel to the axis of the pipe; — circumferential (B) – A crack or fracture which is mainly around the circumference of the pipe; — complex (C) - A group of cracks or fractures which cannot be described as longitudinal or circumferential; — helical (D).
Quantification	The width of the fissure in millimetres.
Circumferential location	The position should be recorded.

b

As can be seen from the figures above, each defect type is represented by a unique code that consists of three letters and one or two characterization(s). The first letter describes the application of the code, for instance, B for pipeline or D for manhole inspection. The second letter describes the type of code, for example, codes relating to the fabric of the pipeline (BA...). The third letter of the code determines the specific observation between the defects, for instance, code “BAJ” is used for each observed “displaced joint” while “BAB” is used for each observed “fissure”. Moreover, the characterization extends the description of a certain defect with additional information. The characterization is registered with complimentary letters based on defects’ nature, for example, “BAB B/A” refers to a “crack” that is parallel to the pipe’s long axis while “BAB C/B” refers to a “fracture” that is around the pipe’s circumference (Le Gauffre, et al., 2007); (van der Steen, et al., 2014).

Quantifications of the defect are used to estimate its damage severity, which essentially assigns classes 1–5 to the defect regarding the different levels of damage (1-5, from good to bad, some may also include 0). The quantifications are usually based on measurable variables, for instance, the damage severity of a “fissure” defect is mainly determined by the width of the fissure in mm (see figure b).

I. State of Art of Impact Echo Sewer inspection

The impact echo is a wide-used non-destructive evaluation method for many forms of concrete structure (e.g., plates, columns, beams, and hollow cylinders like pipe and tunnel). Through decades of development, it has also been proved capable to give a good estimation on the condition of a concrete pipe, which includes: **1).** the pipe wall thickness; **2).** the location (or even extent) of minor surface defects (e.g., cracks) and internal defects (e.g., delamination and voids) (Colla, et al., 2003; Kommireddi, et al., 2004; Rizzo, 2010; Sansalone, et al., 1998); **3).** the presence of cavities around the pipe in wet soil conditions (Kang, et al., 2017).

The expected operation of inspecting sewers with impact echo is similar to in-pipe GPR, which is sending a robotic platform equipped with an in-pipe version of impact echo system into the pipe, assuming such a system is available. Theoretically, the in-pipe impact echo system is supposed to contain a source of controlled impacts and an appropriate transducer that is tightly mounted against the pipe wall (Rajani, et al., 2004). However, mounting the transducer on the sewer inner surface tightly and recycle it afterward remains an unsolved challenge, a more feasible way is to execute the impact echo acoustically by replacing the surface-coupled transducer with a contactless transducer (e.g., an air-coupled microphone) and place it very close to the impact spot (Cernat, 2019; Pleijsier, 2019). The setup for an in-pipe impact echo inspection and its working principle can be seen in Figure 0-26.

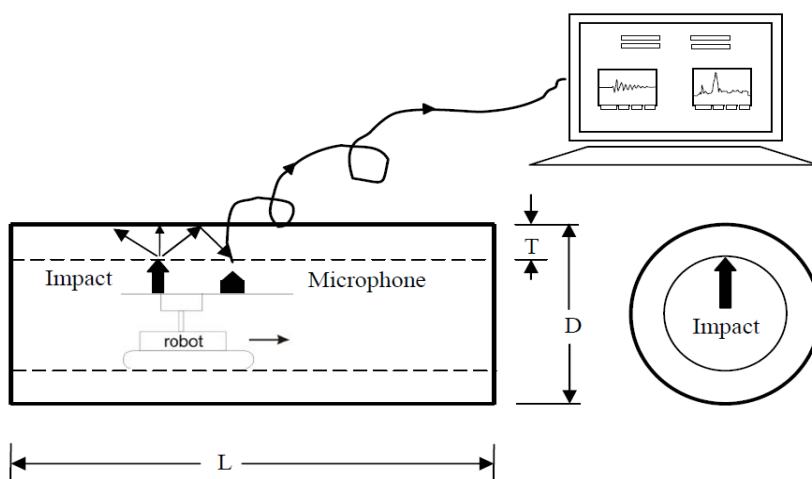


Figure 0-26: Setup and working principle of impact echo detection in a pipe, adapted from (Kommireddi, et al., 2004).

During the in-pipe impact echo survey, a mechanical impact is excited to the sewer inner surface at a certain spot (by striking/tapping with a falling weight or pneumatic hammer). The impact induces short-duration, low-frequency²² stress waves, which propagate into the structure and get reflected by internal defects due to the difference in acoustic impedance (Colla, et al., 2003). When the reflected waves return to the surface, they induce surface vibrations that excite air particles, which is measured and recorded by the microphone adjacent to the impact spot (Pleijsier, 2019). The collected data is displayed on the oscilloscope in waveforms and amplitude spectra, and then transformed into a computer-based data acquisition system and used to evaluate the integrity of the concrete structure (Sansalone, et al., 1998).

Two types of data display are often seen in impact echo data processing, the time domain waveform (time vs. volts), and the frequency domain waveform (frequency vs. amplitude), see Figure 0-27 left and right. Note these are still raw data displays, which are supposed to be further processed and interpreted for the actual data visualization (i.e., visualizing the interpreted results while using the post-processed data as source data of defects).

²² The frequency depends on the form of structure, the impact frequency used for a pipe is usually higher than normally required on a concrete slab.

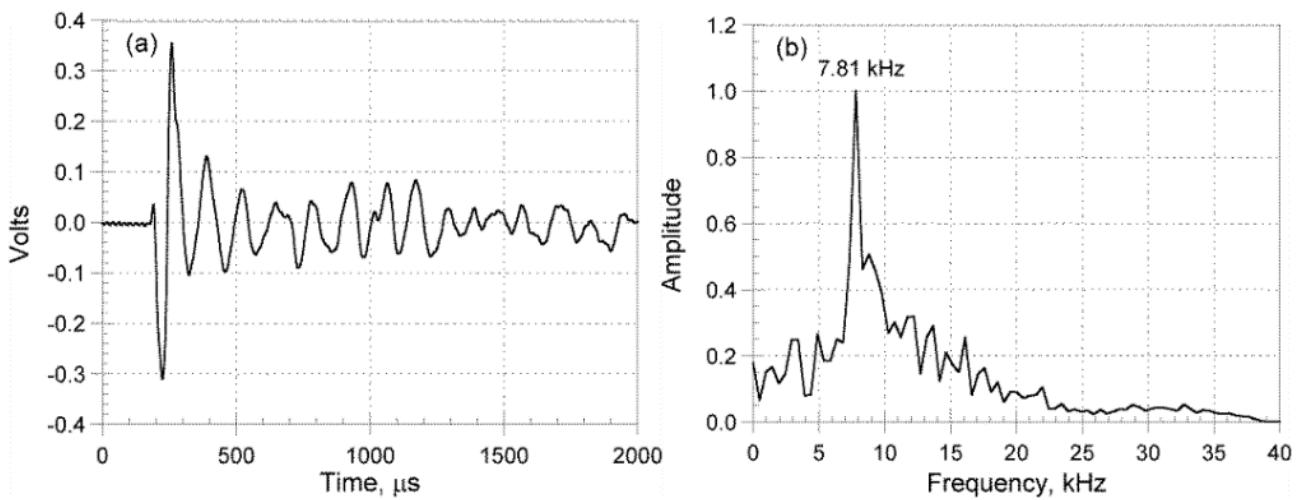


Figure 0-27: Left: Time-domain waveform; right: amplitude spectrum showing the peak of thickness mode frequency, source form (Carino, 2015).

The time vs. volts plot can be understood as the strength of the air particles' excitement caused by the surface displacement (caused by the reflected P-waves) change over time. Although it is concluded in (Cernat, 2019) that the time evolution of the waves yields to a good characterization of the substrate of a concrete object, the interpretation process is very time-consuming and requires a high level of data processing skills. Hence the frequency analysis was later developed (Carino, 2001). With the help of FFT (Fast Fourier Transform), plots of frequency vs. amplitude like Figure 0-27 (right) can be obtained from the time domain waveform. The resulted spectrum shows the amplitudes of various frequencies as peaks in the spectrum, which can be used to estimate the characteristics of the tested object. For example, the thickness frequency can be used to estimate the thickness of the tested object or the depth of the reflecting interface (Carino, 2001; Carino, 2015).

As mentioned, impact echo inspections can verify the thickness of the tested concrete object, and find flaws within the concrete that indicate the concrete is no longer a solid coherent substance, e.g., delamination and voids (Carino, 2015; Pleijsier, 2019). Two criteria are developed in (Carino, 2015) to determine such flaws: **1).** the size (d) of the flaw; **2).** the depth (T) of the flaw. By adjusting the WTDR (width-to-depth ratio, $\frac{d}{T}$) and experiments, four scenarios were generalized to indicate if such flaws can be detected (Carino, 2015):

- For $\frac{d}{T} < \frac{1}{4}$, the flaw cannot be detected, see Figure 0-28a, the response shows the concrete is in good condition.
- For $\frac{1}{4} < \frac{d}{T} < \frac{1}{3}$, the flaw can be detected. As seen in Figure 0-28b, the thickness frequency peak shows a shift compared to Figure 0-28a, which indicates the presence of the flaw but its depth can not be determined. This is because the flaw is too small to reflect sufficient energy to set up a resonance condition related to its depth.
- For $\frac{d}{T} > \frac{1}{3}$, the flaw can be detected and its depth can be determined. Similar to Figure 0-28b, a shifted thickness frequency peak can first be expected due to the diffracted waves. Since the flaw is larger, the received wave also contains a frequency peak corresponding to the flaw's depth, which is presented by the second frequency peak in Figure 0-28c.

- d. For $\frac{d}{T} > 1.5$, the flaw can be detected and the impact echo response will show the tested object has a thickness equal to the flaw depth. Similar to Figure 0-28c, a shifted thickness frequency peak can be expected and a second frequency peak for the depth of the flaw can be expected, see Figure 0-28d.

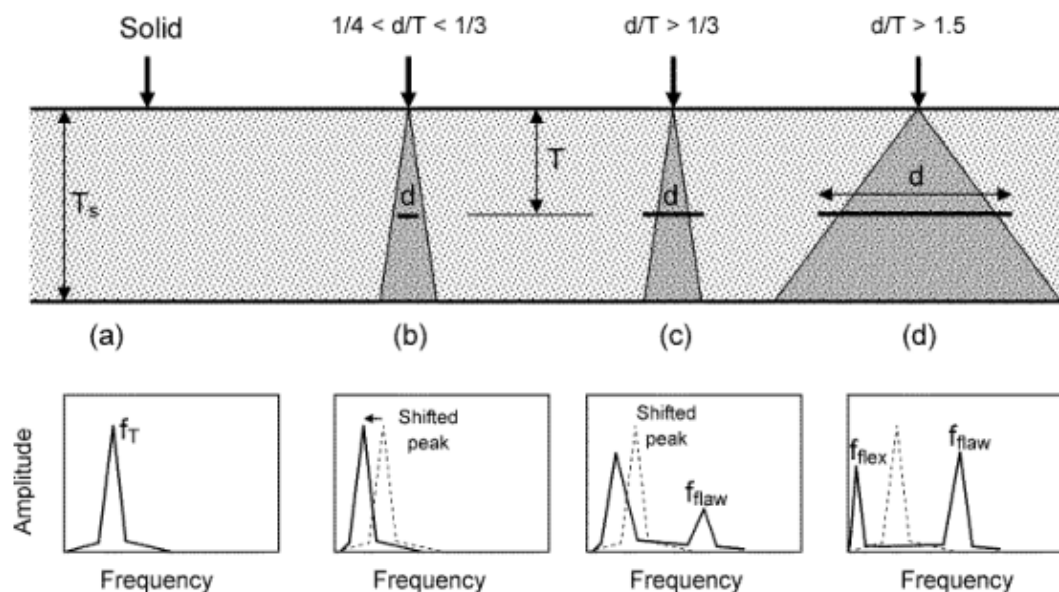


Figure 0-28: Effect of relative flaw size on impact echo responses, source form (Carino, 2015).

As seen from the above explanation, the responses in the impact echo data displays cannot show defects directly. Hence the current impact echo data interpretation can only be performed in a relative way, which is by comparing the “good” spots with the “bad” spots” to determine the existence of a defect and estimate its further information (Pleijssier, 2019), e.g., comparing Figure 0-28a with Figure 0-28b. This means before a specially designed data processing software/algorithm was available, interpretation of the impact echo inspection data will still require an expert’s level of data processing skills. This is a major limitation that needs to be overcome before further popularizing and implementing this technology as a new sewer inspection method.

In summary, as a wide-used quantitative inspection technology for concrete condition assessment, the impact echo method has also shown great potential for sewer condition assessment. However, studies yet have shown no impact echo products or prototypes have been developed for sewer inspections. Besides that, applying impact echo as a sewer inspection method requires a high level of data processing skills to interpret the collected data into meaningful sewer condition information. More importantly, through searching the literature, the author found that there are currently no standardized visualization methods/concepts available to present the impact echo inspection data, let alone for the sewer condition assessment purposes.

Therefore, the TRL of impact echo sewer inspection is concluded as lower than the level of Development 4: Experimental pilot (see full TRL table in Appendix D). This means to implement the impact echo method in the sewer inspection field successfully, more effort should be put on its data interpretation and visualization while the technology itself is still under development. Hence, this thesis introduces this technology as a complementary sewer inspection method, attempts to find a standard routine to process and interpret raw impact echo data, and suitable methods to visualize the interpreted sewer condition information.

J. Solution to Unavailable Impact Echo Simulation

As planned, the COMSOL software should have been used to generate the raw sewer inspection data collected by impact echo. The simulated impact echo data should have been processed and interpreted as done in section 3.1. But unfortunately, the attempt to execute the impact echo simulation through the University of Twente HPC (High-Performance Computing cluster) did not succeed. Thus this section proposes a solution to deal with this problem.

Due to the missing of simulation data, the impact echo sewer inspection data analysis is consequently not an option. What is left available are the scenarios developed for the simulation, which are some specific defects (see Figure 0-29 and the bullet points). These simulation scenarios are the key to this solution, they can be regarded as results interpreted from the inspection data and visualized by the later designed visualizations. Because the raw simulation/inspection data is usually used as source data of the defect in conventional data visualizations (see page 2 and 30), the missing evidence to defects will not cause much influence to the entire visualization (see Figure 1-2, photos and videos of the defects are not uploaded). Simply speaking, it is still possible to design for the impact echo sewer inspection data visualization based on these scenarios by making a fake claim such as: after an impact echo inspection, several defects were found in the pipe but the raw inspection data is somehow lost.

The simulation of impact echo inspection considers the defect types of pipe wall thickness reduction, voids and delamination within the pipe wall and (minor) cracks on the pipe inner/outer surface (see more about them in Appendix C). Below are the four scenarios developed for simulating these four defects (note the pipe geometry used is the same as used in the in-pipe GPR simulation, the pipe is made of unreinforced concrete and has an inner diameter of 600mm and thickness of 95mm.):

- **Thickness reduction**(surface damage). The surface damage usually occurs location at the invert (6 o'clock), the thickness loss is 30mm (around 30% of the total pipe wall thickness).
- **Internal voids**. A sphere air-filled void is located within the pipe wall at 12 o'clock, with a diameter of 30mm (around 30% of the pipe wall thickness).
- **Delaminations**, circumferential range from 3:00 to 4:30, thickness 0.1mm.
- **Cracks on the pipe outer surface**. A circumferential crack ranges from 12 to 5 o'clock, with a width of 5mm.

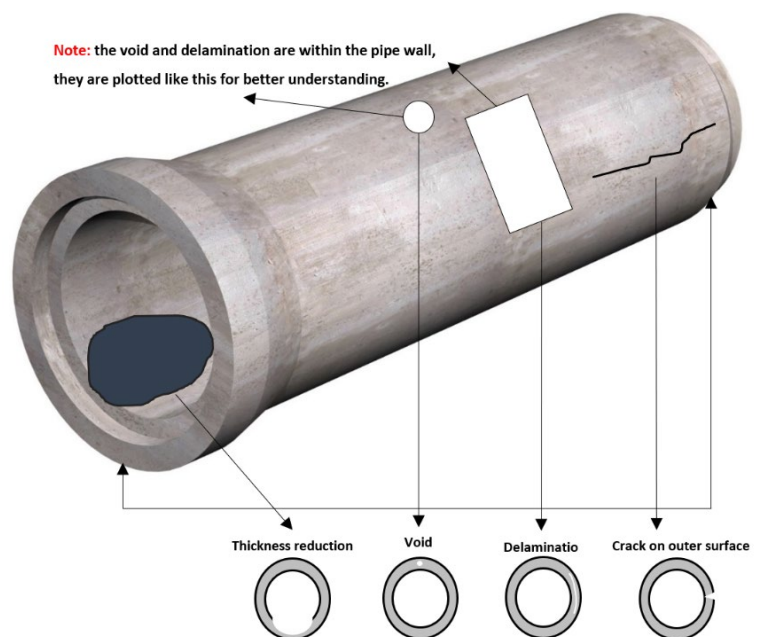


Figure 0-29: Schematic of the impact echo simulation scenarios.

The defects described by these simulation scenarios will be visualized in the later designed impact echo sewer inspection data visualization. Note that the longitudinal location and severity of them will be assumed late

K. Selecting Optimal Visualization Alternatives for Impact Echo & Sewer Condition Data Integration

This section follows the same procedures as in section 4.2.3 and Table 4-4, but the purpose is not only for selecting the most suitable data visualization alternative of in-pipe GPR collected from the pipe's exterior environment, but also for visualizing the condition data of/within the pipe wall collected by impact echo inspections, and one integrated alternative for visualizing the condition data collected from multiple sources. In short, three alternatives will be finally selected for different purposes, which is why the **area of application** criterion and the **final scores** column in Table 0-3 are split into groups of "in-pipe GPR", "impact echo" and "integrated" to specify the available choices for each purpose.

Table 0-3: MCDA of comparison and selection for final designs of the in-pipe GPR and impact echo data visualization alternatives, "-" means the alternative is not suitable for this purpose.

Alternatives	Criteria	Area of application (30%)			Scaling (25%)	Depiction (15%)	Ease of creation (15%)	Future proof (10%)	Viewing perspective (5%)	Final Scores		
		In-pipe GPR	Impact echo	Integrated						In-pipe GPR	Impact echo	Integrated
3. 2D representation of pipewall- soil interface		2	1	1	2	1	2	2	1	1.8	1.5	1.5
2. 2D Pipe wall condition linear representation		-	2	-	2	1	2	1	1	-	1.7	-
1. 2D pipe fold-out view		-	2	-	2	2	2	1	1	-	1.85	-
6. 2D color-coded defects map		-	2	-	2	2	2	1	1	-	1.85	-
4. 3D pipe with inspection data projected on outer surface		1	1	1	1	1	1	1	2	1.05	1.05	1.05
8. 3D pipe reconstruction		1	1	2	1	2	1	2	2	1.3	1.3	1.6
11. 3D Stereo AR sewer data visualization		1	1	2	1	2	0	2	2	1.15	1.15	1.45

Other than the optimal inspection data visualization alternative for the in-pipe GPR method discussed after the MCDA in section 4.2.3. As can see from the highlighted items in Table 0-3 above, the **2D pipe fold-out view (1)** and **2D color-coded defects map (6)** are selected in combination to visualize the condition data of/within the pipe wall collected by impact echo inspections. Moreover, the **3D pipe reconstruction (8)** is selected as the integrated visualization alternative for visualizing sewer condition data collected from multiple sources. The following paragraphs brief the major reasons for selecting these alternatives as final visualizations of choice, and elaborate on the main limitations/imperfections they still own, which need to be modified/improved in the later design phase.

Impact Echo data visualization: Combining 2D pipe fold-out view (1) & 2D color-coded defects map (6)

These two alternatives are selected as a combination to visualize the condition data of/within the pipe wall collected by impact echo inspections. The **2D color-coded defects map (6)** is specially designed to visualize the surface/internal defects on/within the slab-like concrete structures while the **2D pipe fold-out view (1)** is not originally designed for the impact echo method but it can be adjusted to achieve such a visualization purpose²³. Most importantly, the "map-based view"²⁴ of **2D color-coded defects map (6)** still needs to be adapted for representing the pipe's geometry for sewer condition assessment, the "pipe fold-out view" of the **2D pipe fold-out view (1)** can be a very good replacement for that. The combination and adaption of these two alternatives can also be related to the predefined requirement 6).

The **2D representation of pipewall- soil interface** and **2D Pipe wall condition linear representation** can also visualize sewer conditions within the pipe wall. However, they both are limited to provide condition information at several circumferential positions of the pipe instead of all. Hence they are not considered as the final choice for the impact echo sewer inspection data visualization. Also, there are several 3D alternatives with the potential to visualize defects on/within the pipe wall, but again, the inherent deficiency of them is a considerable issue.

Integrated data visualization: 3D pipe reconstruction (8)

Compared to other 3D alternatives, this alternative is selected because it has a higher potential on integrating and visualizing sewer condition data from multiple sources (i.e., only this alternative considers the pipe thickness while modelling, which represents the space within the pipe wall). Moreover, its viewing perspective is relatively easy-to-make and provides a rotatable that allows users to see all the defects.

But be noted, the original "3D pipe reconstruction" visualization concept is not feasible for the researched in-pipe GPR and impact echo methods, customized adjustments are needed to make this alternative feasible in this thesis (e.g., build the 3D pipe model and 3D objects for corresponding defects manually). Besides that, the condition of the pipe's exterior environment also needs to be incorporated since the original alternative has not yet included it.

²³ 2D data visualizations are inherently limited on visualizing the thickness of and defects' depth within the inspected object in spatial dimensions. The conventional way is to represent the thickness with coded colors and denote the defects on the map-based view (see the footnote below).

²⁴ The "map-based" visualization concept means visualizing the inspection data on a 2D map that represents the top view of the inspected object, particularly suitable for slab-like structures.

L. Additional Sewer Defect Codes Development

A particular problem mentioned about the selected data visualization alternatives is, none of them have incorporated the European sewer defects coding system, which plays a very important role in conventional sewer condition assessment. As briefed while introducing the CCTV data visualization (see section 1.1), the sewer defects coding system categorizes and digitizes the visual data and text-descriptive information into codes, which are particularly useful for the sewer management software (i.e., easier to store and process) and make the sharing and communication among users much easier and efficient²⁵ (McDonald, et al., 2001). Most importantly, the coding system provides a systematic approach to describe and measure the condition of a defect, which greatly helps to reduce subjective opinions from the inspector and results in more objective and accurate sewer condition assessment (BS_EN_13508-2:2003+A1, 2011; McDonald, et al., 2001).

Simply speaking, the sewer defects coding system standardized the visualization of the CCTV sewer inspection data. Although it is currently only used in CCTV and other visual sewer inspections, it should not and will not be limited by the inspection technology. Over the past decades, the sewer defects coding system has been updated a few times, some old codes were modified, and new codes were added. It is not only a convention within the sewer inspection industry but also the users' demand and a future trend to encode new defects, make them compatible with and complementary to the current sewer condition assessment. With these concerns, additional sewer defect codes are developed for the defects of interest in this thesis (see more of the defects in Appendix C) based on the current sewer defect coding system in (BS_EN_13508-2:2003+A1, 2011). By studying the European sewer defects coding system in Appendix H, some ground rules of developing new defect codes are established below. Note part of these rules is established based on the suggestions from the sewer management professionals.

- 1) A definition of the defect type should be given.
- 2) The format of the code should be the same as the coding system in (BS_EN_13508-2:2003+A1, 2011).
- 3) The naming of new codes must be different than the existing ones to provide clarity about the data origin (since the new defects are collected by inspection technologies different than CCTV).
- 4) Characterizations (up to two types) and quantifications (up to two types) should be suggested to better describe and measure the condition (severity) of the defect.

Based on these ground rules, additional sewer defect codes for the defects of interest in this thesis are developed in Table 0-4 on the next page.

²⁵ For example, during the interview the author had with the Hengelo sewer managers, they pointed out that the measured values of defects in a sewer pipe are recorded in a “.ribx” file, which is consisted of the defects codes. This file can be easily imported into, recognized by and displayed on the sewer management system of the Hengelo municipality (and other common-used sewer management software).

Table 0-4: Additional sewer defect codes developed for the defects assigned to in-pipe GPR and impact echo.

Defects assigned to the inspection technology	Defect definition	Developed codes	Additional information			
			Location	Characterizations	Qualifications (for measuring the severity of defects)	
In-pipe GPR	External void	An empty space in the vicinity of the pipe outer surface that reduces the support from soil.	A new <i>code "RBAP"</i> is developed based on the code "BAP". "R" represents the origin of the data source - in-pipe GPR.	The longitudinal location and circumferential position should be recorded.	<p>Characterization 1: A/B if the void was filled with air or water.</p> <p>Characterization 2: A/B if the void was observed in the vicinity of other defects that may cause soil erosion or not.</p>	<ul style="list-style-type: none"> Distance to the pipe. Void size, the severity increases as the void size increases (mainly considering the void depth in this thesis due to the detection limitation, assuming the void is a sphere).
	Unknown object	—	RBAQ	The longitudinal location and circumferential position should be recorded.	—	<ul style="list-style-type: none"> Distance to the pipe.
Impact echo	Pipe wall thickness reduction	—	A new <i>code "EBAR"</i> is developed. "E" represents the origin of the data source - impact echo.	The longitudinal location and circumferential position of the starting and finishing points should be recorded.	—	<ul style="list-style-type: none"> The reduced thickness in mm (or the ratio between the reduced thickness and total wall thickness). The size of the area with thickness losses.
	Internal void	An empty space within the pipe wall that reduces the pipe's structural integrity.	A new <i>code "EBAS"</i> is developed, continued after "EBAR".	The longitudinal location and circumferential position should be recorded.	—	<ul style="list-style-type: none"> Void size (the severity increases as the void size increases).
	Delamination	A separation of layers within the pipe wall (usually in the interface of concrete - reinforcement - lining) that reduces the pipe's structural integrity.	A New <i>code "EBAT"</i> is developed, continued after "EBAS".	The longitudinal location and circumferential position of the starting and finishing points should be recorded.	—	Both size, depth of the delamination matters. It is more comprehensive to determine the severity via the WTDR (width-to-depth ratio, $\frac{d}{T}$).
	Surface cracks	(Invisible) cracks on the pipe inner/outer surface that reduce the structural integrity.	A new <i>code "EBAB"</i> is developed based on the code "BAB".	The longitudinal location and circumferential position of the starting and finishing points should be recorded.	<p>Characterization 1: A/B if the crack is in the pipe inner/outer surface.</p> <p>Characterization 2: A/B/C/D if the orientation of the crack is longitudinal, circumferential, complex, or helical.</p>	<ul style="list-style-type: none"> Crack width in mm.

Be noted:

- As of 2020, the new Dutch national sewer inspection standard leaves the defects severity classification for the sewer manager to decide, which is done through the sewer management software incorporated with the severity classification agreement. The sewer manager can adjust the upper and lower limits of the agreement based on his/her experience and preferences. Thus in this thesis, only characteristics and quantifications that can be used to determine the severity are suggested.
- Some of the new codes are adapted from the existing codes with essential adjustments, e.g., *RBAP* for external voids.
- For correction, the location (both longitudinal and circumferential) of the defect might cause different severity but it is essential information of a defect anyway, thus it is not considered as a quantification for the severity estimation.
- Be noted:** The aim of developing the additional sewer defect codes is not to get them approved/accepted by the authority, instead, it means to propose that it is not only a convention within the sewer inspection industry but also the users' demand and a future trend to encode new defects and make them compatible with and complementary to the current sewer condition assessment. This is an indispensable step towards new sewer condition data visualization alternatives.

PS: These developed codes have been evaluated and approved by professionals from the sewer inspection and management filed.

M. Impact Echo Sewer Inspection Data Visualization Method

The determined final solution for visualizing the impact echo inspection data is to use the **2D color-coded defects map (6)** as the main body and combine the **2D pipe fold-out view (1)**. The main body of the new visualization method was initially used to present the condition of the surface and within the slab-like concrete structures, which has an inherent limitation on visualizing the thickness changes and the depth of defects in spatial dimensions. Therefore, coded-colors are conventionally used to denote the thickness and defects information on a “map-based” view (see the example H), which means presenting the inspection data on a 2D map that represents the top view of the inspected object (particularly suitable for slab-like structures, but not pipe-like structures, e.g., tunnels or sewers).

In this case, although the idea of applying the **2D color-coded defects map (6)** to visualize the sewer condition of the pipe surface and within the pipe wall perfectly matches with its visualization capability, the “map-based” view needs to be adapted to represent the pipe’s geometry for the sewer condition assessment. The adaption of the “map-based” view is where the combination lies. For this purpose, the idea of “unfolding” the pipe from the **2D pipe fold-out view (1)** can then be used to replace the “map-based” view in the new visualization method. Other than that, page 66 and the design requirements also require the new visualization method to incorporate the sewer defect codes. Here another benefit of combining these two selected alternatives emerges, the sewer defects codes from the **2D pipe fold-out view (1)** can be transplanted into the new visualization method. The graphical design below then presents these combinations.

Be noted, because the impact echo simulation data and corresponding data processing and interpretation are not available, four arbitrary defects are visualized in the design as a practical example of this new data visualization method. This example assumes an impact echo inspection has been executed to the same sewer pipe as assumed in section 4.3 and certain processing techniques/procedures²⁶ have been applied to process and interpret the inspection data. According to the interpretation, four defects were detected, see the simulation scenarios from section J (the longitudinal location and severity of the defects presented in the design are assumed).

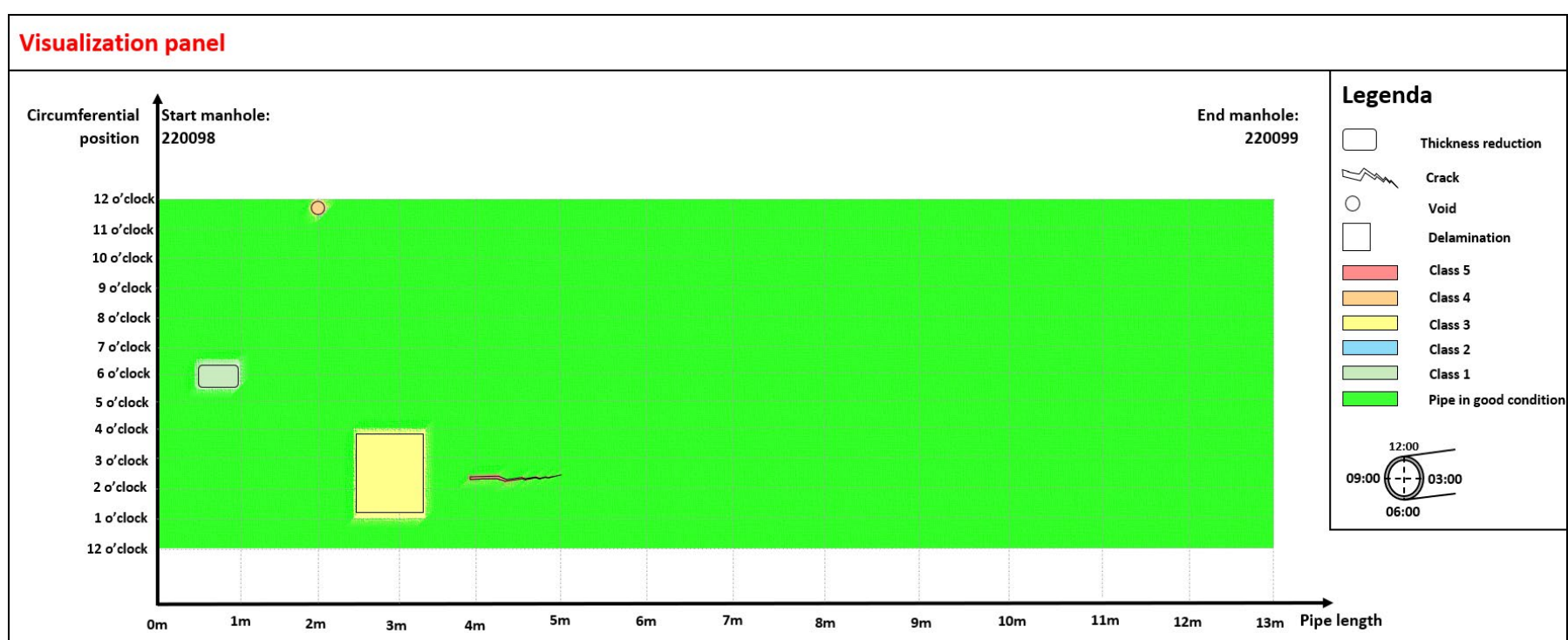


Figure 0-30: The impact echo sewer inspection data visualization with the simulation scenarios presented.

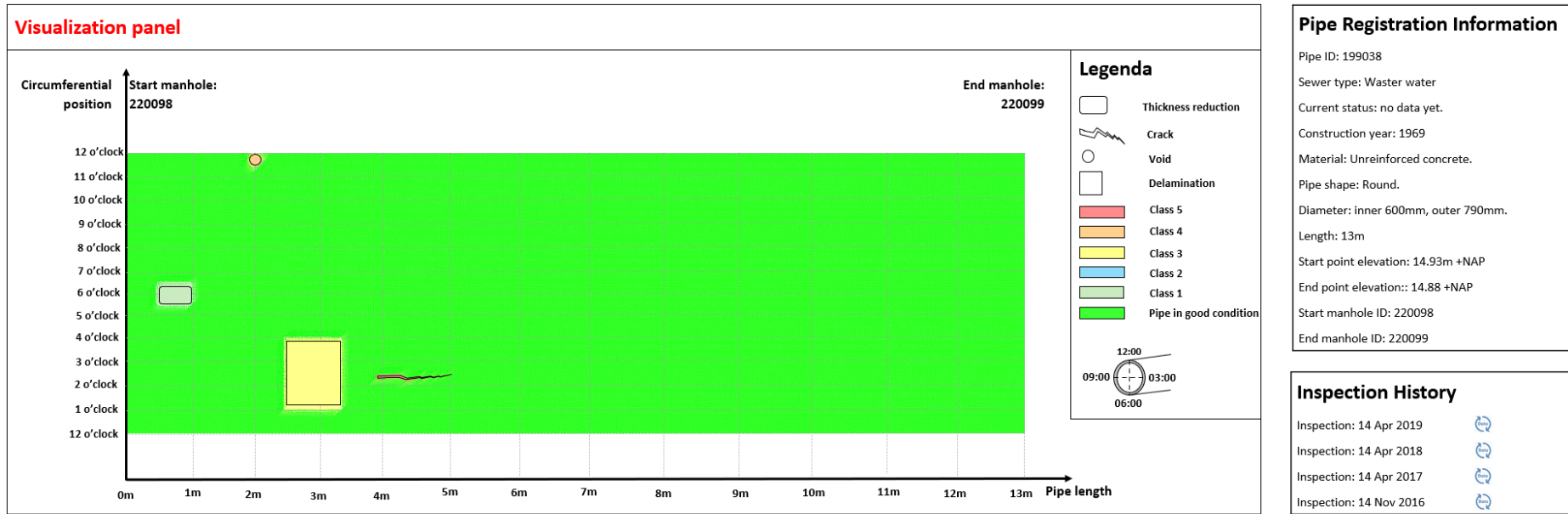
As seen in Figure 0-30, the “map-based” view is replaced by a pipe fold-out view, to some extent, the pipe fold-out view can be regarded as an application of the “map-based” visualization concept in pipes. The X-axis represents the pipe length and direction of inspection, the Y-axis represents the pipe’s circumferential positions, denoted by clock directions. The pipe fold-out view is formed by a color-coded thickness tomogram, where most parts of the pipe are colored green (indicating the pipe is in good condition). But defects such as the pipe wall thickness loss, voids, delamination, and surface cracks, are colored differently than the “healthy” parts. These colored parts provide an outline of the defect, then shapes (see the legenda at the right of Figure 0-30) are added to highlight and distinguish the range and type of them. Be noted, in this example, the colors used for the defects are the same colors used for the severity classes²⁷, because they are already different than the color for “good condition” and the severity of the defects are assumed as known. In simple words, the green “healthy” color can be regarded as the white background in CCTV data visualizations (see Figure 1-2).

Due to the use of the pipe fold-out view, the visualization panel of the new impact echo sewer inspection data visualization is inevitably alike to the CCTV data visualization method (see Figure 1-2). But the innovation of this new visualization is about the depiction of the pipe fold-out view and defects. Imagining the impact echo inspection has scanned the pipe inner surface by tapping it densely, e.g., thousands of tapping points were collected. These data points are then used to form up (or projected to) the pipe fold-out view, which is somehow very similar to the LIDAR scanning data visualization in the example E and 3D data projection visualizations 4 and 5. In case of an impact echo inspection with discrete tapping points, the raw data can still be used to form up an outline of the pipe fold-out view and the interpreted results (e.g., if a defect is found in a specific tapping point) can be overlaid on it. But the resolution/accuracy of the visualization will be reduced (e.g., size/range of defects might not be presented).

Similar to the modified in-pipe GRP sewer inspection data visualization in the previous section, the new impact echo sewer inspection data visualization also uses the interface layout of *MapKit*, thus the “pipe registration information” and “inspection history” features are placed (see the complete design on next page). More than that, the additional sewer defect codes are used to classify and summarize the defects and their detailed condition information (the same link between the defect shapes and codes are suggested as in the in-pipe GPR inspection data visualization method, see page 40).

²⁶ It is assumed the impact echo data processing and interpretation procedures are similar to the ones introduced in section 3.1, which produce post-processed data like the post-processed in-pipe GPR radargrams. See more about the impact echo data interpretation on page 66.

²⁷ In practices, a transition might be needed after the defective parts were found and before knowing their severities. See example: H, the impact echo tomogram has already used different colors to distinguish defective parts from “healthy” parts. However, the severity is not known yet. So further analysis needs to be carried on these defective and then they can be color-coded according to their severity class.



Source Data

Inspection data not available...

Defect Details

Begin	End	Code	Characterisations	Description	Class	Clock	Source data
.....	-	-	- - -	-	-	-	-
0.5m	1m	EBAR	- - -	Pipe wall thickness reduced around 30mm.	1	6	Not available.
2.0m	-	EBAS	- - -	Air void inside the pipe, diameter around 30mm (assumed as a sphere void).	3	12	Not available.
2.5m	3.3m	EBAT	- - -	Delamination within the pipe wall, thickness of the delamination itself is around 0.1mm.	4	1-4	Not available.
3.5m	4.8m	EBAB	B - -	Longitudinal crack on pipe outer surface, width around 5mm.	5	3	Not available.
.....	-	-	- - -	-	-	-	-

Figure 0-31: The complete interface of the modified impact echo sewer inspection data visualization with the simulation scenarios presented.

Overall, due to the missing of simulation data and corresponding processing and interpretation, this data visualization is less specifically designed for impact echo sewer inspections but more to show how can defects from the space within the pipe wall (including the pipe inner and outer surface) can be visualized. Simply speaking, if the impact echo method is replaced by another technology that has similar detection capability (e.g., ultrasonic inspections), this data visualization method is also applicable.

N. Integrated Sewer Condition Data Visualization Method

As concluded from users' emerging data needs, the sewer asset managers are pursuing a more comprehensive sewer condition assessment, which requires visualizing sewer condition data collected from all pipe spaces in a central platform. Since the "pipe spaces" theory developed in this thesis simply divides the buried pipe into three spaces and assigns each space to be inspected by different technologies, the comprehensive sewer condition assessment then requires to integrate and visualize the sewer condition data collected by each technology. Because the collected data are spatially separated, the most logical way to visualize them is through 3D modelling, which can integrate the sewer condition data in a central platform and present their spatial relationship. In fact, among all available visualization alternatives found in literature, indeed only the 3D alternatives have the potential to fulfill this integration and visualization intention.

The final selected alternative for visualizing the condition data collected from multiple sources is the **3D pipe reconstruction (8)**, which has a high potential to integrate sewer condition data from all pipe spaces. But as mentioned on page 66, "reconstructing a 3D pipe with the inspection data is infeasible in this thesis"²⁸. Therefore, the adjustment proposed in this section is to manually create a 3D CAD pipe model (with thickness and other details) to represent the pipe's designed status and manually register defects onto the model with predefined 3D objects. This somehow changes the "inspecting and visualizing simultaneously (reconstructing the 3D pipe while inspecting)" idea of the original visualization alternative, but it is the most practical way to realize such a 3D sewer inspection data visualization with the available simulation data.

Besides the adjustment, as denoted on page 66 and compared to the design requirement, the remaining imperfections of this visualization alternative are, **1**). it has not yet included the pipe's exterior environment; **2**). it is difficult to provide an overview that presents all defects; **3**). it has not been incorporated with the sewer defect codes. In this section, this visualization alternative is modified in terms of these imperfections. Then the modified visualization is used to visualize the defects presented in the modified in-pipe GPR and impact echo visualizations, and some assumed CCTV inspection data, as an example of integrating sewer condition data collected from multiple sources.

Be noted, for the example of integrating sewer condition data collected from multiple sources, the assumption is that the same sewer pipe as assumed in section 4.3 has been inspected by in-pipe GPR, impact echo, and CCTV. According to the inspection data corresponding processing and interpretation, a pipe wall thickness loss, a void, and delamination within the pipe wall were detected by impact echo; one external void and two unknown objects were detected by in-pipe GPR, and an obstacle is found by CCTV²⁹ (the presented defect types can be seen in the legenda below, the longitudinal location and severity of the defects are assumed).

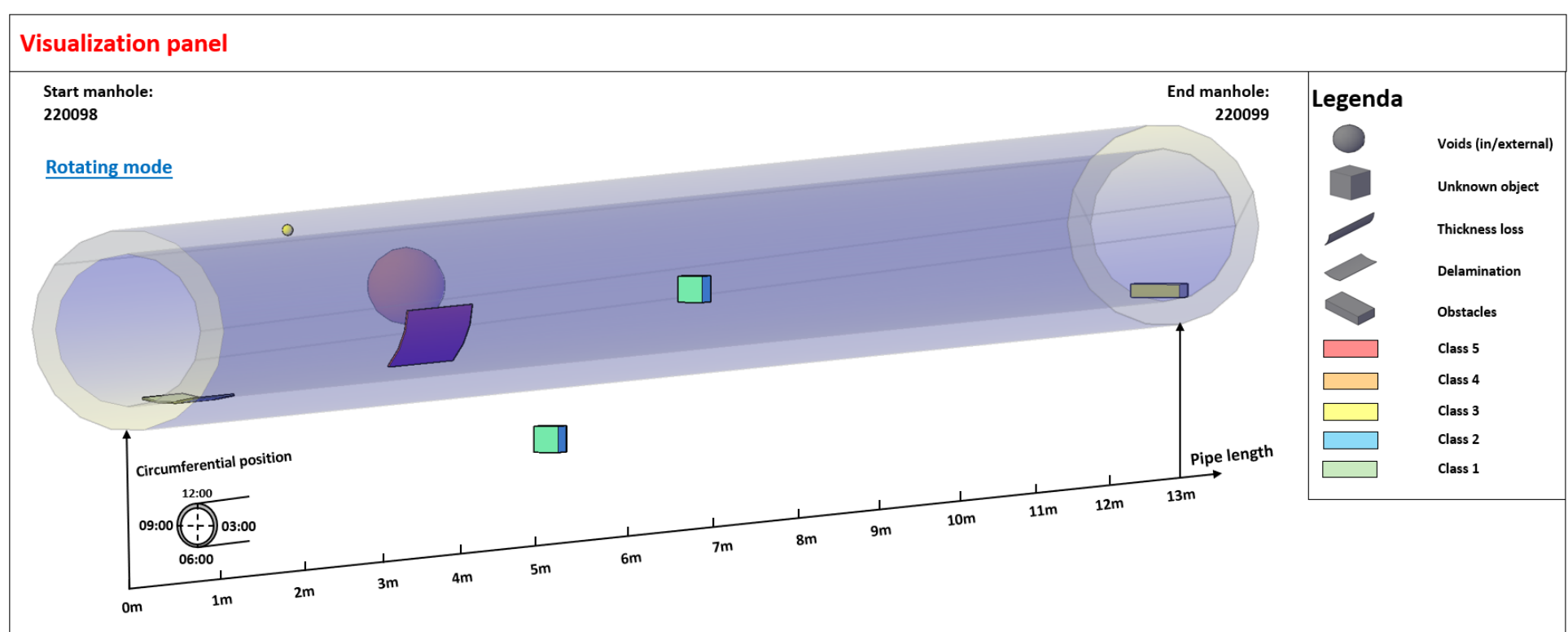


Figure 0-32: The main visualization panel of the modified integrated sewer inspection data visualization.

As seen in the figure above, the visualization panel of the modified integrated sewer inspection data visualization mainly shows a 3D pipe model, which is transparentized and fixed at a certain viewing angle (regarding the pipe's front view as reference (see the right part of Figure 0-33), rotate the 3D pipe -15° vertically and 45° horizontally,). Through the transparent 3D pipe, it can be seen that the defects are then visualized as different 3D objects inside, within, or outside the 3D pipe³⁰. The X-axis represents the pipe length (the arrow indicates inspection direction). Instead of setting a Y-axis in the vertical direction, the location of a defect is denoted by the clock directions and its radial distance to the pipe's outer/inner surface. With these designed elements, the process of adapting the **3D pipe reconstruction (8)** is completed.

From left to right, the 3D pipe first presents the defects detected by impact echo (i.e., the surface damage at 6 o'clock, internal void at 12 o'clock, and delamination at the right haunch of the pipe). Then three objects detected by in-pipe GPR are visualized outside the 3D pipe, distributed at 9 o'clock, 6 o'clock, and 3 o'clock. Finally, at the right end of the 3D pipe, a brick is placed inside the pipe to indicate the "obstacle" detected by CCTV. In this example, the 3D pipe has integrated data collected by different technologies from different pipe spaces, which also indicates that the condition of the pipe's exterior environment has now been included in this visualization.

Several solutions are applied to resolve the "overview" imperfections in this design. Firstly, the 3D pipe is made transparent, which allows users to see through the pipe and see as many defects as possible at once. This may be still unclear for users to understand the spatial relationship between the pipe and defects, hence the "Rotating mode" is designed. See the blue "Rotating mode" button in the top left corner of the 3D pipe in Figure 0-32, after clicking it, a separate window pops up and provides more viewing

²⁸ Since "reconstructing a 3D pipe" from the inspection data is a complicated process and still under development, this thesis poses neither sufficient simulation data nor modeling skills for such a purpose.

²⁹ Be noted, many defects are not presented in this integration since it is difficult to make predefined 3D objects for them (e.g., the outer surface crack visualized in the modified impact echo visualization and other defect types that can be detected by CCTV). It is assumed the presented defects are sufficient to represent defects collected by different technologies from different pipe spaces.

³⁰ Here it is suggested to add as a "viewing setting" button under the "Rotating view" to filter defects in different pipe spaces, i.e., the user can choose to see defects from one or multiple spaces.

perspectives to the users (see the visualization panel in Figure 0-34). The “rotating mode” consists of two parts, the left part allows users to rotate the 3D pipe in a certain range while the right part provides several suggested views (see Figure 0-33 on the next page).

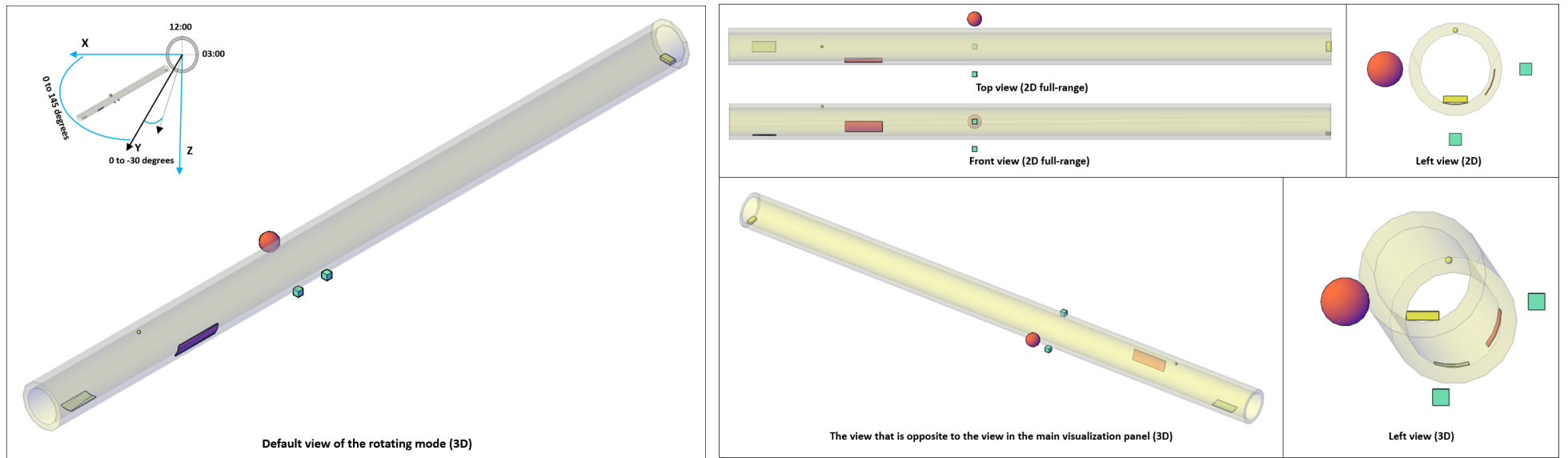


Figure 0-33: Details of the rotating mode, left: rotating view; right: suggested views.

The figure above presents the two parts of the rotating mode more clearly. In the left rotating view, a default view is presented, which is similar to the view presented in the visualization panel. One consideration here is there no need to make the 3D pipe fully rotatable (i.e., 360° all directions), hence the XYZ-axis in the top left corner gives a suggested rotating range, which is from 0 to 145° horizontally and 0 to -30° vertically. Note the front view of the 3D pipe is regarded as reference (see the right part), for example, to rotate the 3D pipe to the position of the default view, the front view needs to rotate downwards by 30° and towards outside the paper by 45°. Noted again, the design of the rotating range can be adjusted according to the users' needs.

Other than the rotating view, this design also suggests providing two groups of fixed views to users as references, see in the right part of Figure 0-33. The first group consists of three orthographic views of the 3D pipe, namely the top view, front view, and the left view. Although the orthographic views are in 2D, they present the length, width, and height of the pipe accurately, which is very important in engineering designs. The second group suggested two fixed 3D views that are typical representatives of seeing the pipe from a different angle. One is the view opposite to the view presented in the visualization panel (downwards by 30° and towards outside the paper by 145°), the other is the 3D left view of the pipe (downwards by around 5° and towards outside the paper by around 85°). Be noted, for all the views provided, the X-axis (representing the pipe length), clock directions and radial axes (denoting defects' distance to the pipe), or solutions to indicate the position of the defects should be given.

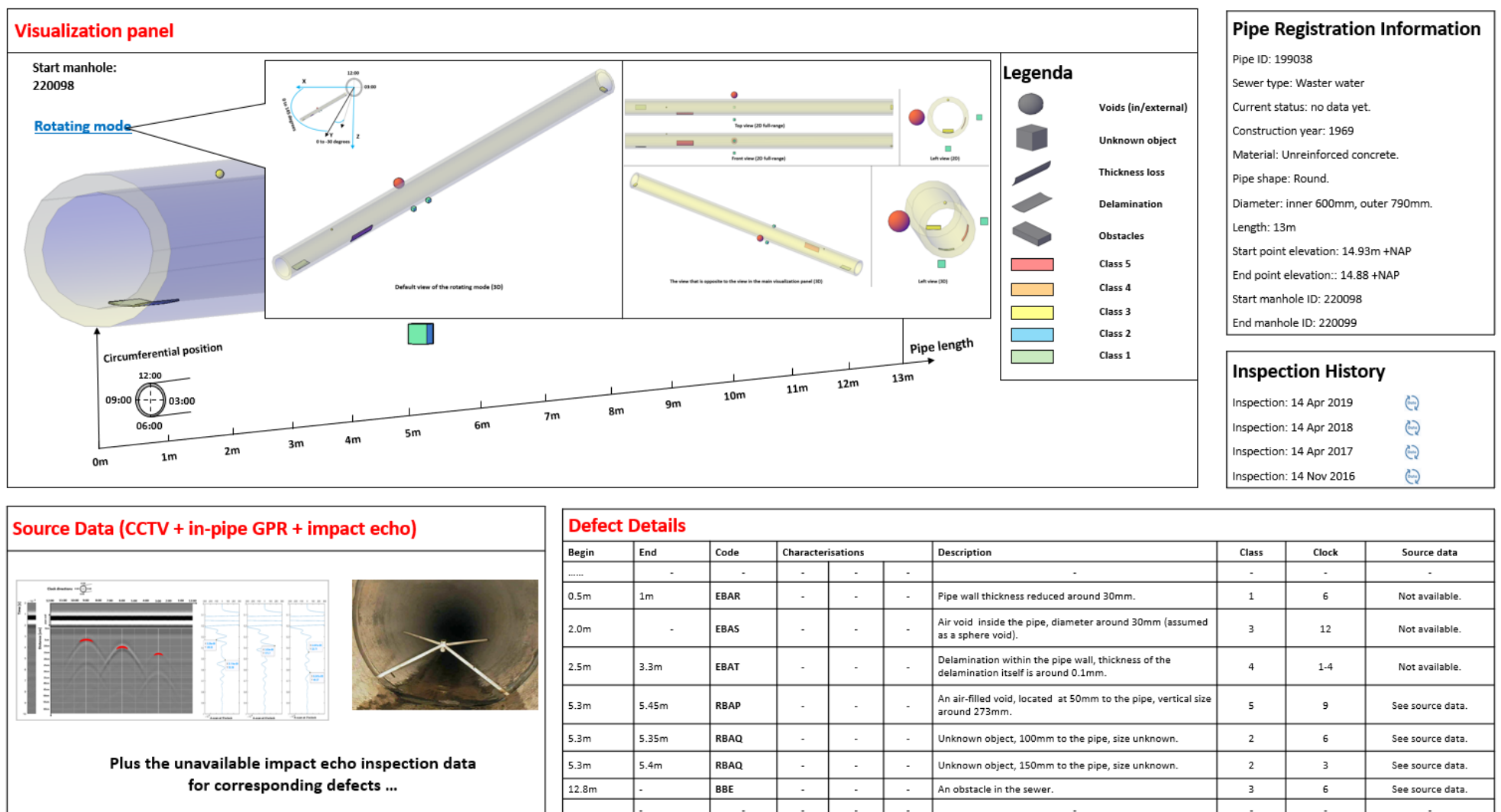


Figure 0-34: The complete interface of the modified integrated sewer inspection data visualization, with sewer condition data from multiple sources presented.

As the previous paragraphs introduced the visualization panel thoroughly, the above figure presents the complete interface of the modified integrated sewer inspection data visualization, which provides the source data of the defects and uses the newly developed sewer defect codes to summarize all the defects. To some extent, the summarised sewer defect codes in a table form also provide a good overview of all the defects and their detailed information (the same link between the defect shapes and codes are suggested as in the in-pipe GPR inspection data visualization method, see page 40). Hence, the second and third imperfections are solved. Similar to the previous two alternatives, the added value features from the **MapKit** interface are added to this visualization to make it more user-friendly. In summary, with the presented design elements and suggestions, the aforementioned imperfections are resolved comprehensively in this modified integrated sewer inspection data visualization.

References

- (EPA), U. S. (2007). *EPA's water infrastructure research plan*.
- Ardito, C., Buono, P., Costabile, M. F., & Lanzilotti, R. (2006). Systematic inspection of information visualization systems. *In Proceedings of the 2006 AVI workshop on BEyond time and errors: novel evaluation methods for information visualization*, 1-4.
- ARSI. (2017). *ARSI*. Retrieved from eurecat.org: <https://eurecat.org/en/portfolio-items/aerial-robot-for-sewer-inspection/>
- Babcock IV, P. S., Stillo, M., Ryan, K., Vincent, E., Sprehn, K., Brill, R. M., & Sun, F. (2020). Augmented reality visualization for pipe inspection.
- Balkaya, M., Moore, I. D., & Sağlamer, A. (2012). Study of non-uniform bedding due to voids under jointed PVC water distribution pipes. *Geotextiles and Geomembranes*, 34, 39-50.
- Benedetto, A., & Pajewski, L. (. (2015). GPR Data Processing Techniques. In *Civil engineering applications of ground penetrating radar* (p. 282).
- Bigman, D. (2017). *5 Need to Know GPR Data Processing Steps*. Retrieved from <http://learnpr.com/5-need-to-know-gpr-data-processing-steps/>
- Bigman, D. (2017, November). *Why Different Materials Produce Different GPR Responses | Ground Penetrating Radar*. Retrieved from learnpr.com: <http://learnpr.com/why-different-materials-produce-different-gpr-responses-ground-penetrating-radar/>
- Blanc, P., Ducastel, B., Cazin, J., Al Blooshi, M., Al Dhaheri, S. S., Al Marzooqi, M. H., & Massabuau, J. C. (2017). First-Time Implementation of Innovative In Situ Biotechnology on an Offshore Platform in Arabian Gulf for Continuous Water Quality Monitoring and Early Leak Detection. *In Abu Dhabi International Petroleum Exhibition & Conference. Society of Petroleum Engineers*.
- Boven, E. v. (2019). *Localization of structural flaws in concrete sewer pipes by physical interaction inspection with a robotic arm*. Retrieved from <http://purl.utwente.nl/essays/79675>
- Browne, M., Ghidary, S., & Mayer, N. (2007). Convolutional Neural Networks for Image Processing with Applications in Mobile Robotics. doi:10.1007/978-3-540-75398-8_15.
- BS_EN_13508-2:2003+A1. (2011). *Investigation and assessment of drain and sewer system outside buildings - Part 2: Visual inspection coding system*. European Committee For Standardization. Provided By P. Wonink. Rolsch.
- BS_EN-752:2017. (2018). *Drain and sewer systems outside buildings - Sewer system management*. European Standard: European Committee For Standardization. Provided By Mr. P. Wonink. Rolsch.
- Caradot, N., Rouault, P., Clemens, F., & Cherqui, F. (2018). Evaluation of uncertainties in sewer condition assessment.
- Carino, N. J. (2001). The impact-echo method: an overview. *In Structures 2001: A Structural Engineering Odyssey*, (pp. 1-18).
- Carino, N. J. (2015). Impact echo: the fundamentals. *International Symposium Non-Destructive Testing in Civil Engineering (NDT-CE)*, Berlin, Germany.
- Carino, N. J., & Sansalone, M. (1990). Flaw detection in concrete using the impact-echo method. *Bridge Evaluation, Repair and Rehabilitation*, (pp. 101-118).

- Cassidy, N. J., & Jol, H. M. (2009). Ground penetrating radar data processing, modelling and analysis. In *Ground penetrating radar: theory and applications* (pp. 141-176).
- Cassidy, N. J., Eddies, R., & Dods, S. (2011). Void detection beneath reinforced concrete sections: The practical application of ground-penetrating radar and ultrasonic techniques.
- Cernat, C. (2019). *Analysis of sensors used for interaction-based condition assessment of concrete*. Retrieved from <http://essay.utwente.nl/78933/>
- Chae, M. J., & Abraham, D. M. (2001). Neuro-fuzzy approaches for sanitary sewer pipeline condition assessment. *Journal of Computing in Civil Engineering*, 15(1), 4-14.
- Colla, C., & Lausch, R. (2003). Influence of source frequency on impact-echo data quality for testing concrete structures. *Ndt & E International*, 36(4), 203-213.
- Costello, S. B., Chapman, D. N., Rogers, C. D., & Metje, N. (2007). Underground asset location and condition assessment technologies. *Tunnelling and Underground Space Technology*, Costello, S. B., Chapman, D. N., Rogers, C. D. F., & Metje, N. (2007). Underground asset location a22(5-6), 524-542.
- Daniels, J. (2000). Ground Penetrating Radar Fundamentals. 10.4133/1.2921864. Retrieved from Daniels, Jeffrey. (2000). Ground Penetrating Radar Fundamentals. 10.4133/1.2921864.
- Dolgiy, A., Dolgiy, A., & Zolotarev, V. (2006). Estimation of subsurface pipe radius using ground penetrating radar data. In *Near Surface 2006-12th EAGE European Meeting of Environmental and Engineering Geophysics European Association of Geoscientists & Engineers.*, (pp. cp-14).
- Donazzolo, V., & Yelf, R. (2010). Determination of wall thickness and condition of asbestos cement pipes in sewer rising mains using Surface Penetrating Radar. 10.1109/ICGPR.2010.5550183.
- Duman, M., & Gurbuz, A. (2015). 3D imaging for ground-penetrating radars via dictionary dimension reduction.
- Duran, O., Althoefer, K., & Seneviratne, L. (2002). State of the art in sensor technologies for sewer inspection. *IEEE Sensors journal*, 2(2), 73-81.
- Ekes, C. (2016). Quantitative pipe condition assessment with Pipe Penetrating Radar.
- Ékes, C., & Maier, J. (2012). Condition Assessments Using Pipe Penetrating Radar: The Metro Wastewater Reclamation District, Denver, CO—Harvard Gulch Interceptor Case Study.
- Ékes, C., & Neduczka, B. (2012). Robot mounted GPR for pipe inspection.
- Ekes, C., Neduczka, B., & Henrich, G. R. (2011). GPR goes underground: pipe penetrating radar. Washington, D.C.
- Ékes, C., Neduczka, B., & Henrich, G. R. (2014). GPR goes underground: Pipe penetrating radar.
- Ekes, C., Neduczka, B., Krause, R., & Lee, R. (2014). Applications of pipe penetrating radar for advanced pipe condition assessments—Clark Regional Wastewater District (WA) Case Study.
- Fenner, R. A. (2000). Approaches to sewer maintenance: a review. *Urban water*, 2(4), 343-356.
- FIU. (2018). *Mapping & Data Visualization*. Retrieved from FIU Libraries: <https://library.fiu.edu/c.php?g=766021&p=5497523>
- Garcia, E., Erdogmus, E., Schuller, M., & Harvey, D. (2017). Novel Method for the Detection of Onset of Delamination in Reinforced Concrete Bridge Decks. *Journal of Performance of Constructed Facilities*.
- Gehrig, M. D., Morris, D. V., & Bryant, J. T. (2004). Ground penetrating radar for concrete evaluation studies. *Technical Presentation Paper for Performance Foundation Association*, 197-200.

- GeoSci. (2019). *CPG Home: Basic Principles*. Retrieved from https://gpg.geosci.xyz/content/GPR/GPR_fundamental_principles.html
- Gong, Q., Zhu, H., Yan, Z., Huang, B., Zhang, Y., & Dong, Z. (2015). Fracture and delamination assessment of prestressed composite concrete for use with pipe jacking method. *Mathematical Problems in Engineering*, 2015.
- GPR-SLICE. (2020). *GPR-SLICE Software - Vector Imaging*. Retrieved from [gpr-survey.com: https://gpr-survey.com/vector-imaging.html](https://gpr-survey.com/vector-imaging.html)
- Han, W. S., Jung, S. K., Shin, J., Lee, J., Yoon, M., Yoon, C. G., & ... Koo, S. O. (2007). A scalable pipeline data processing framework using database and visualization techniques.
- Hong, W. T., Kang, S., Han, W. J., & Lee, J. S. (2017). Investigation of ground cavity using ground penetrating radar. *In 19th International Conference on Soil Mechanics and Geotechnical Engineering*.
- Hwang, J., Kim, D., Li, X., & Min, D. J. (2019). Polarity Change Extraction of GPR Data for Under-road Cavity Detection: Application on Sudeoksa Testbed Data. *Journal of Environmental and Engineering Geophysics*, 419-431.
- Igel, J. (2008). The small-scale variability of electrical soil properties—influence on GPR measurements. *In 12th international conference on ground penetrating radar*, (16-19).
- Ingelise, M. D. (2006). *Ground Penetrating Radar Survey in the Northern [i.e. Northern] Part of the Tyrsting Pilot Area, the BurVal Project: Data Report*. GEUS.
- Kamel, S., & Meguid, M. A. (2008). An Experimental Study of Soil Erosion around Leaking Pipes. *In North American Society for Trenchless Technology No-Dig Conference & Exhibition*.
- Kang, J. M., Song, S., Park, D., & Choi, C. (2017). Detection of cavities around concrete sewage pipelines using impact-echo method. *Tunnelling and Underground Space Technology*, 65, 1-11.
- Kirkham, R., Kearney, P. D., Rogers, K. J., & Mashford, J. (2000). PIRAT—a system for quantitative sewer pipe assessment.
- Kommireddi, C. R., & Gassman, S. L. (2004). Impact Echo Evaluation of Thin Walled Concrete Pipes. *In Pipeline Engineering and Construction: What's on the Horizon? Kommireddi, C. R., & Gassman, S. L. (2004). Impact Echo Evaluation of Thin Walled Concrete Pipes. In Pipeline Engineering and Construction: What's on the Horizon? (pp. 1-10).*, *In Pipeline Engineering and Construction: What's on the Horizon?*
- La, H. M., Gucunski, N., Kee, S. H., & Van Nguyen, L. (2015). Data analysis and visualization for the bridge deck inspection and evaluation robotic system.
- Lawson, S. W., & Pretlove, J. R. (1998). Augmented reality for underground pipe inspection and maintenance.
- Lawson, S. W., Pretlove, J. R., Wheeler, A. C., & Parker, G. A. (2002). Augmented reality as a tool to aid the telerobotic exploration and characterization of remote environments.
- Le Gauffre, P., Joannis, C., Vasconcelos, E., Breyse, D., Gibello, C., & Desmulliez, J. J. (2007). Performance indicators and multicriteria decision support for sewer asset management. *Journal of Infrastructure Systems*, 13(2), 105-114.
- Ling, M., & Chen, J. (2014). Environmental visualization: applications to site characterization, remedial programs, and litigation support.
- Liu, Z., & Kleiner, Y. (2013). State of the art review of inspection technologies for condition assessment of water pipes. *Measurement*, 46(1), 1-15.

- Mac, V. H., Tran, Q. H., Huh, J., Doan, N. S., Kang, C., & Han, D. (2019). Detection of Delamination with Various Width-to-depth Ratios in Concrete Bridge Deck Using Passive IRT: Limits and Applicability.
- Makar, J. M. (1999). Diagnostic techniques for sewer systems. *Journal of Infrastructure Systems*, 5(2), 69-78.
- McDonald, S., & Zhao, J. (2001). Condition assessment and rehabilitation of large sewers. In *Proceedings of International Conference on Underground Infrastructure Research*. Waterloo, Canada: University of Waterloo., pp. 361-369.
- Moore, I. (2008). Assessment of Damage to Rigid Sewer Pipes and Erosion Voids in the Soil, and Implications for Design of Liners. *No-Dig Conference & Exhibition, Dallas, Texas*, Paper C-2e0 .
- Moradi, S., Zayed, T., & Golkhoo, F. (2019). Review on Computer Aided Sewer Pipeline Defect Detection and Condition Assessment. *Infrastructures*, 4(1), 10.
- Mulder, P. (2017). *MoSCoW Method*. Retrieved from <https://www.toolshero.com/project-management/moscow-method/>
- Nahangi, M., & Haas, C. T. (2014). Automated 3D compliance checking in pipe spool fabrication.
- Noshahri, H., olde Scholtenhuis, L., & Dertie, E. (2019). Data Needs-Based Classification of Sewer Condition Assessment Methods. *University of Twente*.
- NYS DOT. (2018). *Geotechnical Design Manual Chapter 21: Geotechnical Aspects of Pipe Design and Installation*. Retrieved from https://www.dot.ny.gov/divisions/engineering/technical-services/geotechnical-engineering-bureau/geotech-eng-repository/GDM_Ch-21_P
- Olson, L. D., Tinkey, Y., & Miller, P. (2011). Concrete bridge condition assessment with impact echo scanning. In *Emerging Technologies for Material, Design, Rehabilitation, and Inspection of Roadway Pavements*, Olson, L. D., Tinkey, Y., & Miller, P. (2011). Concrete bridge condition assessment with impact echo scanning. In *Emerging* 59-66.
- Pasolli, E., Melgani, F., & Donelli, M. (2009). Pasolli, E., Melgani, F., & DA pattern recognition system for extracting buried object characteristics in GPR images. In *2009 IEEE International Geoscience and Remote Sensing Symposium*, (Vol. 4, pp. IV-430). IEEE.
- Pleijssier, A. (2019). *Acoustic condition assessment of concrete sewer pipes using a particle velocity sensor*. Retrieved from <http://essay.utwente.nl/77809/>
- Poluha, B., Porsani, J. L., Almeida, E. R., dos Santos, V. R., & Allen, S. J. (2017). Depth estimates of buried utility systems using the GPR method: Studies at the IAG/USP geophysics test site. *International Journal of Geosciences*, 726-742.
- radarviewllc. (2020). *radarviewllc.com*. Retrieved from Subsurface Void Detection for the Foundation Performance Association: <http://www.foundationperformance.org/pastpresentations/ToddAllenPres-11May05.pdf>
- Rajani, B., & Kleiner, Y. (2004). Non-destructive inspection techniques to determine structural distress indicators in water mains. *Evaluation and Control of Water Loss in Urban Networks*. Retrieved from Rajani, Bogarapu & Kleiner, Yehuda. (2004). Non-destructive inspection techniques to determine structural distress indicators in water mains. *Evaluation and Control of Water Loss in Urban Networks*.
- Reynolds, J. M. (2011). *An introduction to applied and environmental geophysics*. John Wiley & Sons.

- Rhebergen, J. B., Lensen, H. A., van Wijk, R., Hendrickx, J. M., van Dam, R. L., & Borchers, B. (2004). Prediction of soil effects on GPR signatures. *In Detection and Remediation Technologies for Mines and Minelike Targets IX*, 5415, 70.
- Rizzo, P. (2010). Water and Wastewater Pipe Nondestructive Evaluation and Health Monitoring: A Review. *Advances in Civil Engineering*. doi:2010.10.1155/2010/818597
- Saenz, J., Elkmann, N. W., Schulenburg, E., & Althoff, H. (2010). Treading new water with a fully automatic sewer inspection system.
- Sansalone, M. (1997). Impact-Echo: The Complete Story. *ACI Structural Journal*, *Vo. 94, No. 6*, 777-786.
- Sansalone, M. J., & Streett, W. B. (1998). *NDTnet*. Retrieved 2019, from <https://www.ndt.net/article/0298/streett/streett.htm>
- Sansalone, M., Carino, N. J., & Hsu, N. N. (1987). A finite element study of transient wave propagation in plates. *Journal of research of the National Bureau of Standards*, *92(4)*, 267-278.
- Shihab, S., & Al-Nuaimy, W. (2005). Radius estimation for cylindrical objects detected by ground penetrating radar. *Subsurface sensing technologies and applications.*, *6(2)*, 151-166.
- Tableau. (2020). *Data visualization beginner's guide: a definition, examples, and learning resources*. Retrieved from [tableau.com: https://www.tableau.com/learn/articles/data-visualization](https://www.tableau.com/learn/articles/data-visualization)
- Tran, H., Setunge, S., & Shi, L. (2018). A case study on the remaining strength of stormwater drainage pipes.
- van Delft, M. (2019). *Towards feature-based underground void detection with Ground Penetrating Radar from within sewers using Image Processing*. Retrieved from <https://www.ram.eemcs.utwente.nl/about-us/events/towards-feature-based-underground-void-detection-ground-penetrating-radar-within>
- van der Steen, A. J., Dirksen, J., & Clemens, F. H. (2014). Visual sewer inspection: detail of coding system versus data quality? *Structure and infrastructure engineering*, *10(11)*, 1385-1393.
- Walter, C., Saenz, J., Elkmann, N., Althoff, H., Kutzner, S., & Stuerze, T. (2012). Design considerations of robotic system for cleaning and inspection of large-diameter sewers.
- Wirahadikusumah, R., Abraham, D., Iseley, T., & Prasanth, R. (1998). Assessment technologies for sewer system rehabilitation. *Automation in Construction*, *7(4)*, 259-270.
- Yelf, R. (2004). Where is true time zero? *n Proceedings of the Tenth International Conference on Grounds Penetrating Radar, Vol. 1, IEEE*, 279-282.